Quantum Theory of Optical Solitons

by

Yinchieh Lai

S.B.E.E., National Taiwan University (1985)

S.M.E.E., Massachusetts Institute of Technology (1989)

Submitted in partial fulfillment
of the requirements for the degree of

Doctor of Philosophy

in Electrical Engineering and Computer Science

at the

Massachusetts Institute of Technology

August, 1991

© Massachusetts Institute of Technology 1991

Signature of Author _____

Department of Electrical Engineering and Computer Science
August 15, 1991

Certified by _____

Hermann A. Haus
Thesis Advisor

Accepted by _____

Arthur C. Smith
Chairman, Department Committee on Graduate Students

MASSACHUSETTS INSTITUTE
OF TECHNOLOGY

NOV 0 4 1991

LIBRARIES

Quantum Theory of Optical Solitons

by

Yinchieh Lai

Submitted to the
Department of Electrical Engineering and Computer Science
on August 15, 1991 in partial fulfillment of the requirements
for the degree Doctor of Philosophy.

Abstract

A quantum theory of optical solitons is developed. Two kinds of optical soliton phenomena are studied : solitons in optical fibers and self-induced transparency (SIT) solitons. Quantum effects of optical soliton propagation are investigated. Among various quantum effects examined, two of them are of particular interest : the position spreading effect and the squeezing effect. The former places a fundamental upper limit on the achievable bit-rate of proposed long distance communication systems using solitons while the latter may help to overcome the standard quantum limit in precision measurements.

`Thesis Advisor:` Hermann A. Haus
`Title:` Institute Professor

Acknowledgements

Studying at MIT is a great adventure to me. I have to thank a lot of people who have made MIT, at least the part of MIT I am familiar with, an exciting yet comfortable place.

Professors play the most important role in educating young graduate students. They are the source of inspiration. In this respect, the first one I want to thank is my supervisor, Prof. H. A. Haus. We worked together on the ideas presented in the thesis and on many other ideas not presented in the thesis. Without his support and patient guidance, I would not have known how to start. Without his sharp intuition, I would not have known where to put my efforts. The second one to thank is my graduate counselor, Prof. P. L. Hagelstein. I can feel the aspiration from him everytime we had a conservation. The third one I want to thank is Prof. E. P. Ippen. His style of approaching problems and managing things sets another good example for me. I also want to thank Prof. J. H. Shapiro for very carefully reading the thesis and giving valuable comments.

It is friends that make MIT a comfortable place for study. During the past four years, I have the fortune to interact with many good graduate students, postdocs and visiting scientists. I want to thank all of them, especially those in Optics and Quantum Electronics Group, the group I am familiar with. Particularly, I want to mention the following persons. John Moores shares the same office (36-363) with me since I entered this group. We have the same interest in theory and had a lot of discussions on diverse subjects. Katie Hall patiently taught me how to do experiments when we were working together on the ultrafast gain dynamics inside semiconductor diode optical amplifiers. I may not become an experimentalist eventually, but I will always remember those "lab days". Dr. Jyhpyng Wang spent two years (1989-1990) at MIT as a postdoc after his graduation from Harvard. He brought me into the "magic world" of Macintosh, which has facilitated my research a lot.

There are so many friends I want to thank while only limited words can be said here. Anyway, to all my friends at MIT, I will always remember the good time we shared.

To My Parents and Ying-Lin

Table of Contents

List of Figures 6

1. Introduction 7

1.1 Thesis objective ---------- 7
1.2 Historical Background ---------- 9
1.3 Thesis content ---------- 13

2. Solitons in optical fibers 15

2.1 Classical formulation ---------- 15
2.2 Quantum formulation ---------- 17
2.3 Linearization in the Heisenberg picture ---------- 20
2.4 Time dependent Hartree approximation in the Schrödinger picture ---------- 29
2.5 Exact solution in the Schrödinger picture ---------- 34

3. Soliton squeezing in optical fibers 43

3.1 Soliton detection using balanced homodyne scheme ---- 43
3.2 Analytical approach ---------- 46
3.3 Numerical approach ---------- 49
3.4 Squeezing ratio from Hartree approximation ---------- 53
3.5 Soliton gyros with squeezed vacuum injection ---------- 58

4. Solitons in optical fibers with loss and periodic amplification 66

4.1 The equivalent nonlinear Schrödinger equation ---------- 66
4.2 Introduction of gain and loss in quantum mechanics ---- 69
4.3 Linearization approximation and Gordon-Haus limit ---- 70
4.4 Numerical analysis ---------- 73

5. Self-induced transparency solitons 75

5.1 Semiclassical formulation ---------- 75
5.2 Quantization in the scattering data space ---------- 79
5.3 Squeezing ---------- 81

6. Summary and future research directions 86

Appendix 1 90

Appendix 2 91

References 93

List of Figures

[1] Evolution of a rectangular pulses in a optical fiber ---------- 18

[2] Pulse shapes of soliton excitations ---------- 24

[3] Balanced homodyne detection with a pulsed local oscillator 45

[4] Evolution of the contour line of the joint probability --------- 48

[5] Squeezing ratio of solitons in optical fibers ---------- 50

[6] Fiber ring interferometer for squeezing generation ---------- 52

[7] Squeezing spectrum of solitons in optical fibers ---------- 54

[8] Squeezing ratio from Hartree approximation ---------- 56

[9] Fiber ring gyro with squeezed vacuum injection ---------- 59

[10] Squeezing ratio of fiber gyros using solitons ---------- 62

[11] Squeezing ratio of fiber gyros using square pulses ---------- 63

[12] Squeezing ratio of fiber gyros using gaussian pulses ------- 64

[13] Long-haul communication systems using solitons ---------- 67

[14] Optimum squeezing ratio of SIT solitons ---------- 85

Chapter 1

Introduction

1.1 Thesis objective

Solitons, as originally defined, are pulses that propagate in dispersive or absorptive media without changing their pulse shapes, and that can survive after collisions. Two kinds of optical soliton phenomena have been known for a long time : solitons in optical fibers (the nonlinear Schrödinger solitons) and the self-induced transparency (SIT) solitons. Solitons in optical fibers were first predicted by Hasegawa and Tappert[1] in 1973 and were first experimentally observed by Mollenauer et al.[2] in 1980. Since then, the use of solitons in optical fibers for information transmission has been proposed as an attractive alternative to current long-haul communication systems. In the conventional approach to long-haul communication, the signal is transmitted at the frequency where the dispersion of fibers is very small (dispersionless regime). The loss of fiber can be as low as 0.2 dB/km and is compensated using Erbium-doped fiber amplifiers. However, as the length of transmission increases, the effect of the third order nonlinearity (i.e., the self-phase-modulation effect) in optical fibers will show up and place a limit on the transmission bit-rate. On the other hand, if the signal is transmitted in the negative dispersion regime, the dispersion and nonlinearity can achieve balance and solitons are formed. Solitons in optical fibers have been successfully generated using modelocked F-center lasers[2] or using Q-switched semiconductor laser diodes followed by Erbium-doped fiber amplifiers[3]. They have the special property that the interplay between negative group velocity dispersion and the fiber nonlinearity causes their shape to remain unchanged as they transverse the optical fiber. They are also transform-limitted, which facilitates optical switching[4–7]. These properties make the soliton-based long-haul communications system potentially the first large-scale application of modelocked

pulses.

Inclusion of optical amplifiers in the communication link is not without its own problems. The spontaneous emission in optical amplifiers increases the position uncertainty of solitons. This effect places an upper limit (known as the Gordon-Haus limit[8]) on the achievable bit-rate in the long-haul communications system. Although this effect has been studied semi-classically[8], a full quantum theory is needed to analyze the problem rigorously.

With the advance of technology, new effects of soliton propagation may be observed and utilized. The high quantum efficiency of today's detectors makes the quantum noise one of the dominant sources of detector noise. This leads to the possibility of studying quantum effects of soliton propagation. A good example is the soliton squeezing effect. The concept of squeezing (or squeezed states) was first introduced by Yuen[9] in 1976. Up to now, squeezed states have been successfully generated and detected by several research groups[10–19]. In early experiments, the bandwidth of generated squeezed states was narrow because the generation processes were inherently bandwidth-limited. Recently consideration has been given to the high peak power of pulsed lasers to achieve large squeezing. Squeezed pulses generated by parametric down-conversion have been demonstrated[16,17]. A pulse scheme working in the dispersionless region and utilizing Kerr nonlinearity in a optical fiber ring has been carried out in our group[18]. It is expected that, if one uses solitons in the same scheme, the performance should be better because the squeezing phase is constant across the whole soliton. Therefore one does not need to generate a special local oscillator (L.O.) pulse (which is experimentally difficult) to achieve optimum detection. Soliton squeezing in optical fibers has been recently demonstrated by the IBM group[19] . It has also been proposed that one can use solitons to achieve quantum nondemolition measurements[20].

Self-induced transparency, an effect of resonant and coherent coupling between the electromagnetic field and a collection of atoms, was first discovered by McCall and Hahn[21] in 1967. Although many of the theoretical results were originally obtained by McCall and Hahn[22], it was soon recognized[23–26] that the SIT problem

can be completely solved by the inverse scattering formalism of Zakharov-Shabat[27]. Since then, SIT has become one of the few examples of completely solvable nonlinear systems for which we have experimental results[28] to compare with theory. Recently, it was estimated[29] that the self-phase modulation of a 2π soliton and the mutual-phase modulation of two 2π solitons can achieve a very large phase shift for picosecond pulses in the excitonic range of the spectrum in CdS . This makes SIT a promising candidate for the realization of pulsed squeezed states and quantum nondemolition measurements.

To study these new effects, one needs a quantum theory of optical solitons. Unfortunately, past work on these two soliton phenomena is mainly classical or semiclassical. The main objective of this thesis is to develop a rigorous quantum theory of optical solitons so that one can study quantum effects of soliton propagation quantitatively.

1.2 Historical background

The literature on soliton phenomena is a rich one. Different types of nonlinear equations that may have soliton solutions have arisen from different area of research. The most surprising thing is that some important nonlinear equations can be solved analytically from a unified point of view. In this section we will only review the developments that are directly related to optical solitons. Those who are interested in other types of nonlinear systems that have soliton solutions are referred to the books[30–32].

The story of solitons begins with the observation by John Scott Russell[33] in 1844 of the water surface-wave solitons. However, it was until 1895 that Korteweg and deVries[34] wrote down the (unidirectional) governing equation (which is now known as the KdV equation) for this type of solitons. After 70 years, Zabusky and Kruskal[35] did the first numerical study of the KdV equation in 1965 and announced the real discovery of solitons. Stimulated by the numerical results, Gardner et al.[36] quickly discovered a general method (the inverse scattering transform) to solve the KdV equation analytically in 1967. Their discovery is just the beginning

of the theoretical development. One year later, Lax[37] introduced his famous "Lax pair" formulation. The importance of Lax's discovery is that all the solvable (or integrable) nonlinear equations like KdV can be expressed in Lax form.

Almost at the same time, a new soliton phenomenon was discovered in the area of nonlinear optics : the self-induced transparency (SIT) soliton[21,22]. If one assumes a two-level medium and neglects the effect of inhomogeneous broadening, the problem can be described by a single field equation : the sine-Gordon equation, which also arose from the field theory[38]. Besides the sine-Gordon equation, the nonlinear Schrödinger equation, which is the governing equation of optical self-focusing (in one dimension) and optical self-phase-modulation with dispersion (in one dimension), was also well known at that time. So the problem that mathematicians were facing in those days (and even today) is how to solve these nonlinear equations analytically and moreover how to solve them from a unified point of view. The inverse scattering transform developed for the KdV equation seems to be a powerful method. Can it be applied to other problems ?

In 1972 (published in 1971 in the Soviet Union), Zakharov and Shabat[27] found the Lax pair for the nonlinear Schrödinger equation and carried out the solution in the framework of the inverse scattering transform. The sine-Gordon equation was solved independently by Ablowitz et al.[24] and by Lamb[23]. Soon thereafter, Ablowitz et. al.[39] were able to show how to write down the full set of equations that can be solved through the use of the Zakharov and Shabat eigenvalue problem. In this way, one can generate infinite equations that have soliton solutions. The point is that, beginning with any eigenvalue problem, any evolution equation that keep its (inverse scattering) spectrum invariant can be solved by the inverse scattering transform. It was also soon found that the self-induced transparency problem of a two-level medium *with* line-broadening also can be solved in the framework of the Zakharov-Shabat inverse scattering transform[25,26].

With the advance of technology, solitons can be actually generated. The soliton phenomenon in optical fibers is a good example. To lowest order, solitons in optical fibers are described by the nonlinear Schrödinger equation. This leads to the

prediction of their existence by Hasegawa and Tappert[1] in 1973. However, only after modelocked F-center lasers arround the wavelength of 1.55 μm became available, Mollenauer et al.[2] were able to actually generate and observe these solitons in 1980. Since then, a lot of theoretical and experimental work has been carried out. Equations with higher-order dispersion and nonlinearities have been derived and solved analytically in some special cases and numerically in most cases[40]. Some of the highe-order effects like self-frequency shift have also been been observed experimentally[41]. The coupling between the two polarizations in optical fibers brings in new effects[42]. Interesting phenomena have been found and promising applications have been proposed[43].

The development of a quantum theory of solitons can also be dated back to 60's. Two nonlinear equations attracted a lot of attention due to their simple form: the nonlinear Schrödinger equation, which is a nonrelavistic one, and the sine-Gordon equation, which is a relavistic one. Historically, the quantum nonlinear Schrödinger equation arose from a totally different research area : quantum statistical mechanics. It is the evolution equation of a one-dimensional system of bosons with δ-function interactions in the second quantization form[44]. By solving the problem in the Schrödinger picture using Bethe's ansatz method, Lieb and Linger[45], McGuire[46], and Yang[47,48] were able to construct its eigensolutions. They also found the bound state eigensolutions, which are closely related to the soliton phenomenon. Since then, mainly in the 70's, Bethe's ansatz method has been successfully applied to a number of models in statistical physics and quantum field theory[49,50], including the nonlinear Schrödinger equation as just mentioned and also the sine-Gordon equation.

Inspired by the development of classical inverse scattering transform, several groups[51–53] began to develop the quantum inverse scattering method in the the late 70's and early 80's. The quantum inverse scattering method solves the problem in the Heisenberg picture. The creation operators of the eigenstates are constructed algebraically and their commutation relations are derived. Compared to Bethe's ansatz method, the quantum inverse scattering method is definitely more complicated. However, the quantum inverse scattering method is expected to have a greater

applicability.

When we began to study the problem in 1989, we soon found that an important link between quantum and classical soliton theory is missing. That is, how the bound state solutions are related to the classical soliton phenomenon. Nohl[54] was the first one to try to answer this question. Unsatisfied with Nohl's results, Wadati[55] presented an improved theory. Although Wadati's results provide a good basis for our work, his approach is still not fully satisfactory. In our opinion, the construction of soliton states should satisfy the following three criteria:

- A soliton state should be a time-independent superposition of the bound states so that it is a solution of the governing equation.
- One should be able to construct a soliton state with the expectation value of the field operator approaching the classical soliton solution.
- The construction should be generalized to higher order soliton states to provide information about soliton collisions.

One of the achievements of the thesis is to construct soliton states that meet the three criteria listed above. The construction also enables us to study the quantum effects of soliton propagation and soliton collisions[56,57].

In 1987, Carter, Drummond and Shelby et. al.[58,59] solved the quantum nonlinear Schödinger equation numerically based on the linearization approximation. The nonlinear operator equation is linearized around the classical soliton solution. The linear operator equation obtained in this way is then Fourier-transformed into frequency space and the correlation matrix of field operators in the frequency space is calculated numerically. Using this method, they show that solitons are squeezed during propagation. In a later paper, they included the effects of detection in the calculation of squeezing ratio[60].

The linearization approach has the advantage that it reduces the quantum problem to a classical one. This is because in solving a linear equation, one does not

encounter the commutation relations *as long as they are conserved.* The commutation relations enter only when one begins to calculate the second or higher order moments of field operators. However, the numerical approach does not fully exploit the advantages of linearization since not many physical insights can be abstracted from a numerical approach. In the thesis, an analytical theory is developed based on the linearization approximation. The formulation also leads to a novel numerical method for noise analysis of soliton-like systems. Most importantly, the same linearization approach can be used to quantize and solve all the problems that can be solved by the classical inverse scattering transform. In the thesis, this is illustrated by using the SIT problem as an example.

1.3 Thesis content

The structure of the thesis is organized as follows. In Chapter 2, three approaches (linearization approximation, time-dependent Hartree approximation and exact solution based on Bethe's ansatz) are developed to solve the quantum nonlinear Schrödinger equation. The first one is a linear analysis in the Heisenberg picture while the other two are nonlinear analyses in the Schrödinger picture. Each method offers different physical insights into the problem. Especially, the linear analysis provides the basis for the remaining chapters in the thesis. Under the linearization approximation in the Heisenberg picture, a soliton is characterized by four soliton operators (photon number, phase, momentum and position) plus the continuum. Evolution of these operators is derived and the orthogonality relation between the soliton parts and the continuum are proved. On the other hand, in the Schrödinger picture, the soliton is described by the quantum state. In the thesis, we use the time-dependent Hartree approximation and the exact solution based on Bethe's ansatz to construct soliton states. Both fundamental and higher order soliton states are constructed.

In Chapter 3, soliton squeezing effects in optical fibers are studied in the framework of the linearization approximation and Hartree approximation. In light of the projection interpretation of homodyne detection, schemes for squeezing detection

are described and the optimal squeezing ratio is derived analytically. A general numerical approach for calculating squeezing ratios is then presented and applied to the study of fiber gyros using squeezed states.

In Chapter 4, we study the quantum effects of soliton propagation in optical fibers with loss and periodic amplification. When the spacing between optical amplifiers is much shorter than the soliton period, to lowest order, the nonlinear Schrödinger equation (with an additional scaling factor) still can be used to describe the propagation of solitons[61]. However, both loss and amplification introduce their own noise operators. Using the same linearization approach, the evolution equations of the soliton parameters are derived and solved. The position spreading effect is studied and the Gordon-Haus limit is derived rigorously. We also discuss the possibility of overcoming this limit.

In Chapter 5, the self-induced transparency solitons are studied. The quantization is performed in the scattering data space under the linearization approximation. The evolution of the scattering data is derived and the quantum effects of soliton propagation are studied in comparison with the nonlinear Schrödinger solitons. Especially, the concept of generalized squeezing is introduced and examined.

Finally, in Chapter 6, we summarize the achievements in the thesis and mention several possible topics for future studies.

Chapter 2

Solitons in optical fibers

In optical fibers, due to the interplay between negative dispersion and the third order nonlinearity, a class of optical pulses called solitons can propagate without changing their pulse shapes. The objective of this chapter is to develop a quantum theory of soliton propagation in loss-free optical fibers. We first review the classical theory of solitons in optical fibers. The quantum formulation of the problem is then presented and three methods (linearization approach, time-dependent Hartree approximation, and exact solution based on Bethe's ansatz) are developed to solve the quantum problem. The first method is a linear analysis in the Heisenberg picture while the latter two are nonlinear analyses in the Schrödinger picture. Each method offers different physical insights into the problem.

2.1 Classical formulation

Under the slowly varying envelope approximation, the evolution equation of a optical pulse propagating through a nonlinear optical fiber is given by[57]

$$\left[\frac{\partial}{\partial x}+\frac{1}{v_g}\frac{\partial}{\partial t}\right]A(x,t)=i\frac{1}{2}k''\frac{\partial^2}{\partial t^2}A(x,t)-i\kappa A^*(x,t)A(x,t)A(x,t) \qquad (2.1)$$

Here x is the propagation distance, t is the time, $A(x,t)$ is the field envelope of the pulse, $v_g=1/k'$ is the group velocity with k' being the first derivative of the propagation constant with respect to frequency, $k''=\partial v_g^{-1}/\partial\omega=-(\lambda^2/2\pi c)\partial v_g^{-1}/\partial\lambda$ are the second derivatives of the propagation constant with respect to frequency and $\kappa=2\pi n_2/\lambda$ expresses the magnitude of the Kerr nonlinearity. By the following change of variables,

$$\tau=\frac{t-v_g x}{t_o} \quad \text{with} \quad t_o=\frac{\text{Area}}{\hbar\omega}\frac{k''}{\kappa} \qquad (2.2)$$

$$z = \frac{x}{x_o} \quad \text{with} \quad x_o = 2(\frac{\text{Area}}{\hbar\omega})^2 \frac{k''}{\kappa^2} \tag{2.3}$$

$$U = -\text{sign}(k'')\frac{A}{A_o} \quad \text{with} \quad A_o = \frac{\hbar\omega}{\text{Area}}\sqrt{\frac{\kappa}{k''}} \tag{2.4}$$

one can reduce Eq.(2.1) into the following classical nonlinear Schrödinger equation (CNSE) :

$$i\frac{\partial}{\partial z}U(z,\tau) = -\frac{\partial^2}{\partial\tau^2}U(z,\tau) + 2cU^*(z,\tau)U(z,\tau)U(z,\tau) \tag{2.5}$$

Here z is the normalized propagation distance, τ is the normalized time deviation, U is the normalized field amplitude, Area is the effective cross section of the propagating mode and ω is the carrier frequency. The normalization units are chosen in such a way that : (1) the coefficient of the second order derivative term is -1, (2) $c = 1$ in the positive dispersion region and $c = -1$ in the negative dispersion region, and (3) $U(z,\tau)$ represents the photon flux at (z,τ) or, in other words, $\int |U(z,\tau)|^2 d\tau$ is the photon number in the pulse. Since we only have three adjustable normalization parameters, the normalization that satisfies the above three criteria is unique. The normalization units are also given in Eq.(2.2-4). As a numerical example, if one assumes $\lambda = 1.55\mu m$, $\partial v_g^{-1}/\partial\lambda = 3(ps/nm)/km$, $n_2 = 3.18\times10^{-16}cm^2/W$ and Area $= 5\mu m^2$, then $t_o = 1.15\times10^{-6}sec$, $x_o = 4.0\times10^{12}km$ and $A_o = 1.5\times10^{-3}\sqrt{W}/cm$. Although $|c| = 1$ after normalization, we still keep it in the formulation to label the effect of nonlinearity.

The CNSE has been solved analytically by the inverse scattering transform of Zakharov-Shabat[27]. The solution has the following interesting properties :

1. In the negative dispersion region ($c < 0$), it has (bright) soliton solutions (or bound solutions). The fundamental soliton solution is given by :

$$\begin{aligned} U_o(z,\tau) &= \frac{n_o|c|^{1/2}}{2}\exp[ip_o\tau + i\theta(z)] \\ &\quad \text{sech}[\frac{n_o|c|}{2}(\tau - T(z))] \end{aligned} \tag{2.6}$$

with

$$\theta(z) = \theta_o + \frac{n_o^2|c|^2}{4}z - p_o^2 z \tag{2.7}$$

$$T(z) = T_o + 2p_o z \tag{2.8}$$

Here n_o, θ_o, p_o and T_o are four free parameters that characterize a fundamental soliton. They correspond respectively to the photon number, initial phase, momentum (frequency) and initial position of the soliton. Equation (2.7) and (2.8) show the evolution of the phase and position of the soliton as a function of z. In contrast, the photon number and momentum of a soliton do not change during propagation. Following the terminology of inverse scattering transform, $n_o, \theta(z), p_o$ and $T(z)$ will be refered as the soliton parts of the scattering data.

2. Beside soliton solutions, the CNSE also has unbound solutions (the continuum). Figure 1 shows the evolution of a rectangular pulse in an optical fiber. One can clearly see that the continuum parts quickly disperse away and eventually only the soliton parts are left.

3. After two solitons collide, the photon number (and thus the shape) and momenta of each soliton are maintained. The collision simply introduces a time delay and a phase shift to each soliton. If n_1, p_1 and n_2, p_2 are the photon numbers and momentums of two solitons, then the magnitudes of these shifts for the soliton with n_1 photons is given by[27]:

$$\delta\theta_1(n_1, p_1, n_2, p_2) = -2\{\tan^{-1}[\frac{\frac{1}{2}|c|(n_1+n_2)}{p_2-p_1}] - \tan^{-1}[\frac{\frac{1}{2}|c|(n_2-n_1)}{(p_2-p_1)}]\} \tag{2.9}$$

$$\begin{aligned}\delta T_1(n_1, p_1, n_2, p_2) &= \frac{2}{n_1|c|}\{\ln[(p_2-p_1)^2 + \frac{|c|^2}{4}(n_2-n_1)^2] \\ &\quad -\ln[(p_2-p_1)^2 + \frac{|c|^2}{4}(n_2+n_1)^2]\}\end{aligned} \tag{2.10}$$

Expressions for the shifts of the other soliton are analogous.

From the correspondence principle, one would expect these classical results should also arise from the quantum theory. This provides a test for the quantum soliton theory we are going to develop.

2.2 Quantum formulation

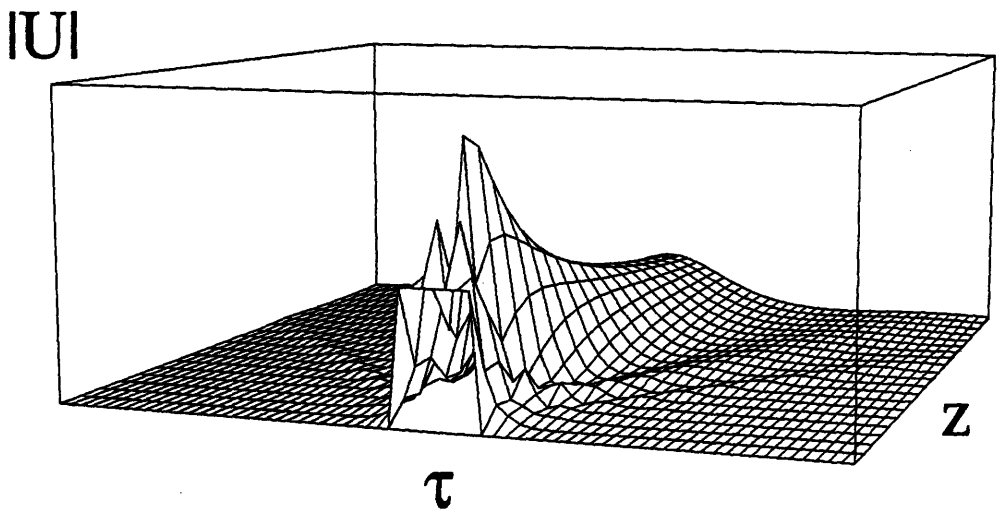

Figure 1 : Evolution of a rectangular pulse in a optical fiber

In quantum theory, field amplitude functions U and U^* become field amplitude operators $\hat{U}$ and $\hat{U}^\dagger$. Since photons are bosons, $\hat{U}$ and $\hat{U}^\dagger$ should obey the following commutation relations :

$$[\hat{U}(z,\tau'),\hat{U}^\dagger(z,\tau)] = \delta(\tau-\tau') \tag{2.11}$$

$$[\hat{U}(z,\tau'),\hat{U}(z,\tau)] = [\hat{U}^\dagger(z,\tau'),\hat{U}^\dagger(z,\tau)] = 0 \tag{2.12}$$

In writing commutation relations like these, $\hat{U}(z,\tau)$ and $\hat{U}^\dagger(z,\tau)$ are also the annilhilation and creation operators of photons at (z,τ), which is consistent with our normalization. Also note that we have chosen to use "equal space" commutation relations instead of the usually used "equal time" commutation relations because it is easier to quantize a traveling wave problem using "equal space" commutation relations.

In the quantum theory, the CNSE becomes the QNSE :

$$i\frac{\partial}{\partial z}\hat{U}(z,\tau) = -\frac{\partial^2}{\partial\tau^2}\hat{U}(z,\tau) + 2c\hat{U}^\dagger(z,\tau)\hat{U}(z,\tau)\hat{U}(z,\tau) \tag{2.13}$$

This is an operator equation in the Heisenberg picture and can be derived from the following Hamiltonian:

$$\hat{H} = [\int \frac{\partial}{\partial\tau}\hat{U}^\dagger(z,\tau)\frac{\partial}{\partial\tau}\hat{U}(z,\tau)d\tau + c\int \hat{U}^\dagger(z,\tau)\hat{U}^\dagger(z,\tau)\hat{U}(z,\tau)\hat{U}(z,\tau)d\tau] \tag{2.14}$$

In the Heisenberg picture, the evolution equation of the operator $\hat{U}$ is given by:

$$i\frac{d}{dz}\hat{U}(z,\tau) = [\hat{U}(z,\tau),\hat{H}] \tag{2.15}$$

Substituting (2.14) into (2.15) and using (2.11)-(2.12) to simplify the expression, the QNSE [(2.13)] is obtained.

The same problem also can be formulated in the Schrödinger picture. Starting from the Hamiltonian in the Schrödinger picture,

$$\hat{H}_s = [\int \frac{\partial}{\partial\tau}\hat{U}^\dagger(\tau)\frac{\partial}{\partial\tau}\hat{U}(\tau)d\tau + c\int \hat{U}^\dagger(\tau)\hat{U}^\dagger(\tau)\hat{U}(\tau)\hat{U}(\tau)d\tau] \tag{2.16}$$

the evolution equation of the quantum state of the system is

$$i\frac{d}{dz}|\psi\rangle = \hat{H}_s|\psi\rangle \tag{2.17}$$

Here $\hat{U}(\tau)$ and $\hat{U}^\dagger(\tau)$ are field operators in the Schrödinger picture and satisfy the following commutation relations :

$$[\hat{U}(\tau'), \hat{U}^\dagger(\tau)] = \delta(\tau - \tau') \tag{2.18}$$

$$[\hat{U}(\tau'), \hat{U}(\tau)] = [\hat{U}^\dagger(\tau'), \hat{U}^\dagger(\tau)] = 0 \tag{2.19}$$

Up to this point, it is interesting to note that although in the Heisenberg picture one has a nonlinear equation, the equation is linear in the Schödinger picture. However, in the Schrödinger picture, the problem is in fact a many-body problem. To show this, one notes that any quantum state of the system can be expanded in Fock space as follows :

$$|\psi\rangle = \sum_n a_n \int \frac{1}{\sqrt{n!}} f_n(\tau_1, \ldots \tau_n, z) \hat{U}^\dagger(\tau_1) \ldots \hat{U}^\dagger(\tau_n) d\tau_1 \ldots d\tau_n |0\rangle \tag{2.20}$$

The state $|\psi\rangle$ is a superposition of states produced from the vacuum state by creating photons at the points $\tau_1, \tau_2 \ldots \tau_n$ with the weighting functions f_n. Since photons are bosons, f_n should be a symmetric function of τ_j. We require a_n and f_n to satisfy the following normalization conditions so that $\langle\psi|\psi\rangle = 1$.

$$\sum_n |a_n|^2 = 1 \tag{2.21}$$

$$\int |f_n(\tau_1 \ldots \tau_n, z)|^2 d\tau_1 \ldots d\tau_n = 1 \tag{2.22}$$

Substituting Eq.(2.16) and (2.20) into (2.17) and using Eq.(2.18) and (2.19), we obtain an equation for $f_n(\tau_1 \ldots \tau_n, z)$:

$$i\frac{d}{dz} f_n(\tau_1 \ldots \tau_n, z) = \Big[-\sum_{j=1}^{n} \frac{\partial^2}{\partial \tau_j^2} + 2c \sum_{1 \le i < j \le n} \delta(\tau_j - \tau_i) \Big] f_n(\tau_1 \ldots \tau_n, z) \tag{2.23}$$

This is just the Schrödinger equation for a one-dimensional system of bosons with delta-function interactions[45–48].

2.3 Linearization approximation in the Heisenberg picture

In this section, we solve the QNSE under the linearization approximation in the Heisenberg picture. We are going to linearize the equation around the fundamental soliton solution and solve the linearized equation to study the evolution of quantum fluctuations. Our starting point is the QNSE [Eq.(2.13)]. From section 1 of this chapter, we know Eq.(2.13) has classical fundamental soliton solution $U_o(z,\tau)$ given by Eq.(2.6). Without loss of generality, *from now on we will always assume* $\theta_o = p_o = T_o = 0$. This simply means we choose the coordinate system that moves along with the soliton pulse center and choose the phase reference that follows the soliton phase. By doing so, the pulse shape is independent of z and the phase is independent of τ.

In the Heisenberg picture, if one linearizes Eq.(2.13) by substituting

$$\hat{U}(z,\tau) = [|U_o(0,\tau)| + \hat{u}(z,\tau)]\exp[i\frac{n_o^2|c|^2}{4}z] \tag{2.24}$$

into Eq.(2.13) and ignoring all the higher order terms of $\hat{u}(z,\tau)$, one has the following linear equation :

$$\begin{aligned} \frac{\partial}{\partial z}\hat{u}(z,\tau) &= i[\frac{\partial^2}{\partial\tau^2} - \frac{n_o^2|c|^2}{4} + 4|c||U_o(0,\tau)|^2]\hat{u}(z,\tau) \\ &\quad +i2|c||U_o(0,\tau)|^2\hat{u}^\dagger(z,\tau) \end{aligned} \tag{2.25}$$

Here $\hat{u}(z,\tau)$ is the perturbation field operator that satisfy the following commuation relations :

$$[\hat{u}(z,\tau),\hat{u}^\dagger(z,\tau')] = \delta(\tau-\tau') \tag{2.26}$$

$$[\hat{u}(z,\tau),\hat{u}(z,\tau')] = [\hat{u}^\dagger(z,\tau),\hat{u}^\dagger(z,\tau')] = 0 \tag{2.27}$$

By separating the real and imaginary parts, Eq.(2.25) can be considered as two coupled differential equations. Written in a vector form, one has

$$\frac{\partial}{\partial z}\hat{\mathbf{u}}(z,\tau) = \mathbf{P}\hat{\mathbf{u}}(z,\tau) \tag{2.28}$$

with

$$\hat{\mathbf{u}} = \begin{bmatrix} \hat{u}_1 \\ \hat{u}_2 \end{bmatrix} \tag{2.29}$$

$$\mathbf{P} = \begin{bmatrix} 0 & -P_1 \\ P_2 & 0 \end{bmatrix} \tag{2.30}$$

$$P_1 = \frac{\partial^2}{\partial\tau^2} - \frac{n_o^2|c|^2}{4} + 2|c||U_o(0,\tau)|^2 \tag{2.31}$$

$$P_2 = \frac{\partial^2}{\partial\tau^2} - \frac{n_o^2|c|^2}{4} + 6|c||U_o(0,\tau)|^2 \tag{2.32}$$

Here $\hat{u}_1$ and $\hat{u}_2$ are the real and imaginary parts of $\hat{u}$.

By eliminating either $\hat{u}_1$ or $\hat{u}_2$ from Eq.(2.28), one obtains the equations for $\hat{u}_1$ and $\hat{u}_2$.

$$\frac{\partial^2}{\partial z^2}\hat{u}_1(z,\tau) = -P_1P_2\hat{u}_1(z,\tau) \tag{2.33}$$

$$\frac{\partial^2}{\partial z^2}\hat{u}_2(z,\tau) = -P_2P_1\hat{u}_2(z,\tau) \tag{2.34}$$

Since P_1 and P_2 do not commute with each other, equations (2.33) and (2.34) are not the same. This suggests one should expand $\hat{u}_1$ and $\hat{u}_2$ in terms of different basis sets : $\hat{u}_1$ in terms of the eigenstates of P_1P_2 and $\hat{u}_2$ in terms of the eigenstates of P_2P_1. Before proceeding to do the expansion, it is important to make the following observations:

1. One should distinguish the eigenstates with the zero eigenvalue and the eigenstates with a nonzero eigenvalue. The former are soliton excitations that travel with the soliton while the latter are the continuum excitation. The eigenstates with the zero eigenvalue are bound states (i.e., they vanish when $|\tau|$ goes to infinity) while the eigenstates with a nonzero eigenvalue are not bound states.

2. The soliton excitations can be easily obtained by perturbing the classical soliton solution Eq.(2.6) with z set to zero. The results are :

$$f_n(\tau) \equiv \frac{\partial U_o(0,\tau)}{\partial n_o} = [\frac{1}{n_o} - \frac{|c|}{2}\tau\tanh(\frac{n_o|c|}{2}\tau)]U_o(0,\tau) \tag{2.35}$$

$$f_\theta(\tau) \equiv \frac{1}{i}\frac{\partial U_o(0,\tau)}{\partial \theta_o} = U_o(0,\tau) \tag{2.36}$$

$$f_p(\tau) \equiv \frac{1}{i}\frac{\partial U_o(0,\tau)}{\partial p_o} = \tau U_o(0,\tau) \tag{2.37}$$

$$f_T(\tau) \equiv \frac{\partial U_o(0,\tau)}{\partial \tau_o} = [\frac{n_o|c|}{2}\tanh(\frac{n_o|c|}{2}\tau)]U_o(0,\tau) \tag{2.38}$$

The four functions are plotted in Fig. 2.

It is easy to prove the following relations:

$$P_1 f_\theta(\tau) = 0 \tag{2.39}$$

$$P_2 f_T(\tau) = 0 \tag{2.40}$$

$$P_2 f_n(\tau) = \frac{n_o|c|^2}{2} f_\theta(\tau) \tag{2.41}$$

$$P_1 f_p(\tau) = 2 f_T(\tau) \tag{2.42}$$

Therefore, f_n and f_T are really eigenstates of P_1P_2 with a zero eigenvalue while f_θ and f_p are eigenstates of P_2P_1 with a zero eigenvalue. Also note that f_n, f_θ are even functions while f_p, f_T are odd functions.

3. Since

$$\mathbf{P}^2 = -\begin{bmatrix} P_1P_2 & 0 \\ 0 & P_2P_1 \end{bmatrix} \tag{2.43}$$

The expansion we just proposed is equivalent to expand $\hat{\mathbf{u}}(z,\tau)$ in terms of the eigenstates of $\mathbf{P}^2$. Therefore, if one defines

$$\mathbf{f_n}(\tau) \equiv \begin{bmatrix} f_n(\tau) \\ 0 \end{bmatrix} \tag{2.44}$$

$$\mathbf{f}_\theta(\tau) \equiv \begin{bmatrix} 0 \\ f_\theta(\tau) \end{bmatrix} \tag{2.45}$$

$$\mathbf{f_p}(\tau) \equiv \begin{bmatrix} 0 \\ f_p(\tau) \end{bmatrix} \tag{2.46}$$

$$\mathbf{f_T}(\tau) \equiv \begin{bmatrix} f_T(\tau) \\ 0 \end{bmatrix} \tag{2.47}$$

then $\mathbf{f_n}$, $\mathbf{f}_\theta$, $\mathbf{f_p}$ and $\mathbf{f_T}$ are eigenstates of $\mathbf{P^2}$ with the zero eigenvalue.

4. Under the following usual definition of inner product

$$\langle \mathbf{f}(\tau)|\mathbf{g}(\tau)\rangle \equiv \int [f_1(\tau)g_1(\tau) + f_2(\tau)g_2(\tau)]d\tau \tag{2.48}$$

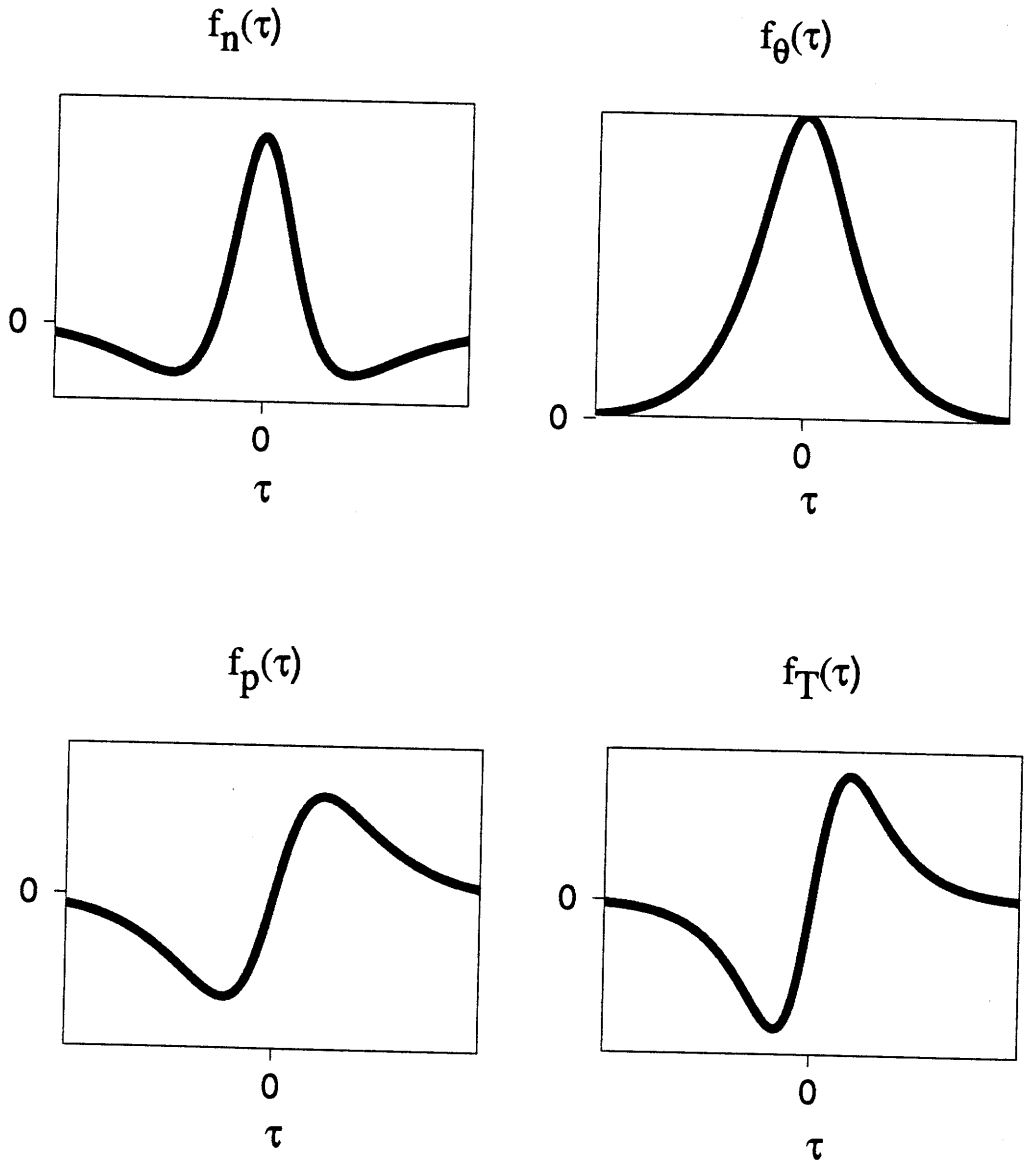

Figure 2: Pulse shapes of soliton excitations

the adjoint operator of $\mathbf{P}$ defined by

$$\langle \mathbf{f}(\tau) | \mathbf{P}\mathbf{g}(\tau) \rangle = \langle \mathbf{P}^{\mathbf{A}}\mathbf{f}(\tau) | \mathbf{g}(\tau) \rangle \tag{2.49}$$

is given by

$$\mathbf{P}^{\mathbf{A}} = \begin{bmatrix} 0 & P_2 \\ -P_1 & 0 \end{bmatrix} \tag{2.50}$$

Also note that

$$(\mathbf{P}^{\mathbf{A}})^2 = -\begin{bmatrix} P_2P_1 & 0 \\ 0 & P_1P_2 \end{bmatrix} \tag{2.51}$$

5. If $\mathbf{f}$ is an eigenfunction of $\mathbf{P}^2$, then $\mathbf{Pf}$ is also an eigenfunction of $\mathbf{P}^2$ with the same eigenvalue. Similiarly, if $\underline{\mathbf{f}}$ is an eigenfunction of $(\mathbf{P}^{\mathbf{A}})^2$, then $\mathbf{P}^{\mathbf{A}}\underline{\mathbf{f}}$ is also an eigenfunction of $(\mathbf{P}^{\mathbf{A}})^2$ with the same eigenvalue. Here we have used underlines to denote eigenfuctions of the adjoint operator $\mathbf{P}^{\mathbf{A}}$.

6. Comparing (2.51) with (2.43), it is easy to show that if $\mathbf{f}$ is an eigenfunction of $\mathbf{P}^2$ and

$$\mathbf{S} = \begin{bmatrix} 0 & 1 \\ 1 & 0 \end{bmatrix} \tag{2.52}$$

then $\mathbf{Sf}$ is an eigenfunction of $(\mathbf{P}^{\mathbf{A}})^2$ with the same eigenvalue. Therefore, if one defines

$$\underline{\mathbf{f}}_{\mathbf{n}}(\tau) \equiv \mathbf{S}\mathbf{f}_\theta(\tau) = \begin{bmatrix} f_\theta(\tau) \\ 0 \end{bmatrix} \tag{2.53}$$

$$\underline{\mathbf{f}}_{\theta}(\tau) \equiv \mathbf{S}\mathbf{f}_{\mathbf{n}}(\tau) = \begin{bmatrix} 0 \\ f_n(\tau) \end{bmatrix} \tag{2.54}$$

$$\underline{\mathbf{f}}_{\mathbf{p}}(\tau) \equiv \mathbf{S}\mathbf{f}_{\mathbf{T}}(\tau) = \begin{bmatrix} f_T(\tau) \\ 0 \end{bmatrix} \tag{2.55}$$

$$\underline{\mathbf{f}}_{\mathbf{T}}(\tau) \equiv \mathbf{S}\mathbf{f}_{\mathbf{p}}(\tau) = \begin{bmatrix} 0 \\ f_p(\tau) \end{bmatrix} \tag{2.56}$$

then $\underline{\mathbf{f}}_{\mathbf{n}}$, $\underline{\mathbf{f}}_{\theta}$, $\underline{\mathbf{f}}_{\mathbf{p}}$ and $\underline{\mathbf{f}}_{\mathbf{T}}$ are eigenstates of $(\mathbf{P}^{\mathbf{A}})^2$ with the zero eigenvalue. The reason for defining $\underline{\mathbf{f}}_{\mathbf{n}} \equiv \mathbf{S}\mathbf{f}_\theta$ instead of $\underline{\mathbf{f}}_{\mathbf{n}} \equiv \mathbf{S}\mathbf{f}_{\mathbf{n}}$ will become clear very soon [see Eq.(2.57-59)].

7. *Mutual orthogonality*: If $\mathbf{f}$ is an eigenfunction of $\mathbf{P^2}$ and $\underline{\mathbf{f}}$ is an eigenfunction of $(\mathbf{P^A})^2$, then they are orthogonal to each other if their eigenvalues are different. Here the orthogonality is defined in terms of the inner product projection. A consequence of the orthogonality relations is that all the four vectors $\underline{\mathbf{f}}_\mathbf{n}$, $\underline{\mathbf{f}}_\theta$, $\underline{\mathbf{f}}_\mathbf{p}$ and $\underline{\mathbf{f}}_\mathbf{T}$ are orthogonal to the continuum of $\mathbf{P^2}$. Moreover, if $k, l = n, \theta, p, T$, then

$$\langle \underline{\mathbf{f}}_\mathbf{k}(\tau) | \mathbf{f}_\mathbf{l}(\tau) \rangle = 0 \quad \text{if} k \neq l \tag{2.57}$$

and

$$\langle \underline{\mathbf{f}}_\mathbf{n}(\tau) | \mathbf{f}_\mathbf{n}(\tau) \rangle = \langle \underline{\mathbf{f}}_\theta(\tau) | \mathbf{f}_\theta(\tau) \rangle = \frac{1}{2} \tag{2.58}$$

$$\langle \underline{\mathbf{f}}_\mathbf{p}(\tau) | \mathbf{f}_\mathbf{p}(\tau) \rangle = \langle \underline{\mathbf{f}}_\mathbf{T}(\tau) | \mathbf{f}_\mathbf{T}(\tau) \rangle = \frac{n_o}{2} \tag{2.59}$$

With all these observations in mind, the expansion can then be written (in a vector form) as

$$\begin{aligned} \hat{\mathbf{u}}(z,\tau) \;=\; & \Delta\hat{n}(z)\mathbf{f}_\mathbf{n}(\tau) + \Delta\hat{T}(z)\mathbf{f}_\mathbf{T}(\tau) + \Delta\hat{\theta}(z)\mathbf{f}_\theta(\tau) + \Delta\hat{p}(z)\mathbf{f}_\mathbf{p}(\tau) \\ & + \text{the continuum} \end{aligned} \tag{2.60}$$

The expansion coefficients $\Delta\hat{n}(z)$, $\Delta\hat{\theta}(t)$, $\Delta\hat{p}(z)$ and $\Delta\hat{T}(z)$ in Eq.(2.60) represent the quantum parts of photon number, phase, momentum and position of the soliton. Since we are only interested in the soliton part, we did not write down the continuum part explicitly in Eq.(2.60). Nevertheless, their analytical expressions can be found in Ref.[77].

$\Delta\hat{n}(z)$, $\Delta\hat{\theta}(t)$, $\Delta\hat{p}(z)$ and $\Delta\hat{T}(z)$ can be determined from $\delta\hat{\mathbf{u}}(z,\tau)$ by projections:

$$\Delta\hat{n}(z) = \frac{\langle \underline{\mathbf{f}}_\mathbf{n}(\tau) | \hat{\mathbf{u}}(z,\tau) \rangle}{\langle \underline{\mathbf{f}}_\mathbf{n}(\tau) | \mathbf{f}_\mathbf{n}(\tau) \rangle} = 2\langle \underline{\mathbf{f}}_\mathbf{n}(\tau) | \hat{\mathbf{u}}(z,\tau) \rangle \tag{2.61}$$

$$\Delta\hat{\theta}(z) = \frac{\langle \underline{\mathbf{f}}_\theta(\tau) | \hat{\mathbf{u}}(z,\tau) \rangle}{\langle \underline{\mathbf{f}}_\theta(\tau) | \mathbf{f}_\theta(\tau) \rangle} = 2\langle \underline{\mathbf{f}}_\theta(\tau) | \hat{\mathbf{u}}(z,\tau) \rangle \tag{2.62}$$

$$\Delta\hat{p}(z) = \frac{\langle \underline{\mathbf{f}}_\mathbf{p}(\tau) | \hat{\mathbf{u}}(z,\tau) \rangle}{\langle \underline{\mathbf{f}}_\mathbf{p}(\tau) | \mathbf{f}_\mathbf{p}(\tau) \rangle} = \frac{2}{n_o}\langle \underline{\mathbf{f}}_\mathbf{p}(\tau) | \hat{\mathbf{u}}(z,\tau) \rangle \tag{2.63}$$

$$\Delta\hat{T}(z) = \frac{\langle \underline{\mathbf{f}}_\mathbf{T}(\tau) | \hat{\mathbf{u}}(z,\tau) \rangle}{\langle \underline{\mathbf{f}}_\mathbf{T}(\tau) | \mathbf{f}_\mathbf{T}(\tau) \rangle} = \frac{2}{n_o}\langle \underline{\mathbf{f}}_\mathbf{T}(\tau) | \hat{\mathbf{u}}(z,\tau) \rangle \tag{2.64}$$

These are the consequences of the mutual orthogonality.

Substituting the expansion (2.60) into (2.28) and using Eq.(2.39)-(2.42) and Eq.(2.61)-(2.64), one obtains the evolution equations of the four soliton operators :

$$\frac{d}{dz}\Delta\hat{n}(z) = 0 \tag{2.65}$$

$$\frac{d}{dz}\Delta\hat{\theta}(z) = \frac{n_o|c|^2}{2}\Delta\hat{n}(z) \tag{2.66}$$

$$\frac{d}{dz}\Delta\hat{p}(z) = 0 \tag{2.67}$$

$$\frac{d}{dz}\Delta\hat{T}(z) = 2\Delta\hat{p}(z) \tag{2.68}$$

The solutions are :

$$\Delta\hat{n}(z) = \Delta\hat{n}(0) \tag{2.69}$$

$$\Delta\hat{\theta}(z) = \Delta\hat{\theta}(0) + \frac{n_o|c|^2}{2}z\Delta\hat{n}(0) \tag{2.70}$$

$$\Delta\hat{p}(z) = \Delta\hat{p}(0) \tag{2.71}$$

$$\Delta\hat{T}(z) = \Delta\hat{T}(0) + 2z\Delta\hat{p}(0) \tag{2.72}$$

The photon number and momentum fluctuations do not change but they cause the spreading of the phase and position. Equations (2.69)-(2.72) also can be obtained directly from perturbing the classical evolution equations from the inverse scattering transform.

From Eq.(2.61)-(2.64), one can easily prove that the four operators obey the usual commutation relations of photon number, phase, position and momentum[63].

$$[\Delta\hat{n}(z), \Delta\hat{\theta}(z)] = i \tag{2.73}$$

$$[\Delta\hat{T}(z), n_o\Delta\hat{p}(z)] = i \tag{2.74}$$

This proves our interpretation of their physical meaning is self-consistent.

If one assumes the quantum state represented by $\hat{u}(0,\tau)$ is the vacuum state, then the variances of these operators at $z = 0$ can be calculated from Eq.(2.61)-(2.64). The results are found to be

$$\langle\Delta\hat{n}^2(0)\rangle = n_o \tag{2.75}$$

$$\langle \Delta\hat{\theta}^2(0) \rangle = \frac{1}{3}[1 + \frac{\pi^2}{12}]\frac{1}{n_o} \approx \frac{0.607}{n_o} \tag{2.76}$$

$$\langle \Delta\hat{p}^2(0) \rangle = \frac{n_o|c|^2}{12} \tag{2.77}$$

$$\langle \Delta\hat{T}^2(0) \rangle = \frac{\pi^2}{3}\frac{1}{n_o^3|c|^2} \approx \frac{3.29}{n_o^3|c|^2} \tag{2.78}$$

It is interesting to note that

$$\langle \Delta\hat{n}^2(0) \rangle \times \langle \Delta\hat{\theta}^2(0) \rangle \approx 0.607 > 0.25 \tag{2.79}$$

$$n_o^2\langle \Delta\hat{p}^2(0) \rangle \times \langle \Delta\hat{T}^2(0) \rangle \approx 0.27 > 0.25 \tag{2.80}$$

We have thus found that a "vacuum fluctuation" excitation of the perturbations does not give a minimum uncertainty state. This is in contrast with the case of a coherent state associated with a sinusoidal steady state which, when linearized, can be viewed as a sinusoid with "vacuum fluctuations". The reason for this state of affairs is that different operators are "projected out" by functions of different shapes. Under these conditions, the operators operating on vacuum do not yield vectors in Hilbert space that are related to each other by an imaginary multiplier as required for a minimum uncertainty state.

The evolution of these variances also can be derived easily.

$$\langle \Delta\hat{n}^2(z) \rangle = n_o \tag{2.81}$$

$$\langle \Delta\hat{\theta}^2(z) \rangle = \frac{0.607}{n_o} + \frac{n_o^3|c|^4}{4}z^2 \tag{2.82}$$

$$\langle \Delta\hat{p}^2(z) \rangle = \frac{n_o|c|^2}{12} \tag{2.83}$$

$$\langle \Delta\hat{T}^2(z) \rangle = \frac{3.29}{n_o^3|c|^2} + \frac{n_o|c|^2}{3}z^2 \tag{2.84}$$

From these equations, one can estimate quantitatively the phase and position spreading. It is also obvious that the phase spreading effect is much stronger than the position spreading effect.

The coupling between photon number and phase also produces squeezing. We shall study this squeezing effect in next chapter.

2.4 Time dependent Hartree approximation in the Schrödinger picture

In this section we present a (nonlinear) approximate analysis by the time-dependent Hartree approximation[64,56]. This approach was first introduced by Yoon and Negele[64] to the study of one-dimensional bosons with δ-function interaction. By following this approach, we construct approximate fundamental and higher-order soliton states[56].

2.4.1 Construction of fundamental soliton states

In this subsections, we switch to the Schrödinger picture and construct fundamental soliton states using the time dependent Hartree approximation. Our starting point is Eq. (2.23). The Hartree approximation is valid when the number of bosons is large. Its basic assumption is that every particle sees the same potential caused by the interaction with other particles. Therefore, we can use a single particle wavefunction to describe a system of particles. To be explicit, we define a Hartree wavefunction by the following Ansatz:

$$f_n^{(H)}(\tau_1, \ldots \tau_n, z) = \Pi_{j=1}^n \Phi_n(\tau_j, z) \tag{2.85}$$

with

$$\int |\Phi_n(\tau, z)|^2 d\tau = 1 \tag{2.86}$$

The functions Φ_n are to be determined by minimizing the following functional:

$$\begin{aligned} I &= \int f_n^{*(H)}(\tau_1, \ldots \tau_n, z)[i\frac{\partial}{\partial z} + \sum_{j=1}^n \frac{\partial^2}{\partial \tau_j^2} \\ &\quad -2c\textstyle\sum_{1\le i<j\le n} \delta(\tau_j - \tau_i)] f_n^{(H)}(\tau_1 \ldots \tau_n, z) d\tau_1 \ldots d\tau_n \\ &= n \int \Phi_n^*[i\tfrac{\partial}{\partial z}\Phi_n + \tfrac{\partial^2}{\partial \tau^2}\Phi_n - (n-1)c\Phi_n^*\Phi_n\Phi_n] d\tau \end{aligned} \tag{2.87}$$

It turns out that the above functional reaches its minimum value if Φ_n obeys the classical nonlinear Schrödinger equation with the nonlinearity scaled by $n-1$.[64]

$$i\frac{\partial}{\partial z}\Phi_n = -\frac{\partial^2}{\partial \tau^2}\Phi_n + 2(n-1)c\Phi_n^*\Phi_n\Phi_n \tag{2.88}$$

This fact is one of the connections between quantum theory and classical theory.

Equation (2.88) under the constraint (2.86) has the following fundamental soliton solution:

$$\begin{aligned}\Phi_{np} &= \tfrac{\sqrt{n-1}}{2}|c|^{1/2}\exp\left[i\tfrac{(n-1)^2}{4}|c|^2 z - ip^2 z + ip\tau + i\theta_o\right] \\ &\quad \times \mathrm{sech}[\tfrac{(n-1)}{2}|c|(\tau - T_o - 2pz)]\end{aligned} \tag{2.89}$$

With Eq.(2.85) and (2.89), the Hartree product eigenstate is given by

$$|n,p,z\rangle_H = \frac{1}{\sqrt{n!}}[\int \Phi_{np}(\tau,z)\hat{U}^\dagger(\tau)d\tau]^n|0\rangle \tag{2.90}$$

Since $|n,p,z\rangle_H$ is an eigenstate of the photon number operator, *in order to have a classical phase, one needs to superimpose these eigenstates over n.* Following the construction of a coherent state in the CW case, a superposition of these eigenstates using a Poissonian distribution of n gives the fundamental soliton state

$$\begin{aligned}|\psi_s\rangle_H &= \textstyle\sum_n \frac{\alpha_o^n}{\sqrt{n!}}e^{-\frac{1}{2}|\alpha_o|^2}|n,p,z\rangle_H \\ &= \textstyle\sum_n \frac{\alpha_o^n}{n!}e^{-\frac{1}{2}|\alpha_o|^2}[\int \Phi_{np}(\tau,z)\hat{U}^\dagger(\tau)d\tau]^n|0\rangle\end{aligned} \tag{2.91}$$

From (2.91), the mean field can be easily calculated:

$$\begin{aligned}{}_H\langle\psi_s|\hat{U}(\tau)|\psi_s\rangle_H &\approx \textstyle\sum_n e^{-|\alpha_o|^2}\frac{|\alpha_o|^{2n}}{n!}\frac{\alpha_o\sqrt{n}}{2}|c|^{1/2}\exp\left[i\frac{n^2}{4}|c|^2 z - ip^2 z + ip\tau + i\theta_o\right] \\ &\quad \times \mathrm{sech}[\tfrac{n}{2}|c|(\tau - T_o - 2pz)]\end{aligned} \tag{2.92}$$

In deriving (2.92), we have used the following approximation :

$$\int \Phi^*_{np}(\tau,z)\Phi_{(n+1)p}(\tau,z)d\tau \approx 1 \tag{2.93}$$

This is a very good approximation as long as the mean photon number is large enough.

Equation (2.92) makes a very important statement. The expectation value of the field is the average of a set of classical solitons. This is a surprising result, because the field propagates in a nonlinear medium, and hence a simple superposition of solutions as the expectation value of the field was not anticipated. Since in Eq.(2.92),

components of different n's have different phase velocities, a soliton experiences phase spreading when it propagates (we have seen this in the linearization approach).

Note that we have used a single value of the "momentum" p, not a superposition. However, $|n, p, z\rangle_H$ is not an eigenstate of the momentum operator $\hat{p}$ and thus a distribution of momenta is in fact associated with the state. In next section, we shall find that a distribution of momenta is necessary to construct a soliton state. Moreover, the Hartree approximation predicts phase spreading due to the selfphase modulation effect. We know that the selfphase modulation effect is caused by the uncertainty of photon number. One may expect that the uncertainty of momentum should cause a dispersion effect of its own, as we have seen in the linearization approach. This dispersion effect is lost under the Hartree approximation and will show up in the exact analysis of the next section.

Also note that the time-dependent Hartree approximation also allows one to study the initial value problem. That is, given an initial wavefunction, one can solve Eq.(2.88) numerically or perturbationally and thus obtains the evolution of the quantum state. This approach has been recently taken by E. M. Wright[74] and was shown to give good results.

2.4.2 Construction of higher order soliton states

In this subsection we use the Hartree approximation to construct two-soliton states and study soliton collision effects[56]. The construction is not as straightforward as that of the fundamental soliton states in the last section because the two-soliton states in collision and two-soliton states not in collision have to be treated differently. When a two-soliton state is in collision, all the photons occupy the same space and interact. Every photon behaves in the same way and therefore has the same wavefunction. However, when a two-soliton state is not in collision, it consists of two independent groups of photons. Photons in different groups behave differently and therefore have different wavefunctions although photons in the same group still interact and can be assumed to have the same wavefunction. Based on the above argument, we construct a two-soliton state that has $n = n_1 + n_2$ photons

with n_1 and n_2 photons bound together respectively. We can assume that the total wavefunction is

$$f^{(c)}_{n_1 n_2}(\tau_1, \ldots \tau_{n_1+n_2}, z) = \Pi_{j=1}^{n_1+n_2} \Phi_{n_1 n_2}(\tau_j, z) \tag{2.94}$$

in collision and

$$f^{(o)}_{n_1 n_2}(\tau_1, \ldots \tau_{n_1+n_2}, t) = \sum_{\{Q\}} \Pi_{j=1}^{n_1} \Phi^{(1)}_{n_1}(\tau_{Q(j)}, z) \Pi_{j=n_1+1}^{n_1+n_2} \Phi^{(2)}_{n_2}(\tau_{Q(j)}, z) \tag{2.95}$$

not in collision. In the latter expansion the summation is over Q, over all possible permutations of $[1, 2, \ldots n_1 + n_2]$ with the grouping of photons into $[1, 2, \ldots n_1]$ and $[n_1 + 1, n_1 + 2, \ldots n_1 + n_2]$ unchanged. The summation appears because $f^{(o)}_{n_1 n_2}$ has to be symmetric with respect to the τ_j's. All the wavefunctions $\Phi_{n_1 n_2}$, $\Phi^{(1)}_{n_1}$, $\Phi^{(2)}_{n_2}$ satisfy the the normalization condition(2.72). The connection between $\Phi_{n_1 n_2}$ and $\Phi^{(1)}_{n_1}$, $\Phi^{(2)}_{n_2}$ can be established by noting that in a sense $\Phi_{n_1 n_2}$ is the "mean" wavefunction of a photon. When the two-soliton state is not in collision, since there are n_1 photons with wavefunction $\Phi^{(1)}_{n_1}$ and n_2 photons with wavefunction $\Phi^{(2)}_{n_2}$, we can conclude that the asymptotic approximation of $\Phi_{n_1 n_2}$ should be

$$\Phi_{n_1 n_2} \longrightarrow \sqrt{\frac{n_1}{n_1 + n_2}} \Phi^{(1)}_{n_1} + \sqrt{\frac{n_2}{n_1 + n_2}} \Phi^{(2)}_{n_2} \tag{2.96}$$

We shall use(2.96) to establish the connection between the wavefunctions before and after collision. This approach is somewhat analogous to the WKB method in quantum mechanics. By substituting Eq.(2.94) into Eq.(2.87) and minimizing the functional, one gets

$$i \frac{\partial}{\partial z} \Phi_{n_1 n_2} = -\frac{\partial^2}{\partial \tau^2} \Phi_{n_1 n_2} + 2(n_1 + n_2 - 1) c |\Phi_{n_1 n_2}|^2 \Phi_{n_1 n_2} \tag{2.97}$$

Substituting Eq.(2.95) into Eq.(2.87) and minimizing the functional, one has

$$i \frac{\partial}{\partial z} \Phi^{(1)}_{n_1} = -\frac{\partial^2}{\partial \tau^2} \Phi^{(1)}_{n_1} + 2(n_1 - 1) c |\Phi^{(1)}_{n_1}|^2 \Phi^{(1)}_{n_1} \tag{2.98}$$

$$i \frac{\partial}{\partial z} \Phi^{(2)}_{n_2} = -\frac{\partial^2}{\partial \tau^2} \Phi^{(2)}_{n_2} + 2(n_2 - 1) c |\Phi^{(2)}_{n_2}|^2 \Phi^{(2)}_{n_2} \tag{2.99}$$

In the above derivation, we have used the fact that $\Phi^{(1)}_{n_1}$ and $\Phi^{(2)}_{n_2}$ are two well-separated functions. This approximation is used frequently in the derivation of this section.

Note that if one substitutes Eq.(2.96) into Eq.(2.97) and separates $\Phi^{(1)}_{n_1}$ and $\Phi^{(2)}_{n_2}$, one obtains Eq.(2.83), (2.84) again. This proves that Eq.(2.96) is consistent with the criteria of the Hartree approximation. Moreover, Eq.(2.98) and (2.99) are the same equations as Eq.(2.88). This justifies our expectation that a two-soliton state not in collision is the product state of two fundamental soliton states.

From Eq.(2.88), the solutions of Eq.(2.98) and (2.99) are :

$$\begin{aligned}\Phi^{(j)}_{n_j} &= \sqrt{\tfrac{n_j-1}{2}}|c|^{\frac{1}{2}}\exp[i\tfrac{(n_j-1)^2}{4}|c|^2 z - ip_j^2 z + ip_j\tau + i\theta_j] \\ &\quad \times \mathrm{sech}[\tfrac{n_j-1}{2}|c|(\tau - T_{jo} - 2p_j z)]\end{aligned} \tag{2.100}$$

with j=1,2 . However, the phases and mean positions can be different before and after collision. The difference can be determined by noting that before and after collision, $\sqrt{\frac{n_1}{n_1+n_2}}\Phi^{(1)}_{n_1} + \sqrt{\frac{n_2}{n_1+n_2}}\Phi^{(2)}_{n_2}$ is the asymptotic approximation of the same $\Phi_{n_1 n_2}$, *i.e.* the asymptotic solution of the CNSE (Eq.(2.88)). It has been shown that the CNSE has two-soliton solutions. Before collision, a two-soliton solution is like two fundamental soliton solutions. After collision, it is still like two fundamental soliton solutions except for a phase shift and a position shift given in Eq.(2.9) and (2.10). With these solutions, one can construct the following Hartree eigenstates before and after collision:

$$|n_1, p_1, n_2, p_2, z\rangle = \frac{1}{\sqrt{n_1! n_2!}}[\int \Phi^{(1)}_{n1}(\tau, z)\hat{U}^\dagger(\tau)d\tau]^{n_1}[\int \Phi^{(2)}_{n2}(\tau, z)\hat{U}^\dagger(\tau)d\tau]^{n_2}|0\rangle \tag{2.101}$$

and the two-soliton states before and after collision:

$$|\psi_s\rangle = \sum_{n_1,n_2} a_1(n_1)a_2(n_2)|n_1, p_1, n_2, p_2, z\rangle \tag{2.102}$$

The natural choices for $a_1(n_1), a_2(n_2)$ are Poisson distributions.

$$a_1(n_1) = \frac{(\alpha_{10})^{n_1}}{\sqrt{n_1!}}e^{-\frac{1}{2}|\alpha_{10}|^2} \tag{2.103}$$

$$a_2(n_2) = \frac{(\alpha_{20})^{n_2}}{\sqrt{n_2!}} e^{-\frac{1}{2}|\alpha_{20}|^2} \tag{2.104}$$

The mean field can be calculated.

$$\begin{aligned} \langle\psi_s|\hat{\phi}(\tau)|\psi_s\rangle &\approx \textstyle\sum_{n_1,n_2} |a_1(n_1)|^2|a_2(n_2)|^2[\alpha_{10}\Phi^{(1)}_{n_1+1}(\tau,z) + \alpha_{20}\Phi^{(2)}_{n_2+1}(\tau,z)] \\ &\approx [\textstyle\sum_{n_1} |a_1(n_1)|^2\alpha_{10}\Phi^{(1)}_{n_1+1}(\tau,z)] \\ &\quad +[\textstyle\sum_{n_2} |a_2(n_2)|^2\alpha_{20}\Phi^{(2)}_{n_2+1}(\tau,z)] \end{aligned} \tag{2.105}$$

before collision and

$$\begin{aligned} &\approx \textstyle\sum_{n_1,n_2} |a_1(n_1)|^2|a_2(n_2)|^2[\alpha_{10}e^{i\delta\theta_1}\Phi^{(1)}_{n_1+1}(\tau-\delta T_1,z)] \\ &\quad +[\textstyle\sum_{n_1,n_2} |a_1(n_1)|^2|a_2(n_2)|^2\alpha_{20}e^{i\delta\theta_2}\Phi^{(2)}_{n_2+1}(\tau-\delta T_2,z)] \end{aligned} \tag{2.106}$$

after collision.

This result also contains the quantum fluctuations produced in the collision. The $\delta\theta_i$'s and δT_i 's $(i = 1, 2)$ are functions of $n_j (j = 1, 2)$ and thus are determined probabilistically.

2.5 Exact solution in the Schrödinger picture

In this section we present an exact (nonlinear) analysis based on Bethe's ansatz method. This approach was first introduced by Lieb and Linger[45], McGuire[46] and Yang[47] to the study of one-dimensional bossons with δ-function interactions. The eigenfunctions of the system were constructed. Following this approach, we construct (exact) fundamental and higher order soliton states.

2.5.1 Construction of fundamental soliton states

In this subsection, we solve Eq.(2.23) exactly to construct fundamental soliton states[57]. The z-dependence in Eq.(2.20) can be factored out by assuming a solution of the form

$$f_n(\tau_1, \ldots \tau_n, z) = f_n(\tau_1 \ldots \tau_n) e^{-iE_n z} \tag{2.107}$$

The equation for $f_n(\tau_1 \ldots \tau_n)$ is

$$\Big[-\sum_{j=1}^{n}\frac{\partial^2}{\partial\tau_j^2}+2c\sum_{1\le i<j\le n}\delta(\tau_j-\tau_i)\Big]f_n(\tau_1\ldots\tau_n)=E_n f_n(\tau_1\ldots\tau_n) \tag{2.108}$$

It turns out that Eq.(2.108) can be solved exactly.

Since f_n is a symmetric and continuous function, it is enough to specify its value in the region $\tau_1 \le \tau_2 \ldots \le \tau_n$. In the regions $\tau_j \ne \tau_i$, all the delta-functions in Eq.(2.108) vanish and the solutions of Eq.(2.108) are of the exponential form

$$\exp i\sum_{j=1}^{n}k_j\tau_j \tag{2.109}$$

To satisfy the symmetry condition, all the permutation terms should be included. Therefore, the general form of the solutions is

$$f_n(\tau_1,\ldots\tau_n)=\sum_{\{Q\}}A_Q\exp\,(i\sum_{j=1}^{n}k_{Q(j)}\tau_j) \tag{2.110}$$

where the summation over $\{Q\}$ is the summation over all possible permutations of $[1,2,\ldots n]$ and $Q(j)$ is the j-th component of Q. The delta functions in Eq.(2.108) impose boundary conditions at the boundaries $\tau_j = \tau_i$. At these boundaries, there is a discontinuity in the slope of the function f_n. It can be shown[52] that these boundary conditions impose the relation among the A_Q's:

$$A_{Q'}=\frac{k_{Q(j+1)}-k_{Q(j)}+ic}{k_{Q(j+1)}-k_{Q(j)}-ic}A_Q \tag{2.111}$$

Here Q' is the permutation derived from Q by interchanging the j-th and $(j+1)$-th components.

Reintroducing the z-dependence, one has

$$f_n(\tau_1,\ldots\tau_n,z)=e^{-iE_nz}\sum_{\{Q\}}A_Q\exp[i\sum_{j=1}^{n}k_{Q(j)}\tau_j] \tag{2.112}$$

for $\tau_1 \le \tau_2 \ldots \le \tau_n$ with the energy expressed by

$$E_n=\sum_{j=1}^{n}k_j^2 \tag{2.113}$$

In general, k_j must be real because the wavefunctions cannot be infinite. However, for negative c, a rising exponential for $\tau_i < \tau_j$ can be matched to a falling exponential for $\tau_i > \tau_j$. Thus *negative values of c make "bound" states possible*, states that cluster around the planes $\tau_i = \tau_j$ in multidimensional space. No such solutions exist for positive c. To be explicit, in the case of $c < 0$, bound state solutions exist if k_j satisfies the following condition.

$$k_j = p + i\frac{c}{2}[n - 2j + 1] \qquad\qquad j = 1, 2, \ldots n \tag{2.114}$$

The reason why we need condition (2.114) can be seen by substituting it into (2.111). We find that all the A_Q vanish except $A_{[1,2,\ldots n]}$. Therefore

$$f_{np}(\tau_1 \ldots \tau_n) = \mathcal{N}_n \exp[ip\sum_{j=1}^{n}\tau_j + \frac{c}{2}\sum_{1\le i<j\le n}|\tau_j - \tau_i|] \tag{2.115}$$

$$\mathcal{N}_n = A_{[1,2,\ldots n]} \tag{2.116}$$

If any other A_Q is nonzero, the wavefunction is not bound. This fact thus leads to the condition (2.114). f_{np} of expression (2.115) is symmetric in the τ_i's and applies to all regions.

If any pair of τ_j values is widely separated, the wavefunction expression (2.115) is very small. This is why these solutions are called bound state wavefunctions. With Eq.(2.115), one can construct the bound states that are the eigenstates of the Hamiltonian.

$$\begin{aligned} |n,p\rangle &= \frac{1}{\sqrt{n!}}\int f_{n,p}(\tau_1 \ldots \tau_n)\hat{U}^\dagger(\tau_1)\ldots\hat{U}^\dagger(\tau_n)d\tau_1 \ldots d\tau_n|0\rangle \\ &\equiv \hat{R}^\dagger(n,p)|0\rangle \end{aligned} \tag{2.117}$$

with the eigenvalue

$$E(n,p) = np^2 - \frac{|c|^2}{12}n(n^2-1) \tag{2.118}$$

The energy is the sum of the net kinetic energy of the bosons with momentum p each and (negative) potential energy due to the binding force of the Kerr nonlinearity $\frac{|c|^2}{12}(n^2-1)$. The dependence on n follows from the functional dependence of the

nonlinearity which is quadratic in $\hat{U}^\dagger(\tau)\hat{U}(\tau)$. Reintroducing the z-dependence, we have

$$|n,p,z\rangle = e^{-iE(n,p)z}|n,p\rangle \tag{2.119}$$

It is easy to prove that $|n,p,z\rangle$ is also the eigenstate of the photon number operator $\hat{N}$ and the momentum operator $\hat{P}$.

$$\hat{N}|n,p,z\rangle = n|n,p,z\rangle \tag{2.120}$$

$$\hat{P}|n,p,z\rangle = np|n,p,z\rangle \tag{2.121}$$

Here the photon number and momentum operators are defined as follows:

$$\hat{N} = \int \hat{U}^\dagger(\tau)\hat{U}(\tau)d\tau \tag{2.122}$$

$$\hat{P} = \frac{i}{2}\int [\frac{\partial \hat{U}^\dagger(\tau)}{\partial \tau}\hat{U}(\tau) - \hat{U}^\dagger(\tau)\frac{\partial \hat{U}(\tau)}{\partial \tau}]d\tau \tag{2.123}$$

The fundamental soliton state is constructed by superimposing these eigenstates in both n and p spaces :

$$|\psi_s\rangle = \sum_n a_n \int g_n(p)|n,p,z\rangle dp \tag{2.124}$$

The natural choices for a_n and $g_n(p)$ are a Poisson distribution and a Gaussian distribution respectively

$$a_n = \frac{\alpha_o^n}{\sqrt{n!}}e^{-\frac{1}{2}|\alpha_o|^2} \tag{2.125}$$

$$g_n(p) = \frac{1}{\sqrt{\Delta p}\sqrt[4]{\pi}}e^{-\frac{1}{2}\frac{|p-p_o|^2}{(\Delta p)^2}}e^{-inpT_o} \equiv g(p)e^{-inpT_o} \tag{2.126}$$

To justify our construction we calculate the mean value of the field operator in the limit of a large photon number. The result is[57] :

$$\begin{aligned}\langle\psi_s|\hat{U}(\tau)|\psi_s\rangle \approx\ & \textstyle\sum_n \frac{|\alpha_o|^{2n}}{n!}\exp[-|\alpha_o|^2]\int \frac{1}{(\Delta p)\sqrt{\pi}}e^{-\frac{(p-p_o)^2}{(\Delta p)^2}} \\ & \textstyle\frac{\alpha_0\sqrt{n}}{2}|c|^{1/2}\{\exp[i\frac{|c|^2n(n+1)}{4}z - ip^2z + ip\tau + i\theta_o] \\ & \textstyle\operatorname{sech}[\frac{1}{2}n|c|(\tau - T_o - 2pz)]\}dp\end{aligned} \tag{2.127}$$

The approximations we used in the derivation are (1) $n_o >> 1$ (2) $\Delta p >> |c|$. We need the second condition to ensure that the soliton pulse shape is a sech function[57].

Equation (2.127) makes a very important statement. The expectation value of the field is the average of a set of classical soliton solutions with different group and phase velocities. The phase velocities depend on the photon number, the group velocities depend on the momentum. This is a surprising result, because the field propagates in a nonlinear medium, and hence a simple superposition of solutions as the expectation value of the field was not anticipated. The result has valuable predictive value. Since the superposition is of many different pulse-shapes with different phase velocities and group velocities, a spreading of the phase and position is to be expected, as we have seen in the linearization approach.

One may think of the position spreading effect as a walk-off of different soliton components. This is in fact rigorously true in the case of coherent excitation. As we have mentioned, in order to have a *sech*-like pulseshape, the superposition bandwidth Δp should satisfy $\Delta p >> |c|$. From Eq.(2.77), we know the bandwidth under coherent excitation is $\Delta p \approx \sqrt{n_o}|c|/\sqrt{12}$. Therefore, under coherent excitation, one can divide the superposition into many sections, each section with a bandwidth $\approx 10|c|$. Thus each section behaves like a soliton with a slightly different momentum and the position spreading is due to the walk-off of these sections.

2.5.2 Construction of higher order soliton states

In this section we construct two-soliton states under the exact analysis[57]. Other higher order soliton states can be constructed in the same way.

We start from the general solution Eq.(2.110) with $n = n_1 + n_2$. If one chooses

$$k_j = p_1 + \frac{ic}{2}[n_1 - 2j + 1] \quad j = 1, \ldots n_1 \tag{2.128}$$

$$k_{n_1+j} = p_2 + \frac{ic}{2}[n_2 - 2j + 1] \quad j = 1, \ldots n_2 \tag{2.129}$$

Then

$$f_{n_1 p_1 n_2 p_2}(\tau_1 \ldots \tau_{n_1+n_2}) = \sum_{\{Q\}} A_Q F_Q(\tau_1, \ldots \tau_{n_1} \ldots \tau_{n_1+n_2}) \tag{2.130}$$

Here F_Q is a symmetric function of τ_j.

$$\begin{aligned} F_Q(\tau_1, \ldots \tau_{n_1+n_2}) &= \exp\left[ip_1 \textstyle\sum_{j=1}^{n_1} \tau_{Q^{-1}(j)} + ip_2 \sum_{j=n_1+1}^{n_1+n_2} \tau_{Q^{-1}(j)}\right] \\ &\quad \times \exp\left[\tfrac{c}{2} \textstyle\sum_{1\le i<j\le n_1} (\tau_{Q^{-1}(j)} - \tau_{Q^{-1}(i)})\right] \\ &\quad \times \exp\left[\tfrac{c}{2} \textstyle\sum_{n_1+1\le i<j\le n_1+n_2} (\tau_{Q^{-1}(j)} - \tau_{Q^{-1}(i)})\right] \end{aligned} \tag{2.131}$$

for $\tau_1 \le \tau_2 \le \ldots \le \tau_{n_1+n_2}$.

In Eq.(2.110) the summation over $\{Q\}$ is the summation over all possible permutations of $[1, 2, \ldots n_1+n_2]$. However, because of the special values of k_j in Eq.(2.128) and (2.129), A_Q is zero if the order of $[1, 2, \ldots n_1]$ or $[n_1+1, \ldots n_1+n_2]$ is permuted. Therefore, in Eq.(2.131) the summation over $\{Q\}$ is the summation over all possible permutations of $[1, 2, \ldots n_1+n_2]$ with the order of $[1, \ldots n_1]$ and $[n_1+1, \ldots n_1+n_2]$ unchanged. In Eq.(2.131), Q^{-1}, the inverse of Q, appears because we have converted the permutation over k into the permutation over τ.

The coefficients A_Q in Eq.(2.130) also have to satisfy Eq.(2.111). It can be seen from Eq.(2.111) that they differ from one another only by a certain phase. As an example and also for later use, we calculate the relation between $A_{\text{in}} = A_{[1,2,\ldots n_1, n_1+1, \ldots n_1+n_2]}$ and $A_{\text{out}} = A_{[n_1+1,\ldots n_1+n_2, 1, \ldots n_1]}$. The result is[57]:

$$A_{\text{out}} = e^{i\theta(n_1,p_1,n_2,p_2)} A_{\text{in}} \tag{2.132}$$

with

$$\begin{aligned} \theta(n_1, p_1, n_2, p_2) &= -\Big\{4 \textstyle\sum_{j=1}^{n_1-1} \tan^{-1}\left[\frac{\frac{1}{2}|c|(n_2-n_1+2j)}{p_2-p_1}\right] \\ &\quad +2\tan^{-1}\left[\frac{\frac{1}{2}|c|(n_2-n_1)}{p_2-p_1}\right] \\ &\quad +2\tan^{-1}\left[\frac{\frac{1}{2}(n_2+n_1)}{p_2-p_1}\right]\Big\} \end{aligned} \tag{2.133}$$

With the solution, one can construct the bound state.

$$\begin{aligned} |n_1,p_1,n_2,p_2\rangle &= \textstyle\sum_{\{Q\}} A_Q \int_{-\infty}^{\infty} F_Q(\tau_1,\ldots\tau_{n_1+n_2}) \\ &\quad \Pi_{j=1}^{n_1+n_2}\hat{U}^\dagger(\tau_j)d\tau_j|0\rangle \\ &= (n_1+n_2)!\textstyle\sum_{\{Q\}} A_Q \int_{\tau_1\le\tau_2\ldots\le\tau_{n_1+n_2}} \\ &\quad F_Q(\tau_1,\ldots\tau_{n_1+n_2})\Pi_{j=1}^{n_1+n_2}\hat{U}^\dagger(\tau_j)d\tau_j|0\rangle \end{aligned} \tag{2.134}$$

Reintroducing the z dependence, one has

$$|n_1,p_1,n_2,p_2,z\rangle = e^{-iE(n_1,p_1,n_2,p_2)z}|n_1,p_1,n_2,p_2\rangle \tag{2.135}$$

with

$$E(n_1,p_1,n_2,p_2) = n_1p_1^2 + n_2p_2^2 - \frac{|c|^2}{12}n_1(n_1^2-1) - \frac{|c|^2}{12}n_2(n_2^2-1) \tag{2.136}$$

The localized two-soliton states can be constructed by superimposing the bound states.

$$|\psi_s\rangle = \sum_{n_1,n_2} a_1(n_1)a_2(n_2)\int\int g_{n_1}(p_1)g_{n_2}(p_2)|n_1,p_1,n_2,p_2,z\rangle dp_1dp_2 \tag{2.137}$$

with

$$a_1(n_1) \equiv \frac{(\alpha_{10})^{n_1}}{\sqrt{n_1!}}e^{-\frac{1}{2}|\alpha_{10}|^2} \tag{2.138}$$

$$a_2(n_2) \equiv \frac{(\alpha_{20})^{n_2}}{\sqrt{n_2!}}e^{-\frac{1}{2}|\alpha_{20}|^2} \tag{2.139}$$

$$\begin{aligned} g_{n_1}(p_1) &\equiv \tfrac{1}{\sqrt{\Delta p_1}\sqrt[4]{\pi}}e^{-\frac{1}{2}\frac{(p_1-p_{10})^2}{(\Delta p_1)^2}}e^{-in_1p_1T_{10}} \\ &\equiv g_1(p_1)e^{-in_1p_1T_{10}} \end{aligned} \tag{2.140}$$

$$\begin{aligned} g_{n_2}(p_2) &\equiv \tfrac{1}{\sqrt{\Delta p_1}\sqrt[4]{\pi}}e^{-\frac{1}{2}\frac{(p_2-p_{20})^2}{(\Delta p_2)^2}}e^{-in_2p_2T_{20}} \\ &\equiv g_2(p_2)e^{-in_2p_2T_{20}} \end{aligned} \tag{2.141}$$

Without loss of generality, we assume $p_{10} > p_{20}$ and $T_{10} < T_{20}$.

The above construction is justified by studying the two-soliton state before collision and after collision. In the two limits, the two-soliton state is composed of two

well separated fundamental solitons. To be explicit, it can be shown[57] that before collision, the two-soliton state is approximately equal to

$$\begin{aligned} |\psi_s\rangle \approx\ & [\textstyle\sum_{n_1} a_1(n_1) \int g_{n_1}(p_1) e^{-iE(n_1,p_1)z} \hat{R}^\dagger(n_1,p_1) dp_1] \\ & \cdot [\textstyle\sum_{n_2} a_2(n_2) \int g_{n_2}(p_2) e^{-iE(n_2,p_2)z} \hat{R}^\dagger(n_2,p_2) dp_2] |0\rangle \end{aligned} \tag{2.142}$$

where the two brackets are identified as the creation operators for fundamental solitons.

After collision,

$$\begin{aligned} |\psi_s\rangle \approx\ & \textstyle\sum_{n_1 n_2} a_1(n_1) a_2(n_2) \int\int e^{i\theta(n_1,p_1,n_2,p_2)} \\ & g_{n_1}(p_1) g_{n_2}(p_2) \exp[-iE(n_1,p_1)z - iE(n_2,p_2)z] \\ & \hat{R}^\dagger(n_1,p_2) \hat{R}^\dagger(n_2,p_2) dp_1 dp_2 |0\rangle \end{aligned} \tag{2.143}$$

with $\theta(n_1,p_1,n_2,p_2)$ defined in Eq.(2.133) and $E(n,p)$ defined in Eq.(2.118). Note that the only difference between Eq.(2.142) and Eq.(2.143) is the phase factor $\theta(n_1,p_1,n_2,p_2)$. To see the effect of this factor, we write Eq.(2.143) as

$$\begin{aligned} |\psi_s\rangle \approx\ & \textstyle\sum_{n_1,n_2} a_1(n_1) a_2(n_2) \exp[i\theta(n_{10},p_{10},n_{20},p_{20}) \\ & + i\frac{\partial\theta}{\partial n_1}(n_1 - n_{10}) + i\frac{\partial\theta}{\partial n_2}(n_2 - n_{20})] \\ & [\textstyle\int g_{n_1}(p_1) \exp[i\frac{\partial\theta}{\partial p_1}(p_1 - p_{10}) - iE(n_1,p_1)z] \hat{R}^\dagger(n_1,p_1) dp_1] \\ & [\textstyle\int g_{n_2}(p_2) \exp[i\frac{\partial\theta}{\partial p_2}(p_2 - p_{20}) - iE(n_2,p_2)z] \hat{R}^\dagger(n_2,p_2) dp_2] |0\rangle \end{aligned} \tag{2.144}$$

Here we have used the expansion

$$\begin{aligned} \theta(n_1,p_1,n_2,p_2) \approx\ & \theta(n_{10},p_{10},n_{20},p_{20}) + \frac{\partial\theta}{\partial n_1}(n_1 - n_{10}) \\ & + \frac{\partial\theta}{\partial n_2}(n_2 - n_{20}) + \frac{\partial\theta}{\partial p_2}(p_1 - p_{10}) + \frac{\partial\theta}{\partial p_2}(p_2 - p_{20}) \end{aligned} \tag{2.145}$$

All the derivatives of θ are evaluated at $(n_{10},n_{20},p_{10},p_{20})$.

It is now clear that the two-soliton state after collision is still composed of two well separated fundamental solitons except for a phase shift and a "position" shift.

The mean phase shift for the first soliton is

$$\begin{aligned}\delta\theta_1 &\approx \frac{\partial\theta}{\partial n_1}(n_{10},p_{10},n_{20},p_{20}) \\ &\approx \theta(n_{10}+1,p_{10},n_{20},p_{20})-\theta(n_{10},p_{10},n_{20},p_{20})\end{aligned} \tag{2.146}$$

and the "position" shift is

$$\delta\tau_1 \approx \frac{1}{n_{10}}\frac{\partial\theta}{\partial p_1}(n_{10},p_{10},n_{20},p_{20}) \tag{2.147}$$

For the second soliton the phase shift is

$$\begin{aligned}\delta\theta_2 &\approx \frac{\partial\theta}{\partial n_2}(n_{10},p_{10},n_{20},p_{20}) \\ &\approx \theta(n_{10},p_{10},n_{20}+1,p_{20})-\theta(n_{10},p_{10},n_{20},p_{20})\end{aligned} \tag{2.148}$$

and the "position" shift is

$$\delta\tau_2 \approx \frac{1}{n_{20}}\frac{\partial\theta}{\partial p_2}(n_{10},p_{10},n_{20},p_{20}) \tag{2.149}$$

It can be shown[52] that when n_{10}, n_{20} are large , the magnitude of $\delta\theta_1$ and $\delta\tau_1$ in Eq.(2.146) and (2.147) approach the classical results.

The increase of the uncertainties due to a collision can be estimated by expanding $\theta(n_1,p_1,n_2,p_2)$ to second order. The phase uncertainty for the first soliton is

$$\begin{aligned}\delta\theta_1 &\approx |\frac{\partial^2\theta}{\partial {n_1}^2}|\Delta n_1 + |\frac{\partial^2\theta}{\partial n_1\partial p_1}|\Delta p_1 \\ &\quad +|\frac{\partial^2\theta}{\partial n_1\partial n_2}|\Delta n_2 + |\frac{\partial^2\theta}{\partial n_1\partial p_2}|\Delta p_2\end{aligned} \tag{2.150}$$

and the position uncertainty is

$$\begin{aligned}\delta T_1 &\approx |\frac{\partial^2\theta}{\partial n_1\partial p_1}|\Delta n_1 + |\frac{\partial^2\theta}{\partial {p_1}^2}|\Delta p_1 \\ &\quad +|\frac{\partial^2\theta}{\partial p_1\partial n_2}|\Delta n_2 + |\frac{\partial^2\theta}{\partial p_1\partial p_2}|\Delta p_2\end{aligned} \tag{2.151}$$

These results also can be obtained directly by perturbing the classical relations (2.9) and (2.10).

Chapter 3

Soliton squeezing in optical fibers

Solitons get "squeezed" during propagation. In this chapter, we explain what is the definition of squeezing, why soliton get squueezed and how to calculate the squeezing ratio using the linearization approach and the time-dependent Hartree approximation. Analysis of a fiber ring gyro system is also presented.

3.1 Soliton detection using balanced homodyne scheme

Before studying the soliton squeezing effect in optical fibers, in this section we discuss the way to detect the quantum fluctuations of optical solitons, or more specific, about the way to detect the four soliton operators introduced in Chapter 2, section 3. From expressions (2.61)-(2.64), one notes that all the four operators are related to the field operators by a (inner-product) projection. Therefore, if one can find detection scheme whose operations are simply projections, then one can detect all the four operators and their linear combinations. It turns out the balanced homodyne detection with a pulsed local oscillator behaves just as described.

The fundamental setup of balanced homodyne detection is shown in Fig. 3. A 50-50 beam splitter and two balanced photodetectors form the principal part of the setup. The input signal is mixed with the local oscillator (L.O.) pulse through the beam splitter and detected by the photodetectors. The difference of the output currents is monitored by a spectrum analyzer. To predict the performance of homodyne detection schemes, a quantum treatment of optical pulse detection is necessary. The problem of wideband optical detection has been treated by many authors recently[65,66]. Although in the literature, there is still disputation about the response of photodetectors to photon flux or energy flux, the difference of predictions

from two pictures are very small for a quasi-chromatic field, unless the magnitude of squeezing is very large. In the thesis, a wideband photodetector is modeled as an ideal photon flux detector followed by a filter which represents the finite bandwith of the electronics. The description of homodyne detection for optical pulses follows directly from this photodetector model and a projection interpretation can be given. In Fig. 3, we also show the models and symbols for the photodetectors, input signal, L.O. pulse, beam splitter, and spectrum analyzer. The c-number function $u_L(\tau)$ is the pulse from the local oscillator. We assume that the local oscillator is powerful enough for it to be treated as a classical function. The operation of the spectrum analyzer is modeled as a Fourier transformer followed by a variance detector.

In Appendix 1, we show that the output of the whole setup is the variance of the following operator :

$$\begin{aligned} \hat{M}(z) &= H(k)\int [u_L(\tau)\hat{u}^\dagger(z,\tau) + u_L^*(z,\tau)\hat{u}(\tau)]\exp(ik\tau)d\tau \\ &= H(k)\int [\mathrm{Re}[u_L(\tau)]\hat{u}_1(z,\tau) + \mathrm{Im}[u_L(\tau)]\hat{u}_2(z,\tau)]\exp(ik\tau)d\tau \end{aligned} \tag{3.1}$$

Here $H(k)$ is the Fourier transform of the detector response function $h(\tau)$. For simplicity, in the following analyses we will assume the detector is ideally broadband and thus $H(k)$ is simply a constant (independent of k).

If one introduces vector notation, then the operator $\hat{M}$ is simply the inner product of $\mathbf{f_L}$ and $\hat{\mathbf{u}}$.

$$\begin{aligned} \hat{M}(z) &= \langle \mathbf{f_L}(\tau)|\hat{\mathbf{u}}(z,\tau)\rangle \\ &\equiv \int [f_{L1}(\tau)\hat{u}_1(z,\tau) + f_{L2}(\tau)\hat{u}_2(z,\tau)]d\tau \end{aligned} \tag{3.2}$$

with

$$\mathbf{f_L}(\tau) \propto \begin{bmatrix} \mathrm{Re}[u_L(\tau)]\exp(ik\tau) \\ \mathrm{Im}[u_L(\tau)]\exp(ik\tau) \end{bmatrix} \tag{3.3}$$

We also require the following normalization condition :

$$\int \mathbf{f_L}^\dagger \mathbf{f_L} d\tau = 1 \tag{3.4}$$

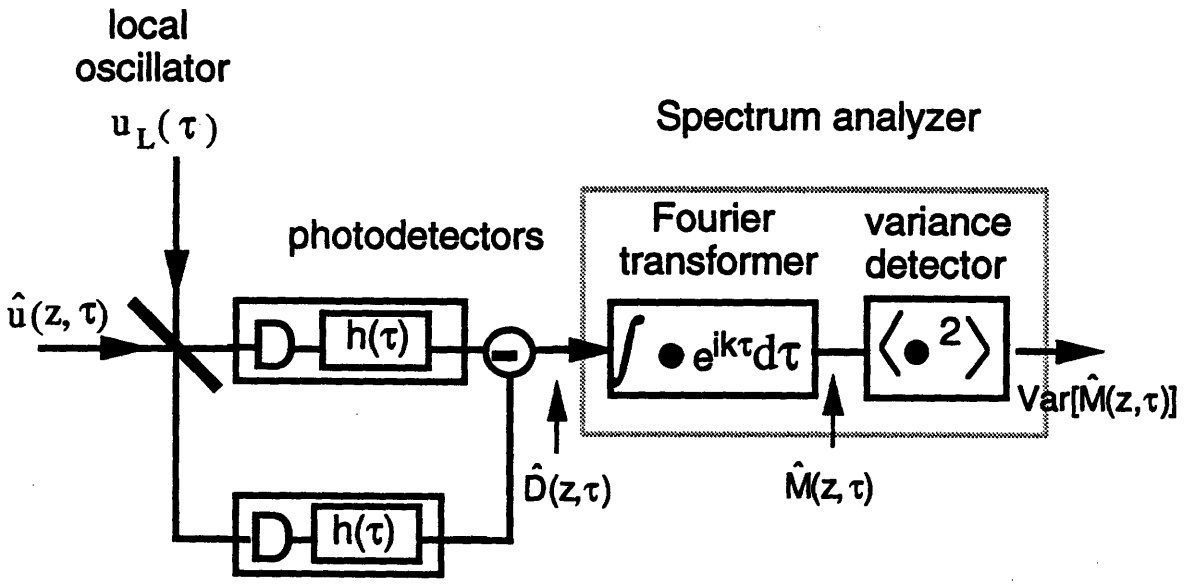

Figure 3 : Balance homodyne detection with a pulse local oscillator

so that when the incoming field is the vacuum state, $\langle \hat{M}^\dagger \hat{M} \rangle = \frac{1}{4}$ (the shot noise level).

Expression (3.2) suggests the following projection interpretation : the homodyne detection followed by a spectrum analyzer detects the "projection" of the input field operator into the characteristic function of the detection; the characteristic function of the detection is simply the local oscillator times $\exp(ik\tau)$. The meaning of "projection" should be understood as the inner product defined in Eq.(2.48) or Eq.(3.2).

Note that in the definition (3.3), $\mathbf{f_L}$ is a complex vector in general. However, most of the time we are only interested in the case of $k = 0$. When $k = 0$, $\mathbf{f_L}$ is real.

3.2 Analytical approach

From section 1 of this chapter, we know how to suppress the contribution of the continuum and detect the four soliton operators and their linear combination using homodyne detection. From section 3 of Chapter 2, we also know that the photon number fluctuations are coupled to the phase fluctuations during propagation and the momentum fluctuations are also coupled to the position fluctuations [see (2.69)-(2.72)]. This coupling produces correlation between the photon number and phase fluctuations and between the momentum and position fluctuations. If one can take advantage of this correlation by detecting a suitable linear combination of $\Delta\hat{n}(z)$, $\Delta\hat{\theta}(z)$, $\Delta\hat{p}(z)$ and $\Delta\hat{T}(z)$, one is able to reduce the detected noise and observe "squeezing". For nonlinear Schrödinger solitons, the problem is even simpler because $\Delta\hat{n}(z)$ and $\Delta\hat{\theta}(z)$ form a pair, $\Delta\hat{p}(z)$ and $\Delta\hat{T}(z)$ form a pair, and there is no coupling between two pairs. Obviously, one only needs to consider the pair that can give rise to a larger squeezing (that is, the photon number and phase pair). Here, the definition of "squeezing" is understood as follows. One makes a measurement of the input state (which is assumed to be a vacuum state) and make the *same* measurement of the output state. If the quantum noise of the second measurement is less than the first measurement, then one says he observes "squeezing" and the

ratio of two outcomes is the squeezing ratio.

Another way to visualize how squeezing occurs is to plot the contour line of the joint probability function of $\Delta\hat{n}(z)/\sqrt{\langle\Delta\hat{n}^2(0)\rangle}$ and $\Delta\hat{\theta}(z)/\sqrt{\langle\Delta\hat{\theta}^2(0)\rangle}$ (see Fig. 4). At $z = 0$, the two operators are uncorrelated and thus the probability function is circular. At $z > 0$, the distribution becomes elliptical due to the coupling. If one tunes the detector to detect the component in the direction of the minor axis, he will see a reduction of the detection noise. This is the squeezing effect.

Now let us calculate the squeezing ratio. By choosing the characteristic function of the homodyne detection to be

$$\mathbf{f_L} = 2[c_n\underline{\mathbf{f}}_\mathbf{n} + c_\theta\underline{\mathbf{f}}_\theta] \tag{3.5}$$

one can detect the operator

$$\hat{M}(z) = [c_n\Delta\hat{n}(z) + c_\theta\Delta\hat{\theta}(z)] = [c_n + \frac{2c_\theta}{n_o}\Phi(z)]\Delta\hat{n}(0) + c_\theta\Delta\hat{\theta}(0) \tag{3.6}$$

with all contributions from the continuum suppressed. Here $\Phi(z) = \frac{n_o^2|c|^2}{4}z$ is the classical phase shift of the soliton.

At $z = 0$, $\hat{u}(0,\tau)$ is assumed to represent the vacuum state. The normalization condition (3.4) requires

$$c_n^2\langle\Delta\hat{n}^2(0)\rangle + c_\theta^2\langle\Delta\hat{\theta}^2(0)\rangle = \frac{1}{4} \tag{3.7}$$

so that $\langle\hat{M}^2(0)\rangle = \frac{1}{4}$ (the shot noise level).

The squeezing ratio is then given by :

$$\begin{aligned} R(z) &\equiv \frac{\langle\hat{M}^2(z)\rangle}{\langle\hat{M}^2(0)\rangle} \\ &= 4[c_n + \frac{2c_\theta}{n_o}\Phi]^2\langle\Delta\hat{n}^2(0)\rangle + 4c_\theta^2\langle\Delta\hat{\theta}^2(0)\rangle \end{aligned} \tag{3.8}$$

The minimum value of $R(z)$ as a function of z is achieved by adjusting c_n and c_θ under the constraint (3.7) and is found to be

$$R_{opt}(z) = 1 + \Phi_1^2(z) - \Phi_1(z)\sqrt{1 + \Phi_1^2(z)} \tag{3.9a}$$

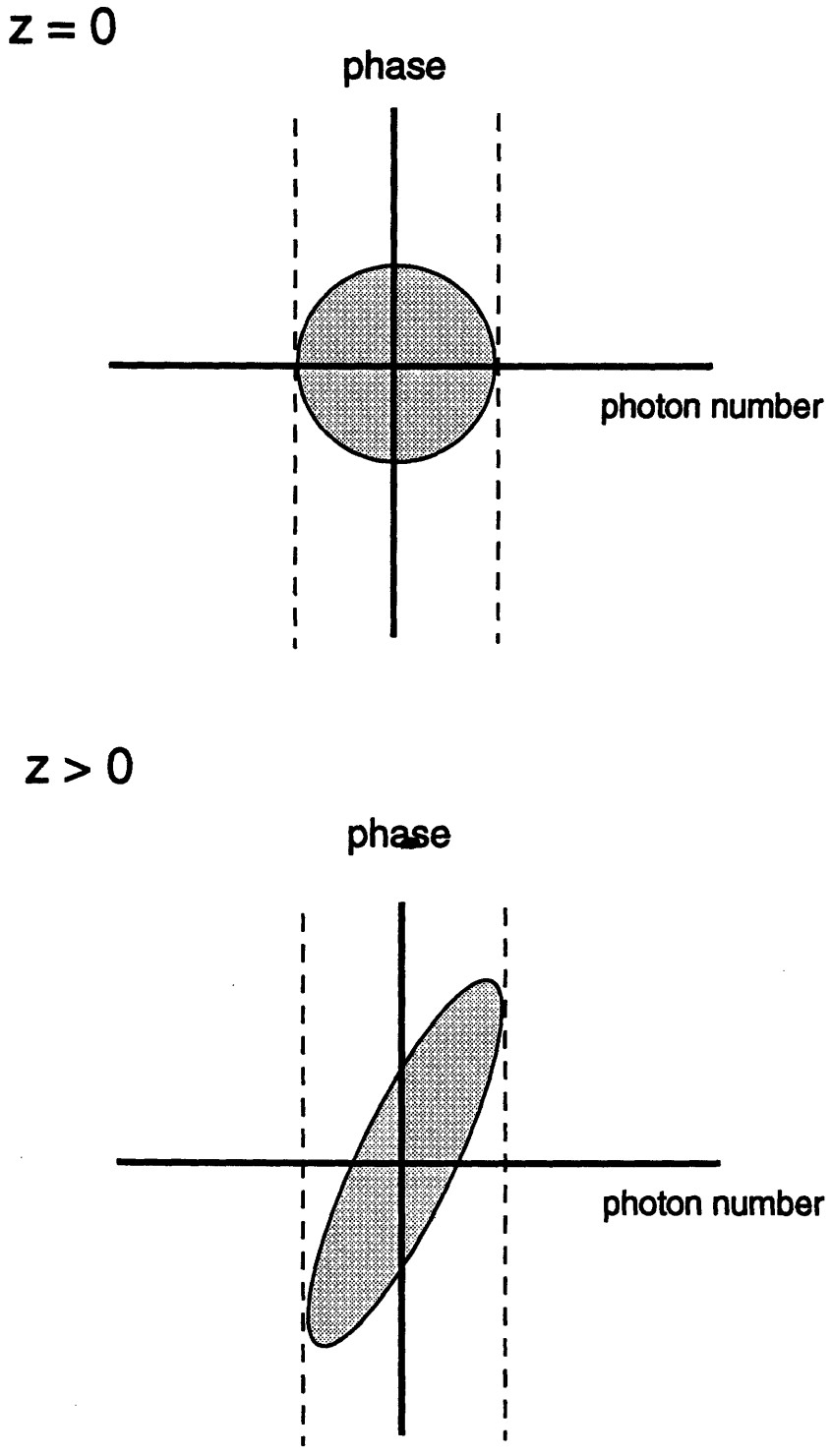

Figure 4: Evolution of the contour line of the joint probability function of $\Delta\hat{n}(z)/\sqrt{\langle\Delta\hat{n}^2(0)\rangle}$ and $\Delta\hat{\theta}(z)/\sqrt{\langle\Delta\hat{\theta}^2(0)\rangle}$

with

$$\Phi_1(z) \equiv \frac{2}{n_o}\Phi(z)\sqrt{\frac{\langle\Delta\hat{n}^2(0)\rangle}{\langle\Delta\hat{\theta}^2(0)\rangle}} \tag{3.9b}$$

$R_{opt}(z)$ as a function of the nonlinear phase $\Phi(z)$ is plotted in Fig. 5. Since the contribution of the continuum is totally suppressed, this is also the optimum squeezing ratio one can achieve. From the values of c_n and c_θ that minimize R, one can determine the optimum local oscillator according to Eq.(3.5).

3.3 Numerical approach

Although the analytical approach provides us the optimum detection scheme and the optimum squeezing ratio, it does not allow us to calculate the squeezing ratio for an arbitrarily given local oscillator. In this section, we develop a numerical approach that enables us to do so. The starting point is the linearized equation (2.26).

Since $\mathbf{P}$ is independent of z, Equation (2.28) has the following formal solution:

$$\hat{\mathbf{u}}(z,\tau) = \exp[\mathbf{P}z]\hat{\mathbf{u}}(0,\tau) \tag{3.10}$$

According to the projection interpretation of homodyne detection, we are only interested in the projection of the field operator. Therefore,

$$\begin{aligned}\langle\mathbf{f_L}(\tau)|\hat{\mathbf{u}}(\mathbf{z},\tau)\rangle &= \langle\mathbf{f_L}(\tau)|\exp[\mathbf{P}z]\hat{\mathbf{u}}(\mathbf{0},\tau)\rangle \\ &= \langle\exp[\mathbf{P^A}z]\mathbf{f_L}(\tau)|\hat{\mathbf{u}}(\mathbf{0},\tau)\rangle \\ &\equiv \langle\mathbf{F_L}(z,\tau)|\hat{\mathbf{u}}(\mathbf{0},\tau)\rangle\end{aligned} \tag{3.11}$$

Here we have used the adjoin operator defined in Chapter 2. Now $\mathbf{F_L}(z,\tau)$ can be evaluated conveniently because only differentiation and 2-by-2 matrix operations are involved.

Equation (3.11) has an interesting interpretation. The original problem is to propagate the operator $\hat{\mathbf{u}}(0,\tau)$ over a distance z and then to project $\hat{\mathbf{u}}(z,\tau)$ into the characteristic function of the detection $\mathbf{f_L}(\tau)$. Equation (3.11) says that one can simply "backpropagate" $\mathbf{f_L}(\tau)$ using the adjoin operator $\mathbf{P^A}$ and then project $\hat{\mathbf{u}}(0,\tau)$

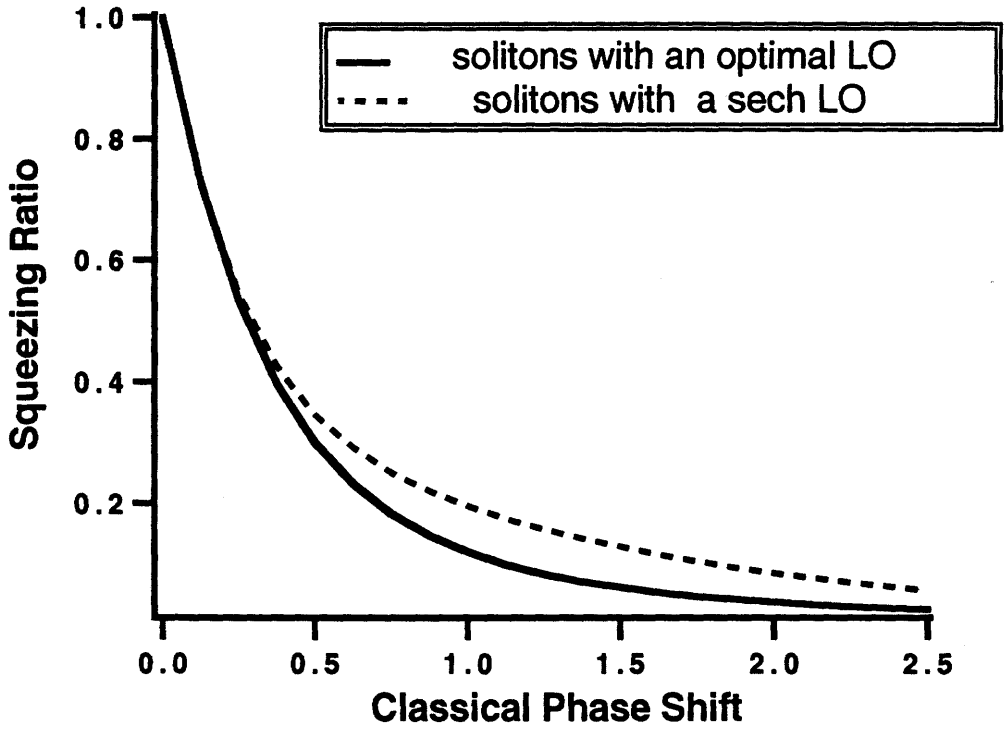

Figure 5: Squeezing ratio of solitons in optical fibers

into it. This is a big simplification because it is easier to visualize the propagation of classical functions than operators. Of course, this kind of backpropagation is only possible for linear problems. In optics, a classic example of this technigue is Siegman's antenna theorem for heterodyne detection.

The above derivation applies equally well to both the classical problem and the quantum problem. For linear problems there is a one-to-one correspondence between the classical theory and quantum theory. Discrepancies occur only when one calculates higher moments.

At $z = 0$, we assume the soliton is a coherent pulse and thus $\hat{u}(0,\tau)$ represents the vacuum state. Based on this assumption, the expectation value of the squared-magnitude of the operator $\hat{M}(z) = \langle \mathbf{f_L}(\tau)|\hat{\mathbf{u}}(z,\tau)\rangle$ then is

$$\langle \hat{M}^{\dagger}(z)\hat{M}(z)\rangle = \frac{1}{4}R(z) \tag{3.12}$$

with the squeezing ratio $R(z)$ given by

$$R(z) = \int \Big[|F_{L1}(z,\tau)|^2 + |F_{L2}(z,\tau)|^2 - 2\mathrm{Im}[|F^*_{L1}(z,\tau)F_{L2}(z,\tau)]\Big]d\tau \tag{3.13}$$

Using Eq.(3.13), one can analyze the performance of homodyne detection with any given local oscillator.

In actual experiments, an interferometric setup (i.e., a fiber ring interferometer, see Fig.6) should be used to separate the squeezed quantum part from the classical soliton pulse and the phase of the local oscillator relative to the phase of the squeezed "vacuum" is adjusted to minimize the noise. Corresponding to this situation, the local oscillator is now given by

$$\mathbf{f_L} = \cos\theta_L \begin{bmatrix} f_{L1} \\ f_{L2} \end{bmatrix} + \sin\theta_L \begin{bmatrix} -f_{L2} \\ f_{L1} \end{bmatrix} \tag{3.14}$$

Here θ_L is the phase adjustment of the local oscillator. Using Eq.(3.14) in the evaluation of Eq.(3.13), one finds the squeezing ratio $R(z)$ is a quadratic function of $\cos\theta_L$ and $\sin\theta_L$.

$$R(z) = A(z)\cos^2\theta_L + 2B(z)\cos\theta_L\sin\theta_L + C(z)\sin^2\theta_L \tag{3.15}$$

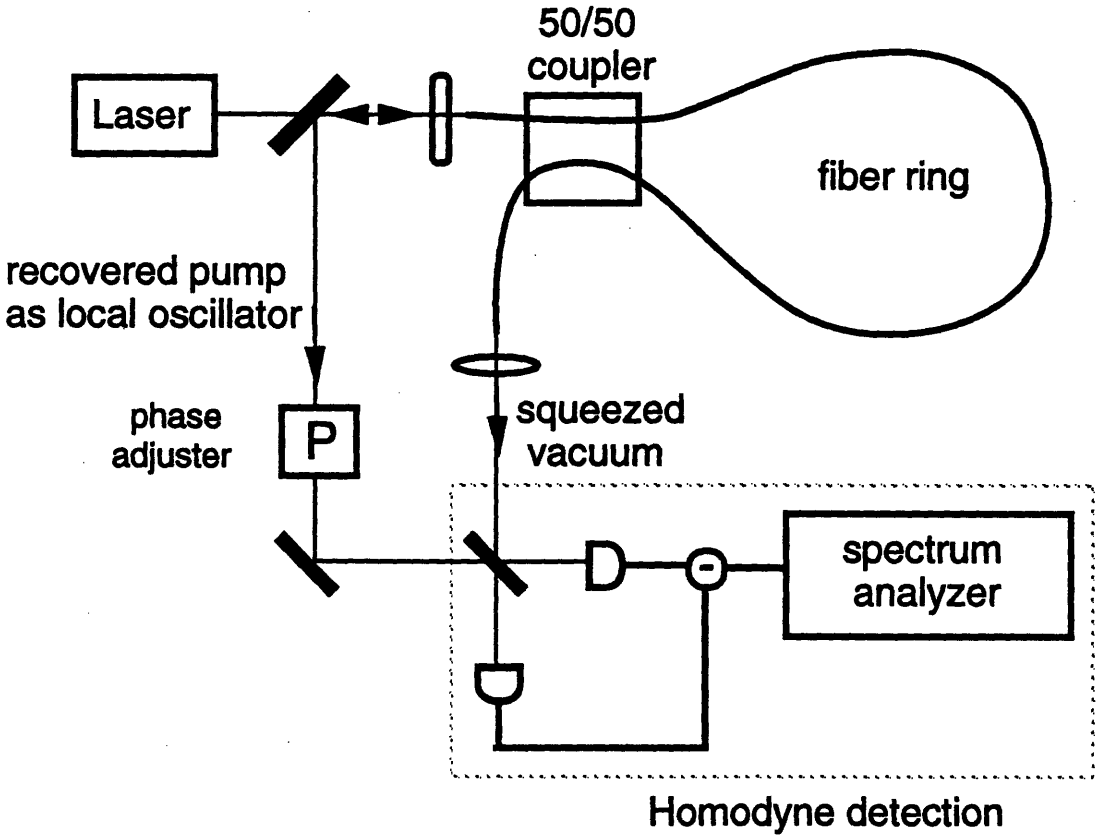

Figure 6: Fiber ring interferometer for squeezing generation

A, B and C are coefficients that can be easily determined. If one defines

$$\begin{bmatrix} F_1 \\ F_2 \end{bmatrix} \equiv \exp[-\mathbf{P}z] \begin{bmatrix} f_{L1} \\ f_{L2} \end{bmatrix} \tag{3.16}$$

$$\begin{bmatrix} F_3 \\ F_4 \end{bmatrix} \equiv \exp[-\mathbf{P}z] \begin{bmatrix} -f_{L2} \\ f_{L1} \end{bmatrix} \tag{3.17}$$

then

$$A(z) = \int [|F_1|^2 + |F_2|^2 - 2\mathrm{Im}(F_1^* F_2)]dz \tag{3.18}$$

$$B(z) = \int [\mathrm{Re}(F_1^* F_3) + \mathrm{Re}(F_2^* F_4) - \mathrm{Im}(F_1^* F_4 + F_3^* F_2)]dz \tag{3.19}$$

$$C(z) = \int [|F_3|^2 + |F_4|^2 - 2\mathrm{Im}(F_3^* F_4)]dz \tag{3.20}$$

The minimum squeezing ratio is then given by

$$R_{min}(z) = \frac{A(z) + C(z) - \sqrt{[A(z) - C(z)]^2 + 4B(z)^2}}{2} \tag{3.21}$$

The recovered soliton pulse can be reused as the local oscillator of the homodyne detection. The squeezing ratio that can be achieved in this way is plotted in Fig.7 as a function of the nonlinear phase shift $\Phi(z)$ and the spectrum analyzer frequency k. One can see that minimum $R(z)$ occurs at $k = 0$ for a fixed $\Phi(z)$. Note that this squeezing is close to, but by no means equal to the optimum result. The squeezing ratio at $k = 0$ is also plotted in Fig. 5 along with the optimum squeezing ratio from Eq.(3.14).

3.4 Squeezing ratio from Hartree approximation

In this section we derive expressions for the squeezing ratio using the Hartree approximation.

From (3.2), we know the homodyne dtection detects the following operator:

$$\begin{aligned} \hat{M}(z) &= \langle \mathbf{f_L}(\tau) | \hat{\mathbf{U}}(\tau) \rangle \\ &\equiv \int [f_{L1}(\tau)\hat{U}_1(\tau) + f_{L2}(\tau)\hat{U}_2(\tau)]d\tau \end{aligned} \tag{3.22}$$

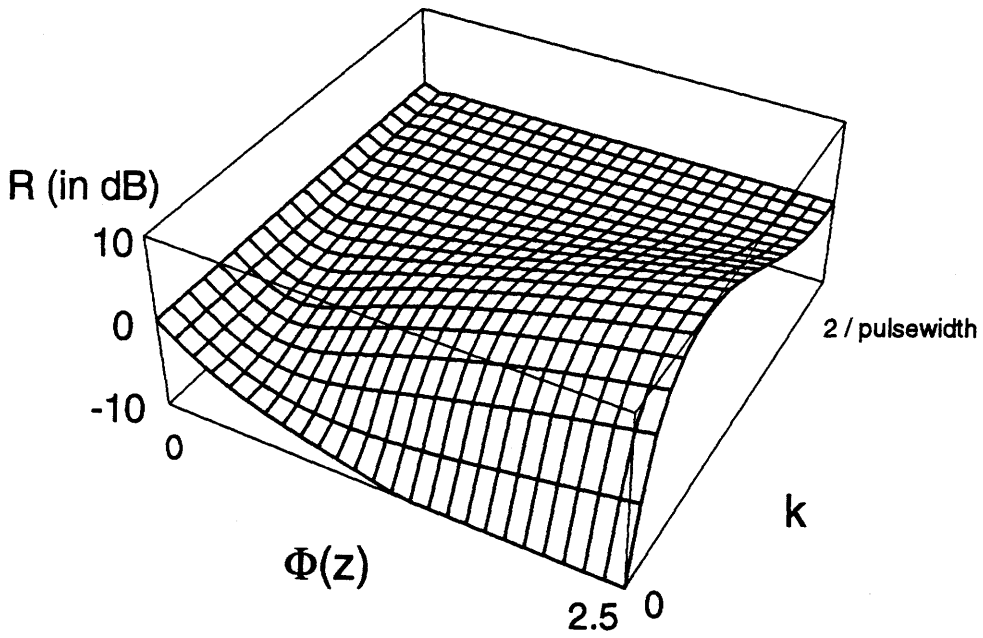

Figure 7 : Squeezing spectrum of solitons in optical fibers

Here we have replaced $\hat{u}(z,\tau)$ by $\hat{U}(\tau)$ because now we are in the Schrödinger picture. For simplicity, we will also assume both f_{L1} and f_{L2} are real functions and $\int(|f_{L1}|^2+|f_{L2}|^2)d\tau = 1$. The variance of the operator $\hat{M}$ then is given by

$$\begin{aligned} \mathrm{Var}[\hat{M}] &\equiv \langle\psi_s|\hat{M}^2|\psi_s\rangle - \langle\psi_s|\hat{M}|\psi_s\rangle^2 \\ &= \tfrac{1}{4}[1+S_1+S_2+S_3] \end{aligned} \tag{3.23}$$

with

$$\begin{aligned} S_1 &= 2\int\int\Big(f_{L1}(\tau_1)f_{L1}(\tau_2)+f_{L2}(\tau_1)f_{L2}(\tau_2)\Big) \\ &\quad\Big[\langle\psi_s|\hat{U}^\dagger(\tau_1)\hat{U}(\tau_2)|\psi_s\rangle - \langle\psi_s|\hat{U}^\dagger(\tau_1)|\psi_s\rangle\langle\psi_s|\hat{U}(\tau_2)|\psi_s\rangle\Big]d\tau_1 d\tau_2 \end{aligned} \tag{3.24}$$

$$\begin{aligned} S_2 &= 2\int\int\Big(f_{L1}(\tau_1)f_{L1}(\tau_2)-f_{L2}(\tau_1)f_{L2}(\tau_2)\Big) \\ &\quad \mathrm{Re}\Big[\langle\psi_s|\hat{U}(\tau_1)\hat{U}(\tau_2)|\psi_s\rangle - \langle\psi_s|\hat{U}(\tau_1)|\psi_s\rangle\langle\psi_s|\hat{U}(\tau_2)|\psi_s\rangle\Big]d\tau_1 d\tau_2 \end{aligned} \tag{3.25}$$

$$\begin{aligned} S_3 &= 4\int\int f_{L1}(\tau_1)f_{L2}(\tau_2) \\ &\quad \mathrm{Im}[\langle\psi_s|\hat{U}(\tau_1)\hat{U}(\tau_2)|\psi_s\rangle - \langle\psi_s|\hat{U}(\tau_1)|\psi_s\rangle\langle\psi_s|\hat{U}(\tau_2)|\psi_s\rangle]d\tau_1 d\tau_2 \end{aligned} \tag{3.26}$$

The first order moment has been given in (2.127) from exact analysis. For the calculation of squeezing ratio, the position spreading effect can be ignored since it is important only after many soliton periods[57]. Thus one has

$$\langle\psi_s|\hat{U}(\tau)|\psi_s\rangle \approx \sum_n |a_n|^2\frac{\alpha_0\sqrt{n}}{2}|c|^{1/2}\exp[i\frac{|c|^2n(n+1)}{4}z]\mathrm{sech}[\frac{1}{2}n|c|\tau] \tag{3.27}$$

Therefore, to evaluate $\mathrm{Var}[\hat{M}]$, one only needs to evaluate the correlation functions of the field operator. Within the Hartree approximation, this is an easy task. Using the (approximate) soliton state constructed in (2.90), one has

$$\begin{aligned} {}_H\langle\psi_s|\hat{U}(\tau_1)\hat{U}(\tau_2)|\psi_s\rangle_H &\approx \textstyle\sum_n a_n^* a_{n+2}\frac{(n+1)\sqrt{n(n+2)}}{4}|c|\exp\left[i\frac{|c|^2(n+1)^2}{2}z\right] \\ &\quad \mathrm{sech}[\tfrac{1}{2}(n+1)|c|\tau_1]\mathrm{sech}[\tfrac{1}{2}(n+1)|c|\tau_2] \end{aligned} \tag{3.28}$$

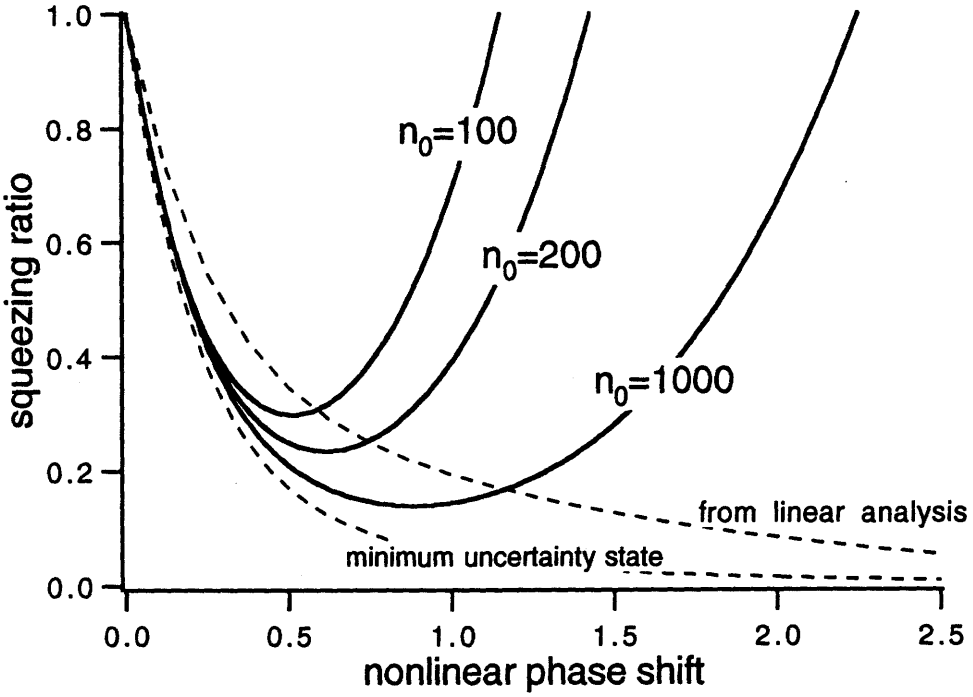

Figure 8 : Squeezing ratio from Hartree approximation

$$
\begin{aligned}
{}_H\langle\psi_s|\hat{U}^\dagger(\tau_1)\hat{U}(\tau_2)|\psi_s\rangle_H \;\approx\; & \textstyle\sum_n a_n^* a_n \frac{n(n-1)}{4}|c| \\
& \operatorname{sech}[\tfrac{1}{2}(n-1)|c|\tau_1]\operatorname{sech}[\tfrac{1}{2}(n-1)|c|\tau_2]
\end{aligned}
\tag{3.29}
$$

Substituting (3.27-29) into (3.23-26), $\mathrm{Var}[\hat{M}]$ and thus the squeezing ratio R can be evaluated numerically. The optimal squeezing ratio for a given local oscillator pulseshape can be obtained readily using the same trick in section 3 of this chapter. The calculated results are shown in Fig.8. There are several interesting things:

1. The squeezing ratio does not decrease monotonically. Eventually it will reach a minimum value and then begins to increase. The reason for this is that when the phase spreading is too large, the shape of joint probability density of the field operators gets bent in order to satisfy the requirement of photon number conservation. This is the difference between the squeezing in a $\chi^{(2)}$ medium and that in a $\chi^{(3)}$ medium[75].

2. However, when the mean photon number gets larger, the minimum point also gets pushed farther and the lowest squeezing ratio gets smaller. This is because when the photon numer (or the field amplitude) becomes larger, the joint probability density can be further stretched without violating the conservation of photon number.

3. In the experiments that have been performed, the photon number of the soliton is of the order of 10^7 or higher. Therefore the minimum point is far off and cannot be observed.

4. Initially, the decreasing of the squeezing ratio from Hartree approximation is steeper than that from the linearization approximation. Strictly speaking, the two figures correspond to two different problems. In the Heisenberg picture under the linearization approximation, we are solving the initial value problem with a vacuum state injection, while in the Schrödinger picture, we are solving the eigenvalue problem and then superimpose eigenstates to construct the soliton state. The soliton state constructed in this way seems to have a smaller

phase noise compared to the quantum state with a vacuum state injection. However, as can be also seen in Fig.8, the phase noise of the Hartree state is still bigger than that of the (ideal) minimun uncertainty state.

3.5 Soliton gyros with squeezed vacuum injection

As an application of the theory developed in the chapter, we are going to consider the following fiber gyro setup (Fig.9). The whole setup contains two fiber loops (both loops are nonlinear). The first loop acts as the squeezer while the second loop is the gyro. The squeezed "vacuum" from the squeezer is injected into the gyro to improve the signal-to-noise ratio. The recovered soliton pulse from the other port of the squeezer is also injected into the gyro to act as the pump. Non-reciprocal couplers are required to direct the squeezed "vacuum" into the gyro and to completely recover the pump. Before entering the gyro, there is a phase shifter that can adjust the relative phase between the squeezed "vacuum" and the pump. Homodyne detection is used to detect the signal from one of the output ports of the gyro and the soliton pulse from the other output port is reused as the local oscillator. Maximum signal energy is achieved by adjusting the phase of the local oscillator while the minimum noise energy is achieved by adjusting the relative phase between the squeezed "vacuum" and the pump (or the local oscillator). As can be shown easily, the signal energy for such gyro setup is given by

$$S = F n_s n_L (\Delta\phi)^2 \tag{3.30}$$

Here n_s is the photon number in one arm of the gyro, n_L is the photon number of the local oscillator, $\Delta\phi$ is phase imbalance of the gyro and F is the pulse-matching factor ($0 \leq F \leq 1$).

$$F = \frac{|\langle \mathbf{f_L}|\mathbf{f_s}\rangle|^2}{\langle \mathbf{f_L}|\mathbf{f_L}\rangle\langle \mathbf{f_s}|\mathbf{f_s}\rangle} \tag{3.31}$$

If we use the same soliton pulse as the oscillator ($\mathbf{f_L} \propto \mathbf{f_s}$), $F = 1$. The noise energy

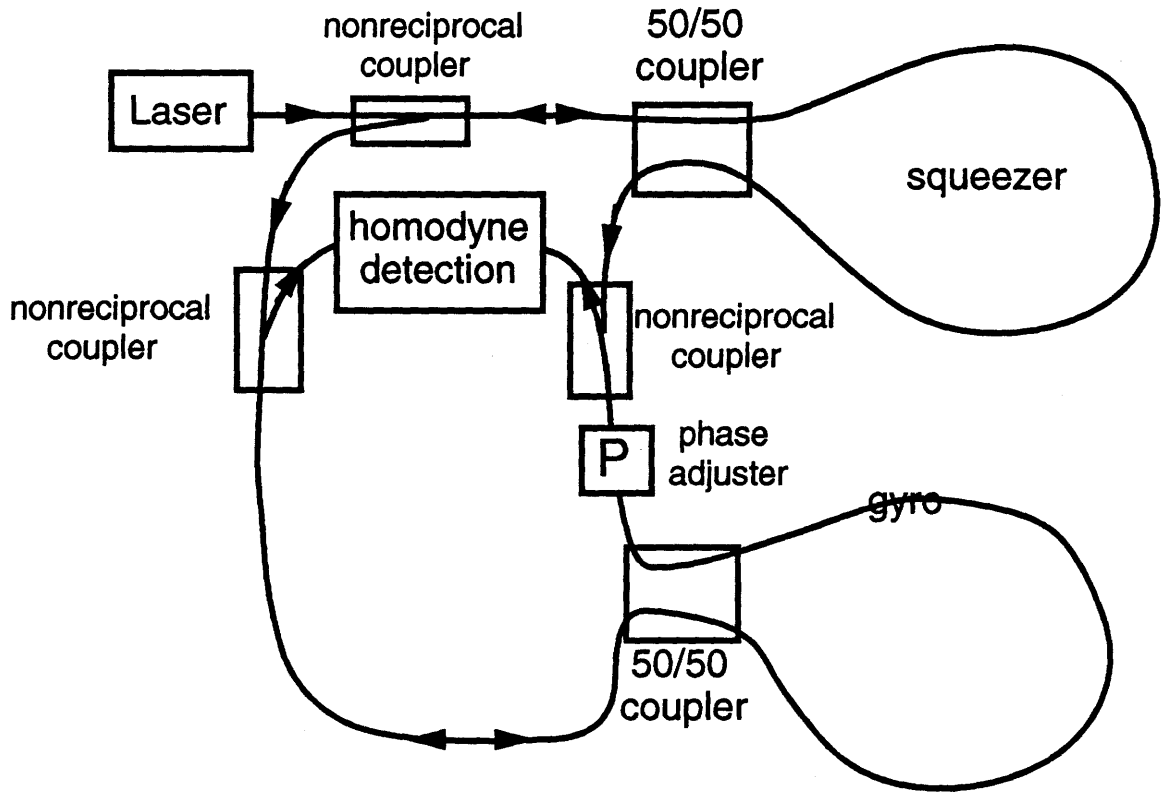

Figure 9: Fiber ring gyro with squeezed vacuum injection

is given by

$$N = \frac{n_L}{4} R \tag{3.32}$$

Here R is the squeezing ratio. When $R = 1$, it is simply the shot noise level. The signal-to-noise ratio then is

$$S/N = \frac{4Fn_s}{R}(\Delta\phi)^2 \tag{3.33}$$

It is now obvious that in order to maximize the signal-to-noise ratio S/N, one needs to minimize the squeezing ratio R.

If the gyro loop is linear, then the squeezing ratio is just what we have calculated in section 3 of this chapter. In this case, if we can shape the soliton pulse from the gyro into the optimum local oscillator pulse shape determined in section 2 of this chapter before it enters the homodyne detector, then in fact we can achieve the optimum squeezing ratio predicted by Eq.(3.8). In practice, this could be achieved by using the femtosecond pulseshaping technique developed by A.M. Weiner et. al[67]. This process could be quite lossy. Since the energy of the local oscillator does not enter in the expression of S/N, the performance of the gyro is not affected as long as the energy of the local oscillator is large enough that the quantum noise dominantes. However, the pulse matching factor F is reduced due to the mismatch between the local oscillator and the signal.

If the gyro loop is nonlinear, then the analysis can only be done numerically. This is because once we rotate the phase of the squeezing "vacuum" relative to the pump before it enters the gyro loop, we have destroyed the orthogonality between the soliton part and the continuum. In Ref.[68], it has been shown that for a gaussian pulse in the dispersionless region, the nonlinearity of the gyro always degrades the overall squeezing. We expect the same statement to be true also for solitons. The question then is how bad is the degradation ?

The method developed in section 3 of this chapter can be applied equally well here. Now the output quantum part is related to the input quantum part by

$$\hat{\mathbf{u}}(z_s + z_g, \tau) = \exp[\mathbf{P}z_g]\mathbf{R}[\theta]\exp[\mathbf{P}z_s]\hat{\mathbf{u}}(0, \tau) \tag{3.34}$$

Here z_s and z_g are lengths of the squeezer and gyro respectively, which also represent the nonlinearities in the squeezer and gyro. $\exp[\mathbf{P}z_g]$ and $\exp[\mathbf{P}z_g]$ are the "propagators" of the squeezer and gyro respectively, and $\mathbf{R}[\theta]$ is the phase rotation matrix

$$\mathbf{R}[\theta] = \begin{bmatrix} \cos\theta & \sin\theta \\ -\sin\theta & \cos\theta \end{bmatrix} \tag{3.35}$$

The operator measured by the homodyne detection is the squared-magnitude of the following operator:

$$\begin{aligned} \langle \mathbf{f_L}(\tau)|\hat{\mathbf{u}}(\mathbf{z_s}+\mathbf{z_g},\tau)\rangle &= \langle \mathbf{f_L}(\tau)|\exp[\mathbf{P}z_g]\mathbf{R}[\theta]\exp[\mathbf{P}z_s]\hat{\mathbf{u}}(\mathbf{0},\tau)|0\rangle \\ &= \langle \exp[\mathbf{P^A}z_s]\mathbf{R}[-\theta]\exp[\mathbf{P^A}z_g]\mathbf{f_L}(\tau)|\hat{\mathbf{u}}(\mathbf{0},\tau) \\ &\equiv \langle \mathbf{F_L}(z_s+z_g,\tau)|\hat{\mathbf{u}}(\mathbf{0},\tau)\rangle \end{aligned} \tag{3.36}$$

Again, the squeezing ratio can be calculated according to equation (3.13).

$$\begin{aligned} R = \int \Big[& |F_{L1}(z_s+z_g,\tau)|^2 + |F_{L2}(z_s+z_g,\tau)|^2 \\ & -2\mathrm{Im}[|F^*_{L1}(z_s+z_g,\tau)F_{L2}(z_s+z_g,\tau)] \Big] d\tau \end{aligned} \tag{3.37}$$

The minimization of R can be easily achieved using the same trick we used at the end of section 3 of this chapter. The minimum squeezing ratio with the same soliton pulse as the local oscillator is plotted in Fig. 10 as a function of the nonlinear phase shift in the squeezer (Φ_s) and in the gyro (Φ_g). One can see that as the nonlinearity in the gyro loop becomes comparable to the nonlinearity in the squeezer loop, it quickly destroys the magnitude of the overall squeezing. Compared to the cases using square pulses Fig. 11 and gaussian pulses Fig. 12 in the dispersionless region, one can see that the effect of the nonlinearity of the gyro loop is more severe for the scheme using solitons than that using square pulses. Nevertheless, the achievable squeezing ratio using solitons is much better than that using gaussian pulses. The reasons are as follows. The squeezing direction is not a constant across a gaussian and thus the local oscillator cannot match the minimum squeezing direction at any point without performing pulse shaping. So the performance of gaussian pulses

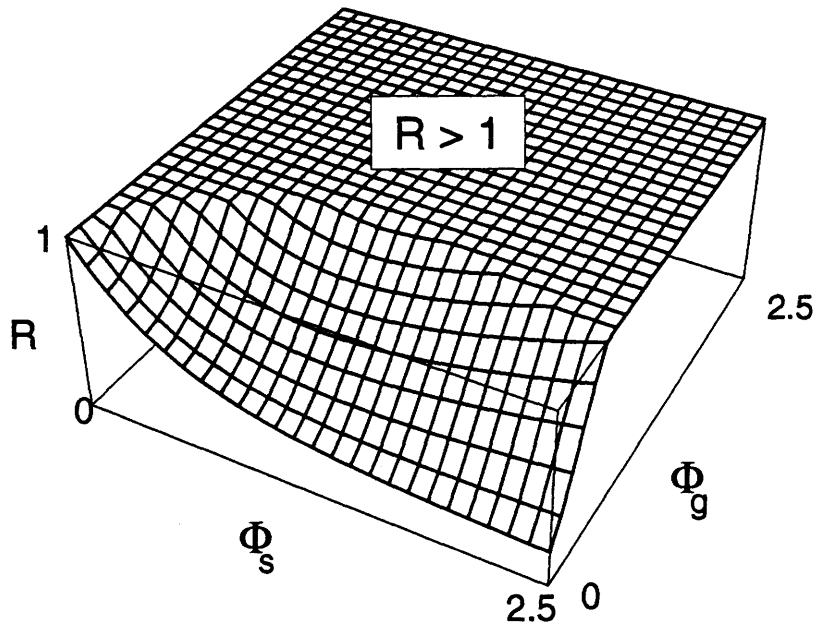

Figure 10 : Squeezing ratio of fiber gyros using solitons.
We cut the portion with R > 1 (the flat region).

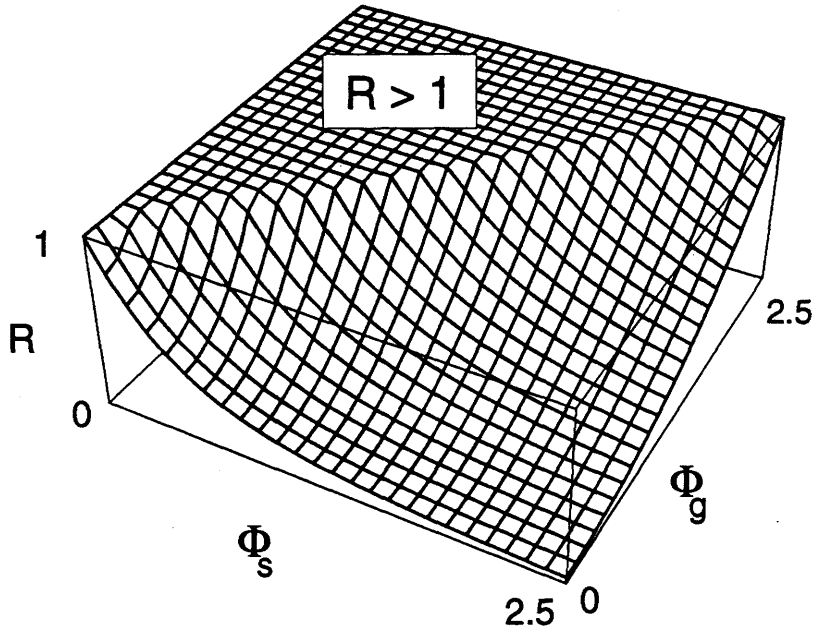

Figure 11 : Squeezing ratio of fiber gyros using square pulses.
We cut the portion with R > 1 (the flat region).

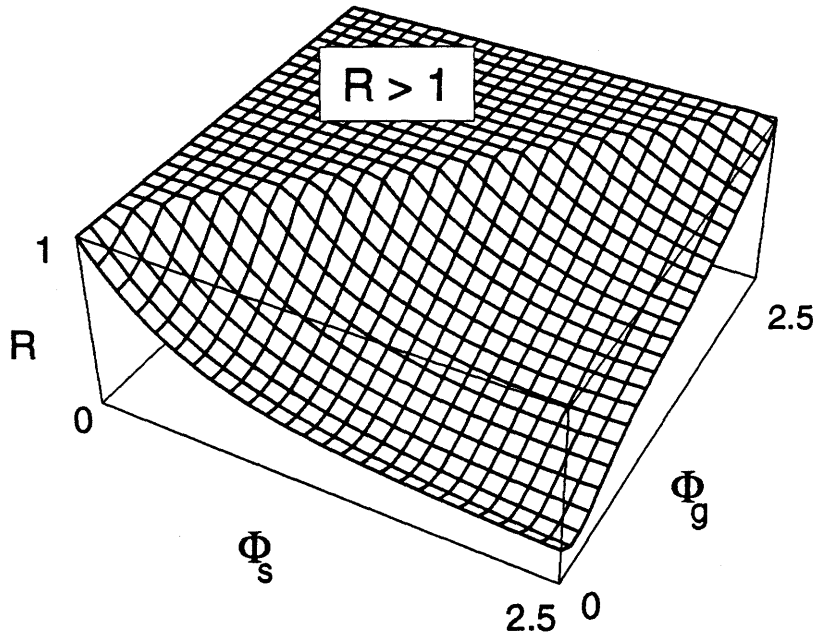

Figure 12 : Squeezing ratio of fiber gyros using gaussian pulses
We cut the portion with R > 1 (the flat region).

is the worst of the three. Solitons have a constant phase and thus do not have this problem. However, as we have explained, the continuum in the squeezer is coupled to the soliton parts in the gyro due to the phase rotation. There is no way to discriminate them. Moreover, since we use the same soliton pulse as the local oscillator, parts of the continuum in the gyro loop also enter the homodyne detection. These two effects make the scheme using solitons more sensitive to the nonlinearity in the gyro loop.

Chapter 4

Solitons in optical fibers with loss and periodic amplification

In long-haul communication systems, Er-doped fiber amplifers are used to compensate the loss of optical fibers (see Fig.13). When the spacing between amplifiers is small compared to the soliton period, the soliton can maintain itself and a equivalent nonlinear Schrödinger equation can be derived. The quantum theory developed in Chapter 2 using the linearization aproach is generalized to take into account the noises introduced by loss and gain.

4.1 The equivalent nonlinear Schrödinger equation

The normalized Schrödinger equation for the fiber with loss is given by

$$i\frac{\partial}{\partial z}U(z,\tau) = -\frac{\partial^2}{\partial \tau^2}U(z,\tau) + 2c|U(z,\tau)|^2U(z,\tau) - i\Gamma U(z,\tau) \tag{4.1}$$

If the attenuation per section is large and the dispersion and phase shift are small, one may treat the GVD and the nonlinearity as perturbations. In this way, one can write

$$U(z,\tau) = U_1(z,\tau)\exp[-\Gamma z] \tag{4.2}$$

with $U_1(z,\tau)$ is a slowly varying function of z compared to $\exp[-\Gamma z]$. Substituting Eq.(4.2) into Eq.(4.1), one has

$$i\frac{\partial}{\partial z}U_1(z,\tau) = -\frac{\partial^2}{\partial \tau^2}U_1(z,\tau) + 2e^{-2\Gamma z}c|U_1(z,\tau)|^2U_1(z,\tau) \tag{4.3}$$

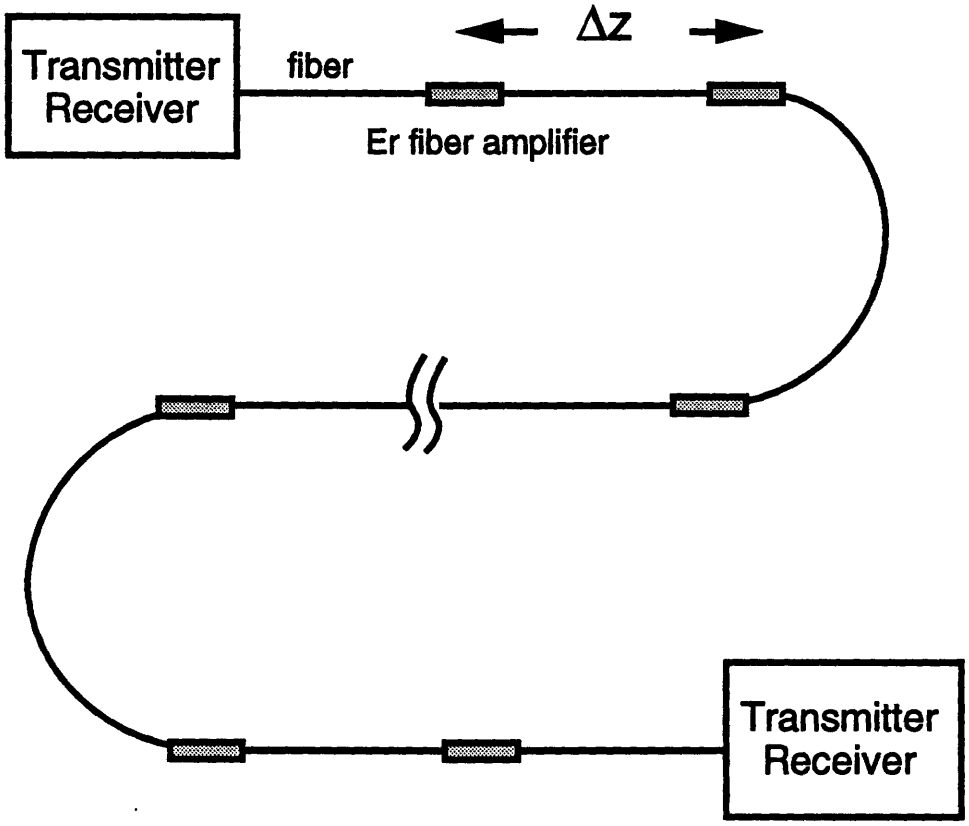

Figure 13: Lomg-haul communication systems using solitons

The change of U_1 after a distance Δz (the spacing between amplifiers) is

$$\begin{aligned} \Delta U_1(z,\tau) &= i\Delta z\frac{\partial^2}{\partial\tau^2}U_1(z,\tau) - i2c[\int_0^{\Delta z} e^{-2\Gamma z}dz]|U_1(z,\tau)|^2U_1(z,\tau) \\ &= i\Delta z\frac{\partial^2}{\partial\tau^2}U_1(z,\tau) - i2c\frac{1-e^{-2\Gamma\Delta z}}{2\Gamma}|U_1(z,\tau)|^2U_1(z,\tau) \end{aligned} \tag{4.4}$$

Treating the length Δz of the fiber as a differential with regard to the perturbations by GVD and the nonlinearity, we have a new Schrödinger equation[56]

$$i\frac{\partial}{\partial z}U_1(z,\tau) = -\frac{\partial^2}{\partial\tau^2}U_1(z,\tau) + 2cr^2|U_1(z,\tau)|^2U_1(z,\tau) \tag{4.5}$$

with the nonlinear coefficient scaled by a factor $r^2 \neq 1$

$$r^2 = \frac{1-e^{-2\Gamma\Delta z}}{2\Gamma\Delta z} \tag{4.6}$$

Therefore, the shape of the "soliton" that would be preserved in this new system is

$$\begin{aligned} U_o(z,\tau) &= \frac{n_o\tau\sqrt{|c|}}{2}\mathrm{sech}\left[\frac{n_o\tau^2|c|}{2}(\tau - T_o - 2p_oz)\right] \\ &\quad \exp\left[i\frac{n_o^2\tau^4|c|^2}{4}z - ip_o^2z + ip_o\tau + \theta_o\right] \end{aligned} \tag{4.7}$$

It should be noted that the "soliton" solution (4.7) behaves soliton-like only globally, i.e., when each section between amplifying stages is treated as a differential distance. Between the amplifiers, the pulse decays essentially without change of width and, thus, does not behave soliton-like. We were able to derive an equivalent lossfree nonlinear Schrödinger equation, because the effects of GVD and of the Kerr nonlinearity within one amplifier spacing is very weak so that the contribution to the pulse shaping could be treated as a differential contribution.

The derivation in this section also can be used in the quantum theory except that in the quantum theory both loss and gain introduce noise operators. Therefore, in the quantum theory one now has the following linearized equation :

$$i\frac{\partial}{\partial z}\hat{U}(z,\tau) = -\frac{\partial^2}{\partial\tau^2}\hat{U}(z,\tau) - 2r^2|c|\hat{U}^\dagger(z,\tau)\hat{U}(z,\tau)\hat{U}(z,\tau) + \hat{n}(z,\tau) \tag{4.8}$$

The question is what is the properties of the noise operator $\hat{n}(z,\tau)$? We will deal with this problem in next section.

4.2 Introduction of loss and gain in quantum theory

In the quantum theory, the properties of the noise operators introduced by loss or gain can be obtained by requiring the conservation of commutation brackets. They can be determined by temporarily ignoring the nonlinearity and dispersion. The simplified equation is

$$\frac{d}{dz}\hat{u}(z,\tau) = -\Gamma\hat{u}(z,\tau) + \hat{\beta}(z,\tau) \tag{4.9}$$

where $\hat{\beta}$ is the noise source. Conservation of commutator brackets requires that[64,65]

$$[\hat{\beta}(z,\tau), \hat{\beta}^{\dagger}(z',\tau')] = 2\Gamma\delta(z-z')\delta(\tau-\tau') \tag{4.10}$$

One may integrate Eq.(4.9) to obtain

$$\hat{u}(\Delta z,\tau) = e^{-\Gamma\Delta z}\int_0^{\Delta z} e^{\Gamma z}\hat{\beta}(z,\tau)dz + \hat{u}(0,\tau)e^{-\Gamma\Delta z} = \hat{N}(\tau) + \hat{u}(0,\tau)e^{-\Gamma\Delta z} \tag{4.11}$$

where

$$\hat{N}(\tau) \equiv e^{-\Gamma\Delta z}\int_o^{\Delta z} e^{\Gamma z}\hat{\beta}(z,t)dz \tag{4.12}$$

We find the commutator of $\hat{N}$ from

$$\begin{aligned}[\hat{N}(\tau), \hat{N}^{\dagger}(\tau')] &= e^{-2\Gamma\Delta z}\int_o^{\Delta z} dz \int_0^{\Delta z} dz' e^{\Gamma(z+z')}[\hat{\beta}(z,\tau), \hat{\beta}^{\dagger}(z',\tau')] \\ &= 2\Gamma e^{-2\Gamma\Delta z}\int_o^{\Delta z} dz e^{2\Gamma z} = (1-e^{-2\Gamma\Delta z})\delta(\tau-\tau')\end{aligned} \tag{4.13}$$

The signal and noise source are amplified by the gain $\sqrt{G} = \exp[\Gamma\Delta z]$. Then the continuum limit is introduced so that the distributed noise source due to the loss, $\hat{n}_l(z,\tau)$ is defined by

$$\hat{n}_l(z,\tau) \equiv \frac{\sqrt{G}\hat{N}}{\Delta z} \tag{4.14}$$

with the commutator

$$[\hat{n}_l(z,\tau),\hat{n}_l^\dagger(z,\tau')] = \frac{G(1-e^{-2\Gamma\Delta z})}{\Delta z}\delta(z-z')\delta(\tau-\tau') = \frac{G-1}{\Delta z}\delta(z-z')\delta(\tau-\tau') \tag{4.15}$$

The reservoir of the noise source is in the ground state (approximately), because at room temperature $\hbar\omega_o \gg kT$. The gain introduces noise of its own. The noise source has the commutator bracket

$$[\hat{n}_g(z,\tau),\hat{n}_g^\dagger(z',\tau')] = -\frac{(G-1)}{\Delta z}\delta(z-z')\delta(\tau-\tau') \tag{4.16}$$

where, again, we made it into a distributed source by division by Δz. The commutator is negative, indicating that the operator $\hat{n}_g$ is a creation operator, $\hat{n}_g^\dagger$ an annihilation operator.

The total noise operator in (4.8) is thus given by

$$\hat{n}(z,\tau) = \hat{n}_l(z,\tau) + \hat{n}_g(z,\tau) \tag{4.17}$$

Note that the commutator of $\hat{n}(z,\tau)$ is equal to zero. This is as it must be if the equivalent "lossless" nonlinear Schrödinger equation is to conserve commutator brackets.

For the noise source associated with the loss, $\langle\hat{n}_l^\dagger\hat{n}_l\rangle$ is zero since the reservoir of the noise source is also in the ground state. On the other hand, for the noise source associated with the gain, $\langle\hat{n}_g\hat{n}_g^\dagger\rangle$ is zero if one assumes total inversion. Using these facts along with the commutation relations, one can calculate fluctuations introduced by these operators. As an example, if one defines

$$\hat{n}_f(z) = \langle\mathbf{f}(\tau)|\hat{\mathbf{n}}(z,\tau)\rangle \tag{4.18}$$

then the autocorrelation of this new defined noise operator is

$$\langle\hat{n}_f(z)\hat{n}_f(z')\rangle = \frac{G-1}{2\Delta z}\int|f(\tau)|^2 d\tau\delta(z-z') \tag{4.19}$$

4.3 Linearization approximation and Gordon-Haus limit

Equation (4.8) can be solved by using the same linearization approach developed in Chapter 2, section 3. Linearizing Eq.(4.8) around the classical soliton solution, one has

$$\begin{aligned}\frac{\partial}{\partial z}\delta\hat{u}(z,\tau) &= i[\tfrac{\partial^2}{\partial\tau^2} - \tfrac{n_o^2|c|^2}{4} + 4|c|r^2|U_o(0,\tau)|^2]\hat{u}(z,\tau) \\ &\quad +i2|c|r^2|U_o(0,\tau)|^2\hat{u}^\dagger(z,\tau) + \hat{n}(z,\tau)\end{aligned} \tag{4.20}$$

Applying the projections (2.61)-(2.64) to both sides of (4.20) with $|c|$ replaced by $|c|r^2$, one obtains the evolution equations of the soliton operators.

$$\frac{d}{dz}\Delta\hat{n}(z) = \hat{n}_n(z) \tag{4.21}$$

$$\frac{d}{dz}\Delta\hat{\theta}(z) = \frac{n_o|c|^2}{2}\Delta\hat{n}(z) + \hat{n}_\theta(z) \tag{4.22}$$

$$\frac{d}{dz}\Delta\hat{p}(z) = \hat{n}_p(z) \tag{4.23}$$

$$\frac{d}{dz}\Delta\hat{T}(z) = 2\Delta\hat{p}(z) + \hat{n}_T(z) \tag{4.24}$$

Here the four noise operators are defined by

$$\Delta\hat{n}_n(z) = \frac{\langle\underline{\mathbf{f}}_\mathbf{n}(\tau)|\hat{\mathbf{n}}(z,\tau)\rangle}{\langle\underline{\mathbf{f}}_\mathbf{n}(\tau)|\mathbf{f}_\mathbf{n}(\tau)\rangle} = 2\langle\underline{\mathbf{f}}_\mathbf{n}(\tau)|\hat{\mathbf{n}}(z,\tau)\rangle \tag{4.25}$$

$$\Delta\hat{n}_\theta(z) = \frac{\langle\underline{\mathbf{f}}_\theta(\tau)|\hat{\mathbf{n}}(z,\tau)\rangle}{\langle\underline{\mathbf{f}}_\theta(\tau)|\mathbf{f}_\theta(\tau)\rangle} = 2\langle\underline{\mathbf{f}}_\theta(\tau)|\hat{\mathbf{n}}(z,\tau)\rangle \tag{4.26}$$

$$\Delta\hat{n}_p(z) = \frac{\langle\underline{\mathbf{f}}_\mathbf{p}(\tau)|\hat{\mathbf{n}}(z,\tau)\rangle}{\langle\underline{\mathbf{f}}_\mathbf{p}(\tau)|\mathbf{f}_\mathbf{p}(\tau)\rangle} = \frac{2}{n_o}\langle\underline{\mathbf{f}}_\mathbf{p}(\tau)|\hat{\mathbf{n}}(z,\tau)\rangle \tag{4.27}$$

$$\Delta\hat{n}_T(z) = \frac{\langle\underline{\mathbf{f}}_\mathbf{T}(\tau)|\hat{\mathbf{n}}(z,\tau)\rangle}{\langle\underline{\mathbf{f}}_\mathbf{T}(\tau)|\mathbf{f}_\mathbf{T}(\tau)\rangle} = \frac{2}{n_o}\langle\underline{\mathbf{f}}_\mathbf{T}(\tau)|\hat{\mathbf{n}}(z,\tau)\rangle \tag{4.28}$$

Using Eq.(4.19), the autocorrelation of these noise operators can be calculated :

$$\langle\hat{n}_n(z)\hat{n}_n(z')\rangle = 2\frac{G-1}{\Delta z}n_o\delta(z-z') \tag{4.29}$$

$$\langle\hat{n}_\theta(z)\hat{n}_\theta(z')\rangle = 2\frac{G-1}{\Delta z}\quad\frac{0.607}{n_o}\delta(z-z') \tag{4.30}$$

$$\langle\hat{n}_p(z)\hat{n}_p(z')\rangle = 2\frac{G-1}{\Delta z}\frac{n_o|c|^2r^4}{12}\delta(z-z') \tag{4.31}$$

$$\langle \hat{n}_T(z)\hat{n}_T(z')\rangle = 2\frac{G-1}{\Delta z}\frac{3.29}{n_o^3|c|^2r^4}\delta(z-z') \tag{4.32}$$

All the cross-correlations are zero.

The solutions of Eq.(4.21)-(4.24) are

$$\Delta\hat{n}(z) = \Delta\hat{n}(0) + \int_0^z \hat{n}_n(z')dz' \tag{4.33}$$

$$\Delta\hat{\theta}(z) = \Delta\hat{\theta}(0)++\int_0^z \hat{n}_\theta(z')dz' + \frac{n_o|c|^2}{2}z\Delta\hat{n}(0) + \frac{n_o|c|^2}{2}\int_0^z\int_0^{z'} n_n(z")dz"dz' \tag{4.34}$$

$$\Delta\hat{p}(z) = \Delta\hat{p}(0) + \int_0^z \hat{n}_p(z')dz' \tag{4.35}$$

$$\Delta\hat{T}(z) = \Delta\hat{T}(0) + \int_0^z \hat{n}_T(z')dz' + 2z\Delta\hat{p}(0) + 2\int_0^z\int_0^{z'} \hat{n}_p(z")dz"dz' \tag{4.36}$$

The variances of these operators can be calculated using Eq.(4.29)-(4.36). As an example, the position uncertainty is

$$\langle\Delta\hat{T}^2(z)\rangle = A_o + A_1 z + A_2 z^2 + A_3 z^3 \tag{4.37}$$

with

$$A_0 = \langle\Delta\hat{T}^2(0)\rangle = \frac{3.29}{n_o^3|c|^2r^4} \tag{4.38}$$

$$A_1 = 2\frac{G-1}{\Delta z}\langle\Delta\hat{T}^2(0)\rangle = \frac{6.6}{n_o^3|c|^2r^4}\frac{G-1}{\Delta z} \tag{4.39}$$

$$A_2 = 4\langle\Delta\hat{p}^2(0)\rangle = \frac{n_o|c|^2r^4}{3} \tag{4.40}$$

$$A_3 = \frac{8}{3}\frac{G-1}{\Delta z}\langle\Delta\hat{p}^2(0)\rangle = \frac{2n_o|c|^2r^4}{9}\frac{G-1}{\Delta z} \tag{4.41}$$

The cubic dependence on z is due to the random walk of the momentum (frequency). The quadratic dependence on z is due to the initial fluctuation of the momentum (frequency). The linear dependence on z is due to the noise-source produced displacement. The constant term is the initial fluctuations of the position.

When z is large, only the cubic term is important. This term reduces to Eq.(16) of Ref.[8] when $r = 1$ and $G - 1 = 2\Gamma\Delta z$, the case treated there. It is known as the Gordon-Haus limit for communication systems using solitons because it places

a upper limit on the product of bit rate (R) and transmission length (z) [8]. To see this, from (4.37) [keeping only the z^3 term], one has

$$R^3 z^3 = \frac{R^3 \langle \Delta \hat{T}^2(z) \rangle}{A_3} \tag{4.42}$$

To achieve a 10^{-9} error rate, assuming a Gaussian distribution one must have

$$\langle \Delta \hat{T}^2(z) \rangle \leq (\frac{t_w}{6.1})^2 \tag{4.43}$$

Here $2t_w$ is the window of detector acceptence for a soliton and usually $t_w = 1/(3R)$. Also note that $n_o|c|r^2/2 = 1.763/t_s$ with t_s being the full width at half power of the solitons and usually $t_s = 1/(10R)$. If one follows these usual design rules, Eq.(4.42) becomes

$$R^3 z^3 \leq 3.8 \times 10^{-4} \frac{\Delta z}{G-1} \tag{4.44}$$

Note that in (4.44), R, z and Δz are normalized quantities. Transforming back to unnormalized quantities, one has

$$\text{bitrate} \times \text{distance} \leq 1.6 \times 10^{13} \left[\frac{\text{spacing}}{G-1}\right]^{1/3} \qquad \text{(km/sec)}$$

If one assumes the spacing between amplifiers is 40km and $G = 10$, one has

$$\text{bitrate} \times \text{distance} \leq 2.6 \times 10^{13} \qquad \text{(km/sec)}$$

With a $10GHz$ bitrate, the maximum transmission distance would be about 2,600km.

One interesting problem is how to overcome the Gordon-Haus limit. One approach is to put a intensity modulator (driven by a microwave source) in the link to directly limit the position spreading. Recently the group at NTT, Japan has claimed that they are able to transmit information at a bit rate as high as 10 Gbit/sec over 1M km[76] using this scheme. Another approach is to introduce bandwidth limitting elements in the link to limit the random walk of the frequency. Right now these are still active research topics.

4.4 Numerical analysis

The numerical approach developed in section 3, chapter 3 also can be applied to soliton-like systems with additional noises. This provides a general method to perform noise analysis of such systems.

The evolution equation of the perturbation field operator is now given by

$$\frac{\partial}{\partial z}\hat{\mathbf{u}}(z,\tau) = \mathbf{P}\hat{\mathbf{u}}(z,\tau) + \hat{n}(z,\tau) \tag{4.45}$$

Here $\mathbf{P}$ is the linear operator given in (2.30-32) and $\hat{n}(z,\tau)$ is the noise operator.

Equation (4.45) has the following formal solution:

$$\hat{\mathbf{u}}(z,\tau) = \exp[\mathbf{P}z]\hat{\mathbf{u}}(0,\tau) + \int_0^z \exp[\mathbf{P}(z-z')]\hat{n}(z',\tau)dz' \tag{4.46}$$

Taking the projection and transfer the operator from the right to the left, one obtains

$$\begin{aligned} \hat{M}(z) &\equiv \langle \mathbf{f_L}(\tau)|\hat{\mathbf{u}}(\mathbf{z},\tau)\rangle \\ &= \langle \mathbf{F_L}(z,\tau)|\hat{\mathbf{u}}(\mathbf{0},\tau)\rangle + \int_0^z \langle \mathbf{F_L}(z-z',\tau)|\hat{n}(z',\tau)\rangle dz' \end{aligned} \tag{4.47}$$

If one assumes the noise is white and has a noise strengh

$$\langle \hat{n}(z,\tau)\hat{n}^\dagger(z',\tau') + \hat{n}^\dagger(z,\tau)\hat{n}(z',\tau')\rangle = N_o\delta(z-z')\delta(\tau-\tau') \tag{4.48}$$

then

$$\langle \hat{M}^\dagger(z)\hat{M}(z)\rangle = \frac{1}{4}[R(z) + N_o\int_0^z R(z')dz'] \tag{4.49}$$

with $R(z)$ given in (3.13). The first term in (4.49) is the quantum noise while the second term is the spreading due to $\hat{n}(z,\tau)$.

For the soliton problem treated in this chapter, the numerical analysis gives the same results as those obtained analytically. This is because for the nonlinear Schrödinger equation, the soliton part and the continumm are not coupled and therefore both approaches are exact under the linearization approximation. However, for other soliton-like systems, if the soliton part is coupled to the continuum, then analytical expressions can be obtained only through approximations and it becomes necessary to compare the analytical solution with the numerical solution. Right now this is also an active research topic.

Chapter 5

Self-induced transparency solitons

Let us consider a medium consisted of a collection of two-level atoms with their resonance frequencies centered around a certain value ζ. If all the atoms are in the ground state and a optical pulse with a carrier frequency around ζ is sent into the medium, then in most cases the optical pulse will experience strong absorption due to the resonant interaction with the medium. However, if both the dephasing time and the carrier relaxation time of the medium are long, a special class of optical pulses [the self-induced transparency (SIT) solitons] can propagate through the medium without experiencing appreciable absorption. This is the well-known self-induced transparency effect and the physical picture is as follows. The front part of the pulse gets absorbed. This excites electrons from the ground state to the upper state. The electrons later return to the ground state and amplify the back part of the pulse. Therefore, the net effect is simply a slowing-down of the propagation of the pulse while the pulse shape remains unchanged. The objective of this chapter is to develop a rigorous quantum theory for these SIT solitons. We first review the conventional semiclassical theory of SIT solitons based on the Zakharov-Shabat inverse scattering transform. Since the nonlinear Schrödinger equation also can be solved in the same framework of Zakharov-Shabat inverse scattering transform, some of the results in section 2.3 [especially, (2.61)-(2.64)] can be applied to the present problem. With these results, we then quantized the problem in the "scattering data" space under the linearization approximation. Squeezing effects of SIT solitons are then studied.

5.1 Semiclassical formulation

The SIT problem is modeled by the following set of equations and boundary

conditions (see Appendix 2):

$$\frac{\partial}{\partial\tau}V_1(z,\tau,\zeta)+i\zeta V_1(z,\tau,\zeta)=\frac{1}{2}U(z,\tau)V_2(z,\tau,\zeta) \tag{5.1}$$

$$\frac{\partial}{\partial\tau}V_2(z,\tau,\zeta)-i\zeta V_2(z,\tau,\zeta)=-\frac{1}{2}U^*(z,\tau)V_1(z,\tau,\zeta) \tag{5.2}$$

$$\frac{\partial}{\partial z}U(z,\tau)=2\langle V_2^*(z,\tau,\zeta)V_1(z,\tau,\zeta)\rangle \tag{5.3}$$

$$V_1(z,-\infty,\zeta)=1 \tag{5.4}$$

$$V_2(z,-\infty,\zeta)=0 \tag{5.5}$$

Here τ is the normalized time, z is the normalized propagation distance, ζ is the normalized frequency deviation, V_1, V_2 are the complex conjugates of the slowly varying amplitudes of the wavefunctions of the two-level atoms and $U(z,\tau)$ is the normalized electric field which represents the photon flux (that is, $\int|U|^2d\tau=$ photon number). We use capital letters for the independent variables in anticipation of the linearization. Small signal variables will be denoted by lower case letters. The brackets in Eq.(5.3) represent an average over all two-level atoms:

$$\langle\ldots\rangle\equiv\int g(\zeta)\ldots d\zeta \tag{5.6}$$

where $g(\zeta)$ is the distribution of two-level atoms over the (normalized) resonance frequencies ζ. Equations (5.1) and (5.2) are just the Zakharov-Shabat equations.

Equation (5.4)-(5.5) have the following 2π soliton solution :

$$U_o(z,\tau)=4\frac{i\rho_1(0)\exp[\frac{i}{2}\langle\frac{1}{\zeta-(\alpha+i\beta)}\rangle z]\exp[-2i(\alpha+i\beta)\tau]}{1+|\frac{\rho_1(0)}{2\beta}|^2\exp[-\langle\frac{\beta}{(\zeta-\alpha)^2+\beta^2}\rangle z]\exp(4\beta\tau)} \tag{5.7}$$

In terms of the terminology of inverse scattering, $\alpha+i\beta$ is the pole position and $\rho_1(0)$ is the residue at $z=0$. The two complex parameters completely determine a 2π soliton. If one defines

$$|c|\equiv\frac{1}{4} \tag{5.8}$$

and introduces new "scattering data" n_o,p_o,T_o,θ_o by means of

$$n_o\equiv\frac{4\beta}{|c|} \tag{5.9}$$

$$p_o \equiv -2\alpha \tag{5.10}$$

$$\theta_o \equiv \arg[\rho_1(0)] + \frac{\pi}{2} \tag{5.11}$$

$$\tau_o \equiv -\frac{1}{2\beta}\ln\frac{|\rho_1(0)|}{2\beta} \tag{5.12}$$

Eq.(5.7) can be put into a more "physical" form:

$$\begin{aligned} U_o(z,\tau) &= \tfrac{n_o|c|^{1/2}}{2}\exp[ip_o\tau + iK(n_o,p_o)z + i\theta_o] \\ &\quad \operatorname{sech}[\tfrac{n_o|c|}{2}(\tau - T_o - G(n_o,p_o)z)] \end{aligned} \tag{5.13}$$

with

$$K(n_o,p_o) \equiv \frac{1}{4}\langle\frac{2(\zeta+p_o/2)}{(\zeta+p_o/2)^2+\frac{1}{16}n_o^2|c|^2}\rangle \tag{5.14}$$

$$G(n_o,p_o) \equiv \frac{1}{4}\langle\frac{1}{(\zeta+p_o/2)^2+\frac{1}{16}n_o^2|c|^2}\rangle \tag{5.15}$$

The meaning of these new parameters can be easily identified: $n_o = \int |U_o(z,\tau)|^2 d\tau$ is the photon number, p_o the momentum per photon (frequency), τ_o the initial position in time, θ_o the initial phase, G the inverse of group velocity and K the wavevector. *Without loss of generality, we will assume from now on* $p_o = T_o = \theta_o = 0$.

The similarity between the solution of SIT and that of CNSE is not surprising. Since both problems can be solved in the framework of Zakharov-Shabat inverse scattering transform, the transformation between the scattering data and the field function is therefore the same. So the only difference of two problems is the way the scattering data evolve. This can be clearly seen by comparing Eq.(5.13) with Eq.(2.6).

By linearization, one obtains the following integro-differential equation for the small signal field function $u(z,\tau)$.

$$\frac{\partial}{\partial z}u(z,\tau) = \langle\lambda(z,\tau,\zeta)\rangle \tag{5.16}$$

with

$$\begin{aligned} \lambda(\tau) &\equiv 2[V_{20}^*(\tau)v_1(\tau) + V_{10}(\tau)v_2^*(\tau)] \\ &= V_{20}^{*2}(\tau)\textstyle\int_{-\infty}^{\tau} u(\tau')V_{20}^2(\tau')d\tau' - V_{10}^2(\tau)\int_{-\infty}^{\tau} u(\tau')V_{10}^{*2}(\tau')d\tau' \\ &\quad + V_{20}^{*2}(\tau)\textstyle\int_{-\infty}^{\tau} u^*(\tau')V_{10}^2(\tau')d\tau' - V_{10}^2(\tau)\int_{-\infty}^{\tau} u^*(\tau')V_{20}^{*2}(\tau')d\tau' \end{aligned} \tag{5.17}$$

Here u is the small signal field function, $\{V_{10}, V_{20}\}$ are the solution of Eqs. (5.1) -(5.2) with $U = U_o$ and λ is the perturbed dipole moment. For convenience, we have not indicated the independent variables z and ζ in Eq. (5.17).

Eq.(5.17) looks formidable to solve. Fortunately one does not need to actually deal with it. Since both SIT and CNSE can be solved in the same Zakharov-Shabat transform, the expansion we developed for the linearized CNSE (QNSE) can be applied to the linearized SIT here. Thus in the vector form, one has

$$\begin{aligned} \mathbf{u}(z,\tau) &= \Delta n(z)\mathbf{f_n}(\tau) + \Delta T(z)\mathbf{f_T}(\tau) + \Delta\theta(z)\mathbf{f_n}(\tau) + \Delta p(z)\mathbf{f_p}(\tau) \\ &\quad + \int [\Delta\rho_r(z,\zeta)\mathbf{u_{cr}}(\tau,\zeta) + \Delta\rho_i(z,\zeta)\mathbf{u_{ci}}(\tau,\zeta)]d\zeta \end{aligned} \tag{5.18}$$

Here we have put in the continuum perturbations. $\Delta\rho = \Delta\rho_r + i\Delta\rho_i$ is the perturbation "residue" of the continuum in the terminology of inverse scattering transform and $\mathbf{u_{cr}}, \mathbf{u_{ci}}$ are the corresponding perturbation functions. The evolution of perturbed scattering data can be obtained by perturbing the evolution equations of scattering data from the inverse scattering theory[25]. For the soliton parts,

$$\frac{d}{dz}\Delta n(z) = 0 \tag{5.19}$$

$$\frac{d}{dz}\Delta\theta(z) = \frac{\partial K}{\partial n_o}\Delta n(z) + \frac{\partial K}{\partial p_o}\Delta p(z) \tag{5.20}$$

$$\frac{d}{dz}\Delta p(z) = 0 \tag{5.21}$$

$$\frac{d}{dz}\Delta T(z) = \frac{\partial G}{\partial n_o}\Delta n(z) + \frac{\partial G}{\partial p_o}\Delta p(z) \tag{5.22}$$

and for the continuum,

$$\begin{aligned} \frac{\partial}{\partial z}\Delta\rho(z,\zeta) &= \frac{i}{2}\int g(\zeta')\frac{1}{\zeta' - \zeta - i0^+}d\zeta'\Delta\rho(z,\zeta) \\ &= [-\frac{\pi}{2}g(\zeta) + \frac{i}{2}P\int g(\zeta')\frac{1}{\zeta' - \zeta - i0^+}d\zeta']\Delta\rho(z,\zeta) \end{aligned} \tag{5.23}$$

Here P indicates principal value.

The solutions are:

$$\Delta n(z) = \Delta n(0) \tag{5.24}$$

$$\Delta\theta(z) = \Delta\theta(0) + \frac{\partial K}{\partial n_o} z\Delta n(0) + \frac{\partial K}{\partial p_o} z\Delta p(0) \tag{5.25}$$

$$\Delta p(z) = \Delta p(0) \tag{5.26}$$

$$\Delta T(z) = \Delta T(0) + \frac{\partial G}{\partial n_o} z\Delta n(0) + \frac{\partial G}{\partial p_o} z\Delta p(0) \tag{5.27}$$

$$\Delta\rho(z,\zeta) = \exp\Big[-\frac{\pi}{2} g(\zeta) z + \frac{i}{2} zP \int g(\zeta') \frac{1}{\zeta' - \zeta - i0^+} d\zeta' \Big] \Delta\rho(0,\zeta) \tag{5.28}$$

In contrast to solitons in optical fibers, the perturbation of photon number is also coupled to the perturbation of position and the perturbation of momentum is also coupled to the perturbation of phase.

Since we use the same expansion as we did for QNSE, the same projections can be used to obtain these perturbation scattering data from the perturbation field function.

$$\Delta n(z) = \frac{\langle \underline{\mathbf{f}}_{\mathbf{n}}(\tau)| \otimes |\mathbf{u}(z,\tau)\rangle}{\langle \underline{\mathbf{f}}_{\mathbf{n}}(\tau)| \otimes |\mathbf{f}_{\mathbf{n}}(\tau)\rangle} = 2\langle \underline{\mathbf{f}}_{\mathbf{n}}(\tau)| \otimes |\mathbf{u}(z,\tau)\rangle \tag{5.29}$$

$$\Delta\theta(z) = \frac{\langle \underline{\mathbf{f}}_{\theta}(\tau)| \otimes |\mathbf{u}(z,\tau)\rangle}{\langle \underline{\mathbf{f}}_{\theta}(\tau)| \otimes |\mathbf{f}_{\theta}(\tau)\rangle} = 2\langle \underline{\mathbf{f}}_{\theta}(\tau)| \otimes |\mathbf{u}(z,\tau)\rangle \tag{5.30}$$

$$\Delta p(z) = \frac{\langle \underline{\mathbf{f}}_{\mathbf{p}}(\tau)| \otimes |\mathbf{u}(z,\tau)\rangle}{\langle \underline{\mathbf{f}}_{\mathbf{p}}(\tau)| \otimes |\mathbf{f}_{\mathbf{p}}(\tau)\rangle} = \frac{2}{n_o}\langle \underline{\mathbf{f}}_{\mathbf{p}}(\tau)| \otimes |\mathbf{u}(z,\tau)\rangle \tag{5.31}$$

$$\Delta T(z) = \frac{\langle \underline{\mathbf{f}}_{\mathbf{T}}(\tau)| \otimes |\mathbf{u}(z,\tau)\rangle}{\langle \underline{\mathbf{f}}_{\mathbf{T}}(\tau)| \otimes |\mathbf{f}_{\mathbf{T}}(\tau)\rangle} = \frac{2}{n_o}\langle \underline{\mathbf{f}}_{\mathbf{T}}(\tau)| \otimes |\mathbf{u}(z,\tau)\rangle \tag{5.32}$$

$$\Delta\rho_r(z,\zeta) = \frac{\langle \underline{\mathbf{u}}_{\mathbf{cr}}(\tau,\zeta)| \otimes |\mathbf{u}(z,\tau)\rangle}{\int \langle \underline{\mathbf{u}}_{\mathbf{cr}}(\tau,\zeta)| \otimes |\mathbf{u}_{\mathbf{cr}}(\tau,\zeta')\rangle d\zeta'} \tag{5.33}$$

$$\Delta\rho_i(z,\zeta) = \frac{\langle \underline{\mathbf{u}}_{\mathbf{ci}}(\tau,\zeta)| \otimes |\mathbf{u}(z,\tau)\rangle}{\int \langle \underline{\mathbf{u}}_{\mathbf{ci}}(\tau,\zeta)| \otimes |\mathbf{u}_{\mathbf{ci}}(\tau,\zeta')\rangle d\zeta'} \tag{5.34}$$

5.2 Quantization in the scattering data space

The quantization of SIT solitons is more subtle than that of the NSE solitons. For a traveling wave (only in one direction) the commutation brackets of the field operator should be conserved even though the field system is coupled to the material system. This may be argued as follows. Suppose the medium is of finite length and light is coupled into and out of the medium without reflection. Then the input and output fields are in free space and therefore have to obey the commutation relations

of free space fields. In principle one can cut the medium at any place and the field at that place has to obey the same commutation relations. Therefore, the commutation brackets are also preserved inside the medium.

Our quantization procedure is as follows[71]. The commutation relations of perturbation field operators are given by Eq.(2.26)-(2.27). The relation between the perturbation field operator and the perturbation scattering data is given by Eq.(5.29)-(5.34) perturbation scattering data. The conservation of the commutator brackets for the field requires the conservation of the commutator brackets for the perturbed scattering data. If the commutator brackets of the scattering data are preserved during evolution, no additional noise operator is needed. Otherwise additional noise operators are introduced to preserve the commutator brackets. This can be easily accomplished in the "scattering data space" due to the decoupling of different "frequency" components.

To check the conservation of commutation brackets, it is easier to start from the evolution equations. The evolution equations of the perturbation scattering data are given by Eq.(5.19)-(5.23). It is easy to show that the commutator brackets of the soliton parts are conserved. However, those of the continuum are not. To see this, note that equation (5.23) is, in fact, the equation for a damped harmonic oscillator. The magnitude squared of $\Delta\rho(t,\zeta)$ decays exponentially.

$$\frac{\partial}{\partial t}|\Delta\rho(t,\zeta)|^2 = -\alpha(\zeta)|\Delta\rho(t,\zeta)|^2 \tag{5.35}$$

with a decay rate

$$\alpha(\zeta) = \pi g(\zeta) \tag{5.36}$$

Conventional laser theories[69,70] show that a damped harmonic oscillator calls for an additional noise operator to preserve the commutator brackets (also see section 2, chapter 4). The noise operator can be introduced formally and/or can be obtained through the concept of a reservoir. Here we follow the first approach and rewrite Eq.(5.23) as

$$\frac{\partial}{\partial z}\Delta\hat{\rho}(z,\zeta) = \frac{i}{2}\int g(\zeta')\frac{1}{\zeta'-\zeta-i0^+}d\zeta'\Delta\hat{\rho}(z,\zeta) + \hat{F}(z,\zeta) \tag{5.37}$$

In principle, one can determine the commutation relations of $\Delta\hat{\rho}(0,\zeta)$ using Eq.(5.33) and (5.34). Suppose, initially

$$[\Delta\hat{\rho}(0,\zeta), \Delta\hat{\rho}^{\dagger}(0,\zeta')] = \rho_o(\zeta)\delta(\zeta-\zeta') \tag{5.38}$$

then to preserve the commutation brackets, $\hat{F}(z,\zeta)$ has to satisfy

$$[\hat{F}(z,\zeta), \hat{F}^{\dagger}(t',\zeta')] = \alpha(\zeta)\rho_o(\zeta)\delta(z-z')\delta(\zeta-\zeta') \tag{5.39}$$

Equations (5.37) and (5.39) are the proper operator equations for the continuum part. We do not study the evolution of the continuum part because, as we have shown, its contribution can be suppressed by suitable detection schemes. Yet it is still interesting to ask for the physical origin of the noise sources. The reservoir theory of a damped harmonic oscillator derives the noise operator from the initial conditions of the reservoir. Here we have the same situation. When we eliminated the atomic variables to derive the classical equation (5.17), the initial conditions of v_1 and v_2 dropped out because they are zero classically. However in quantum theory $\hat{v}_1$ and $\hat{v}_2$ are operators and cannot be set equal to zero.

In the literature, it was proposed by several authors[72,73] to quantize the problem in the scattering data space directly using the classical results of inverse scattering transform without linearization. However, there are two problems with this approach : (1) The commutation relations of the field operators [Eq.(2.11) and (2.12)] cannot be justified. (2) Soliton problems that cannot be derived from a Hamiltonian (like the SIT problem) cannot be treated. The two problems are solved simultaneously under the linearization approach.

5.3 Squeezing

After quantization, the evolution equations for the soliton parts of the SIT problem are given by

$$\Delta\hat{n}(z) = \Delta\hat{n}(0) \tag{5.40}$$

$$\Delta\hat{\theta}(z) = \Delta\hat{\theta}(0) + \frac{\partial K}{\partial n_o} z\Delta\hat{n}(0) + \frac{\partial K}{\partial p_o} z\Delta\hat{p}(0) \tag{5.41}$$

$$\Delta\hat{p}(z) = \Delta\hat{p}(0) \tag{5.42}$$

$$\Delta\hat{T}(z) = \Delta\hat{T}(0) + \frac{\partial G}{\partial n_o} z\Delta\hat{n}(0) + \frac{\partial G}{\partial p_o} z\Delta\hat{p}(0) \tag{5.43}$$

In contrast to solitons in optical fibers, the fluctuations of photon number are also coupled to the fluctuations of position and the fluctuations of momentum are also coupled to the fluctuations of phase.

Because of this, in the consideration of squeezing effects, one needs to consider the linear combination of all the four operators[71]:

$$\hat{M}(z) = c_n\Delta\hat{n}(z) + c_\theta\Delta\hat{\theta}(z) + c_p\Delta\hat{p}(z) + c_T\Delta\hat{T}(z) \tag{5.44}$$

Without loss of generality, we will require

$$c_n^2\langle\Delta\hat{n}^2(0)\rangle + c_\theta^2\langle\Delta\hat{\theta}^2(0)\rangle + c_p^2\langle\Delta\hat{p}^2(0)\rangle + c_T^2\langle\Delta\hat{T}^2(0)\rangle = \frac{1}{4} \tag{5.45}$$

so that $\langle\hat{M}^2(0)\rangle = \frac{1}{4}$ (the shot noise level). The local oscillator time function that will measure the operator is then given by

$$\mathbf{f_L}(\tau) = 2[c_n\underline{\mathbf{f_n}}(\tau) + c_\theta\underline{\mathbf{f}}_\theta(\tau) + \frac{1}{n_o}c_p\underline{\mathbf{f_p}}(\tau) + \frac{1}{n_o}c_T\underline{\mathbf{f_T}}(\tau)] \tag{5.46}$$

Now we are going to use some matrix algebra to calculate the squeezing ratio. First, let us introduce the column matrices

$$\mathbf{y} = \begin{bmatrix} c_n \\ c_\theta \\ c_p \\ c_T \end{bmatrix} \tag{5.47a}$$

$$\hat{\mathbf{a}}(z) = \begin{bmatrix} \Delta\hat{n}(z) \\ \Delta\hat{\theta}(z) \\ \Delta\hat{p}(z) \\ \Delta\hat{T}(z) \end{bmatrix} \tag{5.47b}$$

so that Eq.(5.44) can be written as:

$$\hat{M}(z) = \mathbf{y}^T\hat{\mathbf{a}}(z) \tag{5.48}$$

The correlation matrix of operator vector $\hat{\mathbf{a}}(z)$ is defined as:

$$\mathbf{C}(z) = \frac{1}{2}[\langle \hat{\mathbf{a}}(z)\hat{\mathbf{a}}^{\mathbf{T}}(z)\rangle + \langle \hat{\mathbf{a}}(z)\hat{\mathbf{a}}^{\mathbf{T}}(z)\rangle^{T}] \tag{5.49}$$

The operator vector $\hat{\mathbf{a}}(z)$ is related to the initial operator vector $\hat{\mathbf{a}}(0)$ according to Eq.(5.40)-(5.43).

$$\hat{\mathbf{a}}(z) = \mathbf{S}(z)\hat{\mathbf{a}}(0) \tag{5.50}$$

where the transformation matrix is

$$\mathbf{S}(z) \equiv \begin{bmatrix} 1 & 0 & 0 & 0 \\ \frac{\partial K}{\partial n_o}z & 1 & \frac{\partial K}{\partial p_o}z & 0 \\ 0 & 0 & 1 & 0 \\ \frac{\partial G}{\partial n_o}z & 0 & \frac{\partial G}{\partial p_o}z & 1 \end{bmatrix} \tag{5.51}$$

What the local oscillator actually measures at the output of the medium is $\mathbf{y}^T\hat{\mathbf{a}}(z)$. Thus the fluctuation registered by the local oscillator is

$$\mathbf{y}^T\mathbf{C}(z)\mathbf{y} = \mathbf{y}^T\mathbf{S}(z)\mathbf{C}(0)\mathbf{S}^T(z)\mathbf{y} \tag{5.52}$$

In the matrix form, the constraint (5.45) becomes

$$\mathbf{y}^T\mathbf{C}(0)\mathbf{y} = \frac{1}{4} \tag{5.53}$$

Therefore the squeezing ratio is given by:

$$R(z) = \frac{\mathbf{y}^T\mathbf{C}(z)\mathbf{y}}{\mathbf{y}^T\mathbf{C}(0)\mathbf{y}} = 4\mathbf{y}^T\mathbf{C}(z)\mathbf{y} \tag{5.54}$$

The constraint (5.53) can be handled by the Lagrange multiplier method. The extrema of (5.54) are the eigenvalues of the determinantal equation:

$$\mathbf{S}(z)\mathbf{C}(0)\mathbf{S}^T(z)\mathbf{y} = \lambda\mathbf{C}(0)\mathbf{y} \tag{5.55}$$

or equivalently,

$$\mathbf{C}^{-1}(0)\mathbf{S}(z)\mathbf{C}(0)\mathbf{S}^T(z)\mathbf{y} = \lambda\mathbf{y} \tag{5.56}$$

Thus, the eigenvalues are found by diagonalizing the matrix $\mathbf{C}^{-1}(0)\mathbf{S}(z)\mathbf{C}(0)\mathbf{S}^T(z)$. The lowest eigenvalue tells us the optimum squeezing that can be achieved and

the corresponding eigenvector gives the operator that one should measure in order to achieve the optimum. Full advantage of squeezing can only be taken when the matrix appears in its diagonal form, when the inphase and quadrature components are uncorrelated.

For the SIT problem, assuming the soliton is a "white" soliton at $z = 0$, one has

$$\mathbf{C}(0) = \begin{bmatrix} \langle \Delta \hat{n}_o^2 \rangle & 0 & 0 & 0 \\ 0 & \langle \Delta \hat{\theta}_o^2 \rangle & 0 & 0 \\ 0 & 0 & \langle \Delta \hat{p}_o^2 \rangle & 0 \\ 0 & 0 & 0 & \langle \Delta \hat{T}_o^2 \rangle \end{bmatrix} \tag{5.57}$$

The lowest eigenvalue of Eq.(5.56) gives us the optimum achievable squeezing ratio R.

For homogeneous broadening media, $g(\zeta) = \delta(\zeta - \zeta_o)$, maximum squeezing occurs at $\zeta = 0$ due the symmetry. The optimum squeezing ration as a function of z for a soliton with $n_o = 1.8 \times 10^4$ is plotted in Figure 14. $n_o = 1.8 \times 10^4$ is the number of photons contained in a ps soliton in CdS and the normalization unit for distance is $1.6 \times 10^{-2} \mu m$ (see Appendix 2).

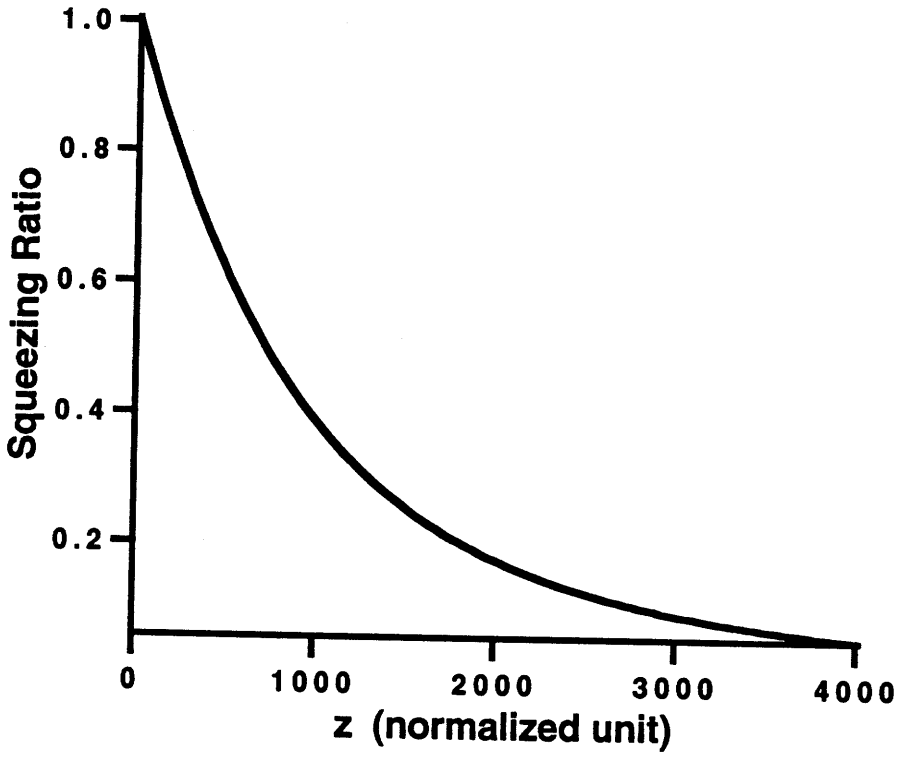

Figure14: Optimum squeezing ratio of SIT solitons

Chapter 6

Summary and future research directions

The objective of the thesis has been to develop a rigorous quantum theory of optical solitons. The investigation has involved the study of solitons in optical fibers and self-induced transparency solitons.

For solitons in optical fibers, the governing equation is the classical nonlinear Schrödinger equation (CNSE). After imposing commutation relations, the CNSE becomes the quantum nonlinear Schrödinger equation (QNSE), which turns out be a valid operator equation since it can be derived from a well defined Hamiltonian. The QNSE has been solved in the Heisenberg picture under linearization approximation. The perturbation field operator is expanded in a special set of basis so that different "frequency" components are decoupled. The soliton parts are characterized by four operators : photon number, phase, momentum and position. All the four operators can be detected using homodyne detection with a complete suppression of the continuum. The evolution of the four operators are determined. The coupling between photon number and phase produces squeezing. An optimum detection scheme using homodyne detection has been presented and the optimum squeezing ratio has been calculated. A general numerical approach for calculating squeezing ratios has been developed and applied to the study of fiber gyros using squeezed soliton.

The QNSE has also been solved in the Schrödinger picture. In the Schrödinger picture the QNSE is equivalent to the evolution equation of a system of bossons with δ-function interaction. The eigenstates of the system can be constructed analytically using Bethe's ansatz method. There are bound eigenstates which are closely related to the soliton phenomena. Both fundamental soliton states and higher order soliton states are constructed by superposition of bound eigenstates. The phase

spreading effect and position spreading effect come out of superposition naturally. The soliton collision effects have also been studied using the constructed higher order soliton states. The system is also studied under the time-dependent Hartree approximation. Approximate eigenstates are constructed by assuming each photon has a same wavefunction. The wavefunction is determined by a variational principle. The phase spreading effect is correctly predicted while the position spreading effect is missing under Hartree approximation. Squeezing ratio calculation based on Hartree approximation is also performed.

Solitons in optical fibers with loss and periodic amplification have been studied in the framework of the linearization approach. An equivalent nonlinear Schrödinger equation has been derived, quantized and solved. Noise operators introduced by both loss and gain give rise to the random walk of soliton frequency (momentum), which in turn causes the spreading of soliton position. This effect places a upper limit (known as the Gordon-Haus limit) on the achievable bit rate of soliton communication system. In the framework of our theory, the Gordon-Haus limit has been derived rigorously. A numerical approach for noise analysis of soliton-like systems is also presented.

The same linearization approach has been directly applied to the study of self-induced transparency solitons by taking the advantage that both the SIT and NSE problems can be solved by the Zakharov-Shabat inverse scattering transform. The same procedure can be applied to all the systems that can be solved in the same framework of Zakharov-Shabat inverse scattering transform. The quantization is performed in the scattering data space by requiring the conservation of commutation relations. In contrast to solitons in optical fibers, the fluctuations of photon number are also coupled to the fluctuations of position and the fluctuations of momentum are also coupled to the fluctuations of phase. The coupling gives rise to a squeezing effect. The correlation matrix technique has been applied to the calculation of squeezing ratio and the determination of optimum receiver structure.

Finally, in view of these developments, we would like to point out some research directions that call for future studies.

1. Although all our developments are on optical solitons, the ideas like solution and superposition in the Schrödinger picture, linearization in the Heisenberg picture or the quantization in the scattering data space under linearization approximation are in fact very general and are applicable to other quantum soliton systems.

2. Recently, the quantum inverse scattering method, which solves the problem exactly in the Heisenberg picture, has been advanced a lot. It would be interesting to compare and combine what we have done with this newly developed method.

3. Quantum effects of soliton propagation in optical fibers need more investigation. The nonlinear Schrödinger equation is correct only to the lowest order. By putting in higher order terms and different polarizations, interesting effects may show up.

4. Since the Gordon-Haus limit plays a fundamental role in long-haul communication systems using solitons, it is of particular interest to find a way to overcome this limit. We have pointed out the possibility of using intensity modulators or/and frequency filters to limit the spreading of position or/and frequency. However, the introduction of modulators or/and filters may perturb the steady state solution and thus call for a general theory of noise analysis of soliton-like systems.

5. Another important class of soliton-like system are the modelocked laser systems. Recently (classical) theory of modelocked laser systems has been advanced a lot due to the stimulus of experimental success. To study their noise properties again calls for a general theory of noise analysis of soliton-like systems.

There are many other interesting topics worthy of investigation. We are pretty sure that the studies on quantum effects of nonlinear pulse propagation will become

richer and richer. We sincerely hope that our studies have made some contributions to this development.

Appendix 1

In this appendix we prove equation (3.1).

From figure 3, the difference of the currents from two photodetectors is given by

$$\begin{aligned} \hat{D}(z,\tau) &= \left[\frac{|u_L(\tau)+\hat{u}(z,\tau)|^2-|u_L(\tau)-\hat{u}(z,\tau)|^2}{2}\right] \otimes h(\tau) \\ &= [u_L^*(\tau)\hat{u}(z,\tau)+u_L(\tau)\hat{u}^\dagger(z,\tau)] \otimes h(\tau) \end{aligned} \tag{A1.1}$$

Here $\otimes$ is the operation of convolution.

After the Fourier transform, one has

$$\begin{aligned} \hat{M}(z) &= \int e^{ik\tau}[u_L^*(\tau)\hat{u}(z,\tau)+u_L(\tau)\hat{u}^\dagger(z,\tau)] \otimes h(\tau)d\tau \\ &= H(k)\int e^{ik\tau}[u_L^*(\tau)\hat{u}(z,\tau)+u_L(\tau)\hat{u}^\dagger(z,\tau)]d\tau \end{aligned} \tag{A1.2}$$

This proves (3.1).

Appendix 2

According to Ref[26], the SIT problem can be modeled by three equations.

$$\frac{\partial}{\partial t}V_1(x',t',\delta') + i\delta' V_1(x',t',\delta') = \frac{1}{2}E'(x',t')V_2(x',t',\delta') \qquad (A2.1)$$

$$\frac{\partial}{\partial t'}V_2(x',t',\delta') - i\delta' V_2(x',t',\delta') = -\frac{1}{2}E'^{*}(x',t')V_1(x',t',\delta') \qquad (A2.2)$$

$$\frac{\partial}{\partial x'}E'(x',t') = 2\langle V_2^{*}(x',t',\delta')V_1(x',t',\delta')\rangle \qquad (A2.3)$$

Here t', x', δ' and E' are the normalized quantities (time, propagation distance, frequency deviation and electric field) used in Ref[26] and are related to the unnormalized quantities t, x, δ and E by

$$t' = \Omega t \qquad (A2.4)$$

$$x' = \frac{\Omega x}{v_c} \qquad (A2.5)$$

$$\delta' = -\frac{\delta}{2\Omega} \qquad (A2.6)$$

$$E' = \frac{2p_{21}E}{i\hbar\Omega} \qquad (A2.7)$$

with

$$\Omega = \frac{\omega_o N_a |p_{12}|^2}{2\hbar\epsilon} \qquad (A2.8)$$

Here N_a is the density of atoms, $p_{21} = p_{12}^{*}$ is the dipole moment per atom, ω_o is the "carrier" frequency and v_c is the velocity of light in the "background" index. We want to renormalize the field so that energy can be expressed in terms of photon number, while keeping the form of equations (A2.1)-(A2.3) unchanged. This can be achieved by the following change of variables:

$$\tau = Kt' \qquad (A2.9)$$

$$z = x'/K \qquad (A2.10)$$

$$\zeta = \delta'/K \qquad (A2.11)$$

$$U = E'/K \qquad (A2.12)$$

This reduces equations (A2.1)-(A2.3) to (5.1)-(5.3). The constant K is determined from the following energy condition:

$$\frac{1}{2\eta}\int |E|^2 d\tau Area = n\hbar\omega_o \qquad (A2.13)$$

which leads to the following expression for K:

$$K = \frac{8\eta\omega_o|p_{21}|^2}{\hbar\Omega Area} \qquad (A2.14)$$

Here $\eta = \sqrt{\frac{\mu}{\epsilon}}$ and $Area$ is the cross section of the beam. The new variables are related to the unnormalized quantities by

$$\tau = \frac{8\eta\omega_o|p_{21}|^2}{\hbar Area}t \qquad (A2.15)$$

$$z = \frac{\hbar\Omega^2 Area}{8\eta\omega_o|p_{21}|^2 v_c}x \qquad (A2.16)$$

$$\zeta = -\frac{\hbar Area}{16\eta\omega_o|p_{21}|^2}\delta \qquad (A2.17)$$

$$U = \frac{Area}{4\eta\omega_o|p_{21}|}E \qquad (A2.18)$$

As a numerical example[29], consider excitons bound to a neutral donor in CdS at 2 °K with an absorption peak wavelengh of λ=487 nm, an exciton intensity $N_a = 1 \times 10^{21}$ m^{-3} and a dipole moment 1×10^{-28} Cm. Assuming the beam crosssection is 1 μm^2 and the pulse duration is 1 ps, and one has :

$$t = 2.2 \times 10^{-9}\tau \quad [\text{sec}]$$

$$x = 1.6 \times 10^{-8}z \quad [\text{m}]$$

$$\delta = -9.1 \times 10^{8}\zeta \quad [\text{Hz}]$$

$$E = 2.4 \times 10^{2}U \quad [\text{V/m}]$$

and the photon number is

$$n_o = 1.8 \times 10^4$$

References

1. A. Hasegawa and F. Tappert, "Transmission of stationary nonlinear optical pulses in dispersive dielectric fibers I. anomalous dispersion", *Appl. Phys. Lett.* **23**, 142-144(1973).

2. L. F. Mollenauer, R. H. Stolen and J. P. Gordon, "Experimental observation of picosecond pulse narrowing and solitons in optical fibers", *Phys. Rev. Lett.* **45**, 1095-1097(1980).

3. M. Nakazawa, F. Suzuki and Y. Kimura, "20-Ghz soliton amplification and transmission with an Er-doped fiber", *Opt. Lett.* **14**, 1065-1067(1989).

4. K. J. Blow, N. J. Doran and B. K. Nayar, "Experimental demonstration of optical soliton switching in an all-fiber sagnac interferometer", *Opt. Lett.* **14**,754-756(1989).

5. N. J. Doran and D. Wood, "Nonlinear-optical loop mirror", *Opt. Lett.* **13**, 56-58(1988).

6. M. N. Islam, E. R. Sunderman, R. H. Stolen, W. Pleibel and J. R. Simpson, "Soliton switching in a fiber nonlinear loop mirror", *Opt. Lett.* **14**, 811-813(1989).

7. J. D. Moores, K. Bergman, H. A. Haus and E. P. Ippen, "Optical switching using fiber ring reflectors", *J. Opt. Soc. Am. B* **8**, 594-601(1991).

8. J. P. Gordon and H. A. Haus. "Random walk of coherent amplified solitons in optical fiber transmission", *Opt. Lett.* **11**, 665-667(1986).

9. H. P. Yuen, "Two-photon coherent states of the radiation field", *Phys. Rev. A* **13**, 2226-2243(1976).

10. R. E. Slusher, L. W. Hollberg, B. Yurke, J. C. Mertz and J. F. Valley, "Observation of squeezed states generated by four-wave mixing in an optical cavity", *Phys. Rev. Lett.* **55**, 2409-2412(1985).

11. R. M. Shelby, M. D. Levenson, S. H. Perlmutter, R. G. DeVoe and D. F.Walls, "Broadband parametric deamplification of quantum noise in an optical fiber", *Phys. Rev. Lett.* **57**, 691-694(1986).

12. L. W. Wu, H. J. Kimble, J. L. Hall and H. Wu, "Generation of squeezed states by parametric down conversion", *Phys. Rev. Lett.* **57**, 2520-2523(1986).

13. M. G. Raizen, L. A. Orozco, M. Xiao, T. L. Boyd and H. J. Kimble, "Squeezed state generation by normal modes of a coupled systems", *Phys. Rev. Lett.* **59**, 198-201(1987).

14. M. W. Maeda, P. Kumar and J. H. Shapiro, "Observation of squeezed noise produced by forward four-wave mixing in sodium vapor", *Opt. Lett.* **59**, 161-163(1987).

15. S. Machida, Y. Yamamoto and Y. Itaya, "Ultrabroadband amplitude squeezing in a semiconductor laser", *Phys. Rev. Lett.* **60**, 792-794(1988).

16. R. E. Slusher, P. Grangier, A. LaPorta, B. Yurke and M. J. Potasek. "Pulsed squeezed light". *Phys. Rev. Lett.* **59**, 2566-2569(1987).

17. T. Hirano and M. Matsuoka, "Broadband squeezing of light by pulse excitation", *Opt. Lett.* **15**, 1153-1155(1990).

18. K. Bergman and H.A. Haus, "Squeezing in fibers with optical pulses", *Opt. Lett.* **16**, 663-665(1991).

19. M. Rosenbluh and R. M. Shelby, "Squeezed optical solitons", *Phys. Rev. Lett.* **66**, 153-156(1991).

20. N. Imoto, H. A. Haus, and Y. Yamamoto, "Quantum non-demolition measurement of the photon number via the optical Kerr effect", *Phys. Rev. A* **32**, 2287-2292(1985).

21. S. L. McCall and E. L. Hahn, "Self-induced transparency by pulsed coherent light", *Phys. Rev. Lett.* **18**, 908-911(1967).

22. S. L. McCall and E. L. Hahn, "Self-induced transparency", *Phys. Rev.* **183**, 457-485(1969).

23. G. L. Lamb, Jr., "Analytical descriptions of ultra-short optical pulse propagation in a resonant medium", *Rev. Mod. Phys.* **43**, 99-129(1971).

24. M. J. Ablowitz, D. J. Kaup, A. C. Newell and H. Segur, "Method for solving the sine-gordon equation", *Phys. Lett.* **30**, 1262-1264(1973).

25. D. J. Kaup, "Coherent pulse propagation : A comparison of the complete solution with the McCall-Han theory and others", *Phys. Rev.* **16**, 704-719(1977).

26. H. A. Haus, "Physical interpretation of inverse scattering formalism applied to SIT", *Rev. Mod. Phys.* **51**, 331-339(1979).

27. V. Zakharov and A. Shabat, "Exact theory of two-dimensional self-focusing and one- dimensional self-modulation of waves in nonlinear media", *Soviet Physics JETP* **34**, 62-68(1972).

28. R. E. Slusher and H. M. Gibbs, "Self-induced transparency in atomic rubidium", *Phys. Rev. A* **5**, 1634-1659(1972).

29. K. Watanabe, H. Nakano, A. Honold and Y. Yamamoto, "Optical nonlinearities of excitonic self-induced transparency solitons : Towards ultimate detection of squeezed states and quantum nondemolition measurement", *Phys. Rev. Lett.* **19**, 2257-2260(1989).

30. M. Lakshmanan, **Solitons**, Spinger-Verlag, 1988.

31. S. E. Trullinger, V. E. Zakharov and V. L. Pokrovs (Editors), **Solitons**, North-Holland, Amsterdam, 1986.

32. M. Barthes and J. Leon (Editors), *Nonlinear Coherent Structures*, Springer-Verlag, 1990.

33. J. Scott Russell, "Report on waves". In **Rept. Fourteenth Meeting of the British Association for the advancement of science**, page 311. John Murray, London, 1844.

34. D. J. Korteweg and G. deVries, "On the change of form of long waves advancing in a rectangular canal, and on a new type of long stationary waves", *Phil. Mag.* **39**, 422-443(1895).

35. N. J. Zabusky and M. D. Kruskal, "Interactions of solitons in a collisionless plasma and the recurrence of initial states", *Phys. Rev. Lett.* **15**, 240-24(1965).

36. C. S. Gardner, J. M. Greene, M. D. Kruskal and R. M. Miura, "Method for solving the Korteweg-deVries equation", *Phys. Rev. Lett.* **19**, 1095-1097(1967).

37. P. D. Lax, "Integrals of nonlinear equations and solitary waves", *Comm. Pure Appl. Math.* **21**, 467-490(1968).

38. T. H. R. Skyrme, *Proc. Roy. Soc. Lond.* **A247**, 260-278(1958).

39. M. J. Ablowitz, D. J. Kaup, A. C. Newell and H. Segur, "The inverse scattering transform-fourier analysis for nonlinear problems", *Stud. Appl. Math.* **53**, 249-315(1974).

40. Y. Kodama and A. hasegawa, "Nonlinear pulse propagation in a monomode dielectric guide", IEEE *J. Quan. Elec.* **23**, 510-524(1997).

41. F. M. Mitschke and L. F. Mollenauer, "Discovery of the soliton self-frequency shift", *Optics Letter* **11**, 659-661(1986).

42. For example, see C. R. Menyuk, "Stability of solitons in birefringent optical fibers II", *J. Opt. Soc. Am. B* **5**, 392-402(1988).

43. For a review, see A. Hasegawa, **Optical Solitons in Fibers**, Springer-Verlag Berlin Heidelberg and AT&T Bell Laboratories 1989.

44. K. Huang, **Statistical Mechanics**, John Wiley, NY, 1963.

45. E. H. Lieb and W. Linger, "Exact analysis of an interacting bose gas. I and II", *Phys. Rev.* **130**, 1605(1963).

46. I. B. McGuire, "Study of exactly solvable one-dimensional n-body problems", *J. Math. Phys.* **5**, 622(1964).

47. C. N. Yang, "Some exact results for the many-body problem in one dimension with repulsive delta-function interactions", *Phys. Rev. Lett.* **19**, 1312(1967).

48. C. N. Yang, "S matrix for the one-dimensional n-body problem with repulsive or attractive δ-function interaction", *Phys. Rev.* **168**, 1920-1923(1967).

49. H. P. Thacker, "Exact integrability in quantum field theory and statistical systems", *Rev. Mod. Phys.* **53**, 253(1981).

50. P. Garbaczewski, **Classical and Quantum Field Theory of Exactly Soluble Nonlinear Systems**. World Scientific Publishing, 1985.

51. H. B. Thacker and D. Wilkinson, "Inverse scattering transform as an operator method in quantum field theory", *Phys. Rev. D* **19**, 3660-3665(1979).

52. D. B. Creamer, H. B. Thacker and D. Wilkinson, "Gelfand-Levitan method for operator fields", *Phys. Rev. D* **21**, 1523-1528(1980).

53. M. Gockeler, "The construction of bound state operators for the cubic Schroedinger field theory", *Z. Phys.* **C7**, 263-269(1981).

54. C. R. Nohl, "Semiclassical quantization of nonlinear Schrödinger equation", *Ann. Phys. (USA)* **96**, 234-260(1976).

55. M. Wadachi and M. Sakagami, "Classical soliton as a limit of the quantum field theory", *J. Phys. Soc. Japan.* **53**, 1933-1938(1984).

56. Y. Lai and H. A. Haus, "Quantum theory of solitons in optical fibers I. time-dependent hartree approximation", *Phys. Rev. A* **40**, 844-853(1989).

57. Y. Lai and H. A. Haus, "Quantum theory of solitons in optical fibers II. exact solution", *Phys. Rev. A* **40**, 854-866(1989).

58. S. J. Carter, P. D. Drummond, M. D. Reid and R. M. Shelby, "Squeezing of quantum solitons", *Phys. Rev. Lett.* **58**, 1841-1843(1987).

59. P. D. Drummond and S. J. Carter, "Quantum field theory of squeezing in solitons", *J. Opt. Soc. Am. B* **4**, 1565-1573(1987).

60. S. J. Carter P. D. Drummond and R. M. Shelby, "Time dependence of quantum fluctuations in solitons", *Opt. Lett.* **14**, 373-375(1989).

61. H. A. Haus, "Quantum noise in a solitonlike repeater system", *J. Opt. Soc. Am. B* **8**, 1122-1126(1991).

62. H. A. Haus, **Waves and Fields in Optoelectronics**. Prentice Hall, 1984.

63. H. A. Haus and Y. Lai, "Quantum theory of soliton squeezing - a linearized approach", *J. Opt. Soc. Am. B* **7**, 386-392(1990).

64. B. Yoon and J. W. Negele, "Time-dependent Hartree approximation for a one-dimensional system of bosons with attractive δ-function interactions", *Phys. Rev. A* **16**, 1451-1459(1977).

65. R. S. Bondurant, "Response of ideal photodetectors to photon flux and/or energy flux", *Phys. Rev. A* **32**, 2797-2802(1985).

66. B. Yurke, "Wideband photon counting and homodyne detection", *Phys. Rev. A* **32**, 311-323(1985).

67. A.M. Weiner, J. P. Heritage and E. M. Kirschner, "High resolution femtosecond pulse shaping", *J. Opt. Soc. Am. B* **5**, 1563-1572(1988).

68. K. Bergman, H.A. Haus and Y. Lai, "Fiber gyros using squeezed pulses", to be published on *J. Opt. Soc. Am. B.*

69. H. Haken, **Laser Theory**, Springer-Verlag Berlin, 1970.

70. H. Haken, **Light I and II.** Springer-Verlag Berlin, 1981.

71. Y. Lai and H. A. Haus, "Quantum theory of self-induced transparency solitons : A linearization approach", *Phys. Rev. A* **42**, 2925-2934(1990).

72. D. J. Kaup, "Exact quantization of the nonlinear Schródinger equation", *J. Math. Phys.* **16**, 2036-2041, 1975.

73. H. A. Haus, K. Watanabe and Y. Yamamoto, "Quantum-nondemolition measurement of optical solitons", *J. Opt. Soc. Am. B* **6**, 1138(1989).

74. E. M. Wright, "Quantum theory of soliton propagation in an optical fiber using the Hartree approximation", *Phys. Rev. A* **43**, 3836-3844(1991).

75. M. Kitagawa and Y. Yamamoto, "Number-phase minimum-uncertainty state with reduced number uncertainty in a Kerr nonlinear interferometer", *Phys. Rev. A* **34**, 3974-3988(1986).

76. M. Nakajawa, E. Yamada, H. Kubota and K. Suzuki, "10 Gbits/s soliton data transmission over one million kilometers", to be published on *Electronics Letters.*

77. D. J. Kaup, "Perturbation theory for solitons in optical fibers", *Phys. Rev. A* **42**, 5689-5694(1990).